Evaluation of SBI and SBI-Airmass as indicators for sunlight access

Tural Doruk Aral & Agnieszka Małgorzata Gębura-Tetiurka

Master thesis in Energy-efficient and Environmental Buildings
Faculty of Engineering | Lund University

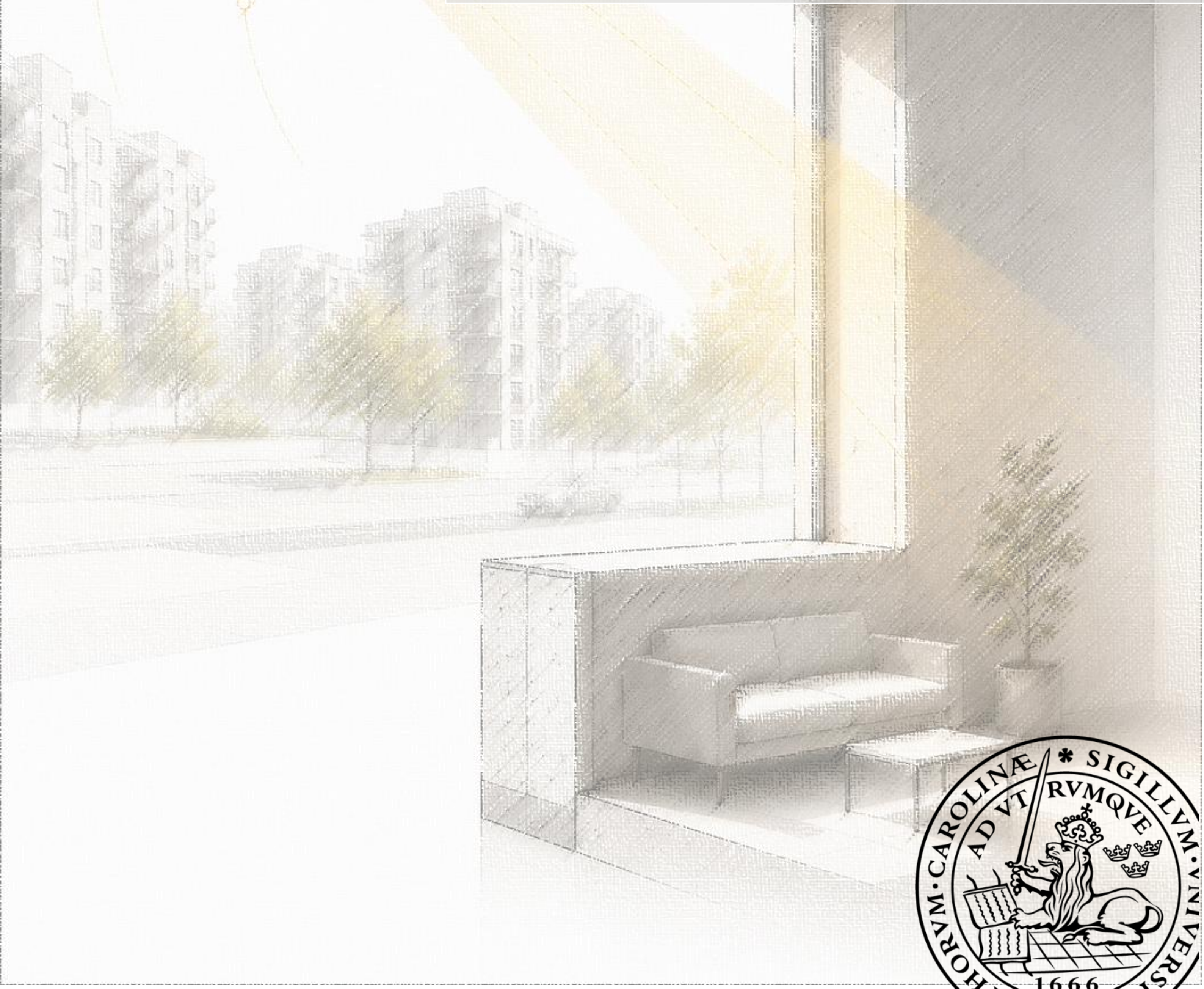

Lund University

Lund University, with eight faculties and a number of research centres and specialized institutes, is the largest establishment for research and higher education in Scandinavia. The main part of the University is situated in the small city of Lund which has about 112 000 inhabitants. A number of departments for research and education are, however, located in Malmö. Lund University was founded in 1666 and has today a total staff of 6 000 employees and 47 000 students attending 280 degree programmes and 2 300 subject courses offered by 63 departments.

Master Programme in Energy-efficient and Environmental Building Design

This international programme provides knowledge, skills and competencies within the area of energy-efficient and environmental building design in cold climates. The goal is to train highly skilled professionals, who will significantly contribute to and influence the design, building or renovation of energy-efficient buildings, taking into consideration the architecture and environment, the inhabitants' behaviour and needs, their health and comfort as well as the overall economy.

The degree project is the final part of the master programme leading to a Master of Science (120 credits) in Energy-efficient and Environmental Buildings.

Examiner: Marie-Claude Dubois (Division of Energy and Building Design)

Supervisor: Niko Gentile (Division of Energy and Building Design), John Mardaljevic (Daylight Experts / Loughborough University, UK) and Paul Rogers (ACC Glas och Fasadkonsult)

Keywords: SBI, SBI-airmass, EN 17037, ASE, ASH, direct sunlight exposure, solar access indicators, aperture-based indicators.

Publication year: 2026

Abstract

The assessment of sunlight access in buildings is constrained by methods that rely on simplified point-based evaluation. EN 17037 sunlight exposure evaluates sunlight at a single point on the aperture under restricted temporal conditions. This limits the representation of how sunlight interacts with the aperture over time. These characteristics reduce its applicability at early design stages. The resulting evaluation does not capture the distribution of direct sunlight across the aperture.

This study examines the aperture-based indicators Sunlight Beam Index (SBI) and SBI-airmass as geometry-driven measures of direct sunlight access. A custom computational workflow was developed in Rhino–Grasshopper using Python to calculate these metrics at the aperture level based on time-resolved solar position data. The analysis combines a parametric study using a reference “shoebox” model with an evaluation of existing buildings in their urban context. The results are examined in relation to SBI and SBI-airmass as well as EN 17037 sunlight exposure, Annual Sunlight Exposure (ASE), and Annual Sunlight Hours (ASH), using correlation analysis, distribution analysis, relationship modelling, and variable importance assessment.

The results show that SBI varies in proportion to aperture area, with orientation, obstruction, and aperture configuration influencing the outcome. SBI-airmass keeps the geometric basis of SBI but adds an airmass factor to account for the reduced strength of low-elevation sunlight. Comparisons with EN 17037 sunlight exposure, ASE, and ASH show that these metrics produce different outcomes under the same conditions due to differences in spatial definition and temporal scope. The relationships between them show a pattern at lower and upper ranges, while variation is observed within intermediate values.

The findings indicate that aperture-based indicators provide a continuous, geometry-dependent description of sunlight access that can be evaluated without interior definition. This allows the assessment of sunlight conditions at stages where only building form and spatial context are defined. SBI and SBI-airmass extend the evaluation of sunlight access by connecting geometric configuration to time-integrated exposure, while remaining distinct from existing methods in both formulation and output.

Preface

This thesis was carried out at Lund University as part of the Energy Efficient and Environmental Building Design Master's programme.

The work focuses on the analysis of access to direct sunlight in residential buildings and the evaluation of the Sunlight Beam Index (SBI) in relation to selected methods used for assessing the sunlight environment, including EN 17037 sunlight exposure, as well as climate-based indicators such as Annual Sunlight Exposure (ASE) and Annual Sunlight Hours (ASH).

The study was based on computer simulations conducted using both simplified reference models and real-case models representing urban conditions. The analysis was performed at two scales: the level of individual apertures and the level of entire rooms.

The real-case models included a range of building types and urban densities, described using a simplified representation of the surrounding context.

The aim of this thesis was to evaluate the behaviour of the SBI metric and to explore its potential application as a tool supporting the analysis of sunlight access in the early stages of the design process.

This thesis was prepared as a joint work by Tural Doruk Aral and Agnieszka Małgorzata Gębura-Tetiurka.

This thesis was developed by the authors. The research design, computational method, simulations, data analysis, results and interpretations presented in this work are the authors' own work.

Artificial intelligence tools, specifically ChatGPT by OpenAI, were used as a language-support tool during the writing process to improve clarity, grammar, wording and academic style. The authors reviewed and approved all AI-assisted revisions, and no AI tool was used to generate the research method, simulation results, data analysis or conclusions.

Acknowledgements

We would like to express our sincere gratitude to our supervisor, Niko Gentile, for his guidance, support, and valuable feedback throughout the development of this thesis. His insights and constructive comments have greatly contributed to the quality of this work.

We would also like to express our gratitude to John Mardaljevic (Daylight Experts / Loughborough University, UK), Paul Rogers and Eftychia Stamataki (ACC Glas och Fasadkonsult AB) for their support and for the valuable discussions that contributed to this research.

We would like to acknowledge the support of the Division of Energy and Building Design at Lund University, which provided the academic environment and resources necessary for this research.

Finally, we would like to thank our families and friends for their continuous support, patience, and encouragement throughout this work.

Table of Contents

1 Introduction and background

1.1 Background

Access to sunlight is increasingly shaped by urban densification. Dense urban form can reduce the daylight available to people and ecosystems, placing access to natural light within the broader discussion of sustainable urban development (Volf et al., 2024). Access to direct sunlight is one of the determinants of quality for residential buildings. Sunlight influences physiological and psychological well-being, thermal conditions, and the perception of indoor environments (Reinhart, Mardaljevic and Rogers, 2013). In residential design, sunlight access is therefore both an urban-scale resource question and a matter of indoor comfort.

Sunlight access indoors is shaped by the geometry of buildings and their surroundings, with urban form limiting access to sunlight. Increased residential density leads to obstruction between buildings, reducing the availability of direct solar exposure and limiting its penetration into interior spaces (Czachura, 2023). This is especially relevant at northern latitudes, where low solar altitude and seasonal variation make sunlight access more dependent on building spacing, orientation, and obstruction. In this context, sunlight access becomes a planning-level condition as well as a room-level comfort issue, as urban layout, density, building spacing, and orientation affect the solar conditions available to dwellings (Czachura, 2023).

Current methods for evaluating sunlight access use different spatial and temporal definitions. Point-based approaches evaluate sunlight at a single location at the aperture. For example, exposure to sunlight as defined by EN 17037 (SSI and CEN, 2021) follows this approach and defines sunlight access using a reference point and a time-bound evaluation period. This makes EN 17037 sunlight exposure useful as a standardised sunlight exposure criterion, although its reference-point definition and restricted evaluation period limit its ability to describe annual sunlight exposure across the aperture (Dervishaj et al., 2023; Dervishaj and Gudmundsson, 2025). Other methods, such as Annual Sunlight Hours (ASH) (Czachura, 2023) and Annual Sunlight Exposure (ASE) (IES, 2012), extend the evaluation across time or across both space and time. ASH records direct sunlight as a binary condition at each timestep, and ASE evaluates the annual occurrence of direct sunlight above a defined exposure threshold. These differences mean that existing metrics describe different aspects of sunlight access and exposure, but do not fully capture how direct sunlight changes across aperture area, season, orientation, obstruction, and angle of incidence.

Aperture-based approaches address this limitation by focusing on the relationship between solar paths and building openings. Aperture-Based Daylight Modelling (ABDM) treats the aperture as the primary element of analysis (Mardaljevic, 2019). The term ABDM refers to the general approach to daylight modelling; ABDM metrics are adopted for assessing different daylight qualities in buildings. In particular, focusing on sunlight, the Sunlight Beam Index (SBI) is an ABDM metric that quantifies the cross-sectional area of direct sunlight passing through an opening and aggregates this quantity over time (Mardaljevic and Roy, 2016). SBI enables the evaluation of sunlight access without predefined interior conditions. It applies to early design stages and urban-scale analysis using aperture geometry, solar position, and external obstruction.

SBI-airmass (Mardaljevic and Brembilla, 2021) extends the SBI formulation. The method applies a correction based on the atmospheric path length of solar rays. Solar rays at low angles travel through a greater air mass. This reduces sunlight intensity. The correction accounts for this effect and adjusts the contribution of sunlight over time. Aperture-based indicators can support early-stage analysis because they rely on aperture geometry, solar position, and external obstruction.

While SBI and SBI-airmass are promising sunlight access indicators, they have not been as extensively tested and studied as other existing sunlight access metrics. This thesis evaluates SBI and SBI-airmass through a controlled shoebox study and urban-context models and compares their behaviour against the sunlight access metrics proposed by EN 17037 sunlight exposure, ASE, and ASH. The results are used to discuss the strengths and weaknesses of SBI and SBI-airmass with respect to existing metrics for practical application. A proposal for SBI thresholds is also provided.

1.2 Aim and research questions

The aim of this study is to contribute to the development and evaluation of aperture-based sunlight access indicators by examining the SBI and SBI-airmass in relation to changes in aperture geometry, orientation, and external obstructions. The analysis examines the sensitivity of these aperture-based indicators and their relationship to established methods for assessing sunlight access, including EN 17037 sunlight exposure, ASE, and ASH. The broader purpose is to assess whether aperture-based metrics can represent direct sunlight access in a way that is more responsive to geometric variation and more suitable for early-stage design assessment.

The study focuses on establishing how these indicators respond to geometric variation and how their results relate to existing assessment approaches, with the intention of examining their potential role in early-stage architectural and urban design.

In particular, the objective of this thesis is to answer the following research question (RQ) and two supporting sub-questions (SQ.1, SQ.2):

RQ: How are SBI, SBI-airmass, and other established sunlight metrics affected by aperture size, geometry, orientation, and surrounding obstructions?

SQ.1: How do SBI and SBI-Airmass compare with the sunlight access metrics EN 17037 sunlight exposure, ASE and ASH?

SQ.2: How can SBI and SBI-Airmass support early design decisions and urban planning?

1.3 Literature review: existing indicators and methods for assessing sunlight access

1.3.1 Scope of sunlight access assessment

This study focuses on the assessment of direct sunlight access in residential buildings. The analysis concerns direct sunlight entering space through apertures. In this context, sunlight access is understood as the availability of unobstructed direct sun rays at a defined point, surface, or aperture over a specified period.

The term sunlighting refers to the provision of access to direct sunlight and is commonly assessed through geometric methods that relate sun position to the analysed point or surface (Czachura, 2023). The result is often expressed as the duration of direct sunlight exposure. Czachura (2023) defines solar access more broadly as the amount and distribution of sunlight within the human living environment, shaped by urban geometry and mutual shading between buildings.

This distinction defines the scope of the review. The following sections therefore focus on methods that assess direct sunlight exposure, annual sunlight availability, excessive sunlight exposure, and aperture-based sunlight access.

1.3.2 EN 17037 Exposure to sunlight

EN 17037 sunlight exposure provides one of the main normative reference points for assessing direct sunlight access in European building practice. Within this study, only the section concerning exposure to sunlight is considered. The method is relevant because it defines sunlight access through exposure duration and is therefore commonly used as a compliance-oriented reference.

Standard EN 17037 sunlight exposure defines the appropriate duration of direct sunlight in a room. The standard assumes that access to sunlight contributes to occupant comfort and interior environmental quality. It recognises that both insufficient and excessive exposure can lead to discomfort (SSI and CEN, 2021).

The evaluation is based on the visibility of the sun at a single reference point located at the centre of the aperture on a selected day (Figure 1) (SSI and CEN, 2021).

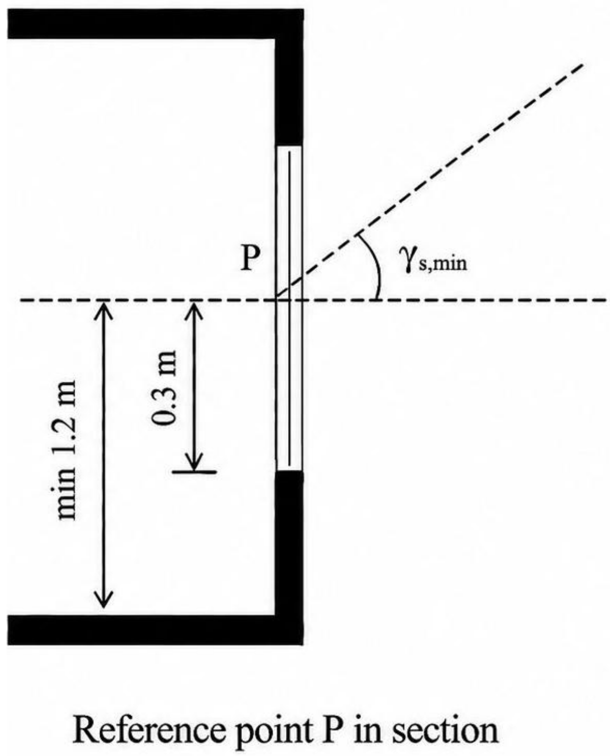

Figure 1 Reference point definition and sunlight exposure criteria in EN 17037 (source: adapted from Dervishaj and Gudmundsson, 2025).

Specifically, the calculations are carried out for:
- A selected reference day between 1st February and 21st March,
- Clear sky conditions,
- Considering the actual building's orientation, including shading from the surrounding area.

The assessment is carried out at a single reference point (point P – Figure 1), located:
- On the inner surface of the window opening,
- Centrally in relation to the aperture geometry,

For spaces with multiple openings, the assessment is based on the opening that provides the highest sunlight access. The standard allows the summation of exposure durations from different openings if these exposures do not occur simultaneously (SSI and CEN, 2021).

The EN 17037 sunlight exposure standard is characterised as follows:
- Single-day analysis; no annual calculations,
- A pass/fail approach; the result either meets or does not meet the requirements,
- Target level of performance: 1.50 h – low, 3,00 h – medium, 4,00 h – high,
- Based on a single measurement point,
- No account is taken of sunlight intensity; only the duration of exposure is analysed.

The main advantage of this method is its clear structure and suitability for compliance assessment. Its limitation is that the result depends on a single reference point and a restricted assessment period. The method does not describe the distribution of direct sunlight across the aperture, nor does it account for aperture area, angle of incidence, or partial shading across the opening. As a result, different aperture configurations may produce the same EN 17037 sunlight exposure result despite receiving different amounts of direct sunlight. This limitation is directly relevant to the present study, which evaluates whether aperture-based metrics can provide additional geometric information.

1.3.3 Annual Sunlight Exposure

Annual Sunlight Exposure (ASE) is included in this review because it represents a different category of sunlight metric. It does not assess minimum access to direct sunlight. Instead, it identifies excessive indoor exposure based on annual threshold exceedance. ASE is therefore relevant as a comparative metric, but it should not be interpreted as equivalent to EN 17037 sunlight exposure, ASH, SBI, or SBI-airmass.

The ASE metric determines the annual percentage of indoor analysis area exposed to direct sunlight above a specified illuminance threshold (Figure 2). ASE:

- Covers the entire year – 8 760 hours,
- Considers only direct sunlight,
- Is based on climate simulations using actual weather data (IES, 2012).

Threshold values define the proportion of the horizontal surface area experiencing intense sunlight that exceeds specific values.

- Illuminance – 1 000 lx,
- Exposure time – 250 hours per year (IES, 2012).

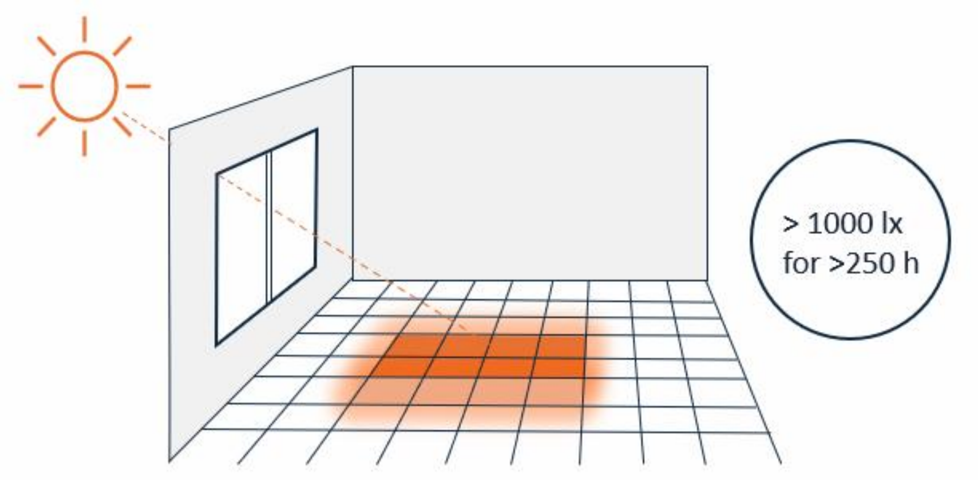

Figure 2 Conceptual representation of Annual Sunlight Exposure (ASE), showing the proportion of the indoor analysis grid receiving direct sunlight above 1,000 lx for more than 250 hours per year.

The calculations are based on an indoor grid of points distributed across the working plane. Each point in the grid is analysed in terms of the number of hours per year during which the threshold for direct solar exposure intensity is exceeded (IES, 2012).

The result is presented as:

- The percentage of the area meeting the threshold exceedance criterion,
- Or as the spatial distribution of exposure within the analysed room (IES, 2012).

ASE is conceptually different from other sunlight metrics. The ASE metric is a measure of excessive exposure to sunlight. It is generally accepted that exceeding a certain percentage of the surface area indicates a risk of excessive sun exposure, whilst values below this level can be considered acceptable (IES, 2012).

Characteristics of the ASE method:

- Annual analysis, accounting for the variability of conditions throughout the year,
- A threshold-based, based on the exceeding of limit values,
- Area-based analysis, with calculations relating to the proportion of the analysed area,
- Consideration of sunlight intensity, via a light intensity threshold,
- Focus on excessive solar exposure.

Most importantly, ASE is assessed indoors, therefore requiring knowledge about the indoor layout of a building.

For this reason, ASE has a different methodological role from the other metrics in this study. A high ASE value indicates a higher risk of excessive indoor exposure. In addition, the metric depends on interior layout, sensor grid definition, and material assumptions. It is therefore less directly related to aperture geometry than SBI and SBI-airmass. In this study, ASE is used as a comparative reference for excessive exposure, not as a direct measure of beneficial sunlight access.

1.3.4 Annual Sunlight Hours

Annual Sunlight Hours (ASH) represents an annual and time-based method for assessing direct sunlight availability (Figure 3). It is relevant to this study because it extends the analysis beyond a single reference day and evaluates sunlight availability over the full year. Its use in urban planning also makes it important for assessing the influence of surrounding geometry.

The ASH metric determines the availability of direct sunlight on an annual basis, based on an analysis of the surrounding geometry and the position of the sun. It is time-based and is used to assess access to sunlight in urban planning analyses (Czachura, 2023).

ASH is described as the average availability of direct sunlight, calculated based on all hours of sunlight during the year. In practice, this involves analysing whether there is an unobstructed path of solar rays for a given area for successive solar vectors throughout the year (Czachura, 2023).

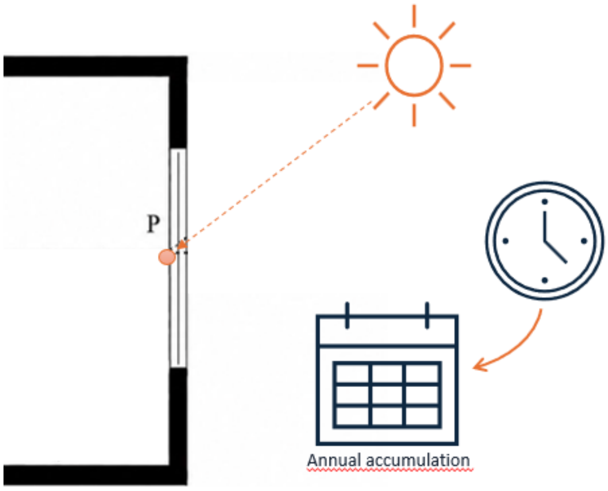

Figure 3 Conceptual representation of Annual Sunlight Hours (ASH), showing the annual accumulation of time during which direct sunlight reaches an unobstructed evaluation point on the aperture.

The calculation method includes:
- Generating the sun's position for all time steps,
- Verifying whether the sun is above the horizon,
- Analysing the visibility of sunlight through ray tracing,
- Assigning a binary value – sunlight (1) / shade (0),
- Summing all instances of direct exposure.

The analysis is applicable to various surfaces, such as facades or outdoor spaces, enabling wide application across different design scales (Czachura, 2023).

Characteristics of the ASH metric:
- Annual analysis, accounting for the full variability of sunlight conditions,
- Continuous approach, no threshold values,
- Temporal analysis, the result indicates the total exposure time,
- Geometric conditions, the result depends on the form of the built environment and surrounding obstacles (Czachura, 2023).

ASH provides an annual description of direct sunlight availability based on exposure duration and surrounding geometry. Its limitation is that it describes exposure duration rather than the amount of direct sunlight passing through an aperture. It does not distinguish between full and partial aperture exposure, and it does not account for angle of incidence. ASH can therefore describe when direct sunlight is available, but not how much of the sunlight beam effectively passes through the aperture. This distinction is central to the comparison with SBI and SBI-airmass.

1.3.5 Solar access metrics in urban planning

Direct sunlight access is strongly determined by urban geometry. Building height, spacing, street orientation, courtyard depth, and development density influence whether direct sunlight reaches façades, apertures, and outdoor spaces. This is particularly relevant in dense urban contexts and at higher latitudes, where low solar altitude increases the effect of mutual shading between buildings (Czachura, 2023).

Czachura (2023) argues that solar access is often assessed at late stages of building design, when changes to the urban configuration are already limited. Assessment at the urban planning stage is therefore important, as building spacing, orientation, massing, and the relationship between neighbouring buildings can still be modified. Solar access metrics can support the evaluation of direct sunlight availability before detailed architectural decisions are fixed.

Czachura (2023) reviewed existing solar access metrics, organised them into a taxonomy, and analysed their relationship with urban density. One of the identified indicators was ASH_F, a façade-based variant of Annual Sunlight Hours. ASH_F represents the average availability of direct sunlight calculated for points on the façade, expressed in relation to all annual sun vectors. In this approach, the façade is used as a simplified assessment surface for estimating sunlighting conditions related to potential access through apertures, without detailed modelling of the interior space.

This distinction is relevant to the present study. Urban-scale metrics describe the effect of built form on direct sunlight availability, but they do not describe the interaction between direct sunlight and an individual aperture. They can indicate the general solar access potential of a façade or area, but they do not directly account for aperture size, aperture shape, reveal depth, frame geometry, partial shading across the aperture, or angle of incidence. This creates a methodological gap between urban-scale solar access assessment and aperture-level sunlight evaluation.

Aperture-based metrics, such as SBI and SBI-airmass, address this gap by linking direct sunlight access to the geometry of a specific opening. Unlike façade-based indicators, they describe the amount of direct sunlight passing through the aperture over time. This allows the effect of aperture geometry and external obstruction to be assessed at the scale relevant to building design.

1.3.6 Limitations of existing sunlight access metrics

The reviewed methods describe different aspects of direct sunlight access. EN 17037 sunlight exposure provides a compliance-oriented assessment based on required exposure duration. ASE identifies the risk of excessive indoor exposure. ASH describes annual sunlight availability. However, none of these methods fully describes the geometric interaction between direct sunlight, the aperture, and the surrounding built form.

The limitations of existing methods can be grouped into four main categories. First, some methods are point-based, meaning that the result depends on a selected assessment point rather than on the entire aperture area. Second, several methods are threshold-based, indicating whether a defined condition is met without describing continuous variation in sunlight access. Third, some methods are restricted to a selected day or period and therefore do not capture annual or seasonal variability. Fourth, existing metrics often do not account for aperture area, angle of incidence, number of apertures, aperture orientation, or partial shading caused by reveals, frames, balconies, or neighbouring buildings.

These limitations are particularly relevant in early-stage design. At this stage, decisions concerning building massing, orientation, aperture placement, and the relationship with surrounding buildings are made before the interior layout is fully defined. Metrics that depend on room configuration or internal sensor grids may therefore be difficult to apply. A method is needed that can assess direct sunlight access without detailed interior modelling, while remaining sensitive to aperture geometry and external obstruction.

1.3.7 Aperture-based sunlight assessment: SBI and SBI-airmass

The aperture-based approach addresses several limitations of point-based, threshold-based, and time-based sunlight metrics. In this approach, the aperture is treated as the primary unit of analysis. Direct sunlight access is assessed through the geometry of the sunlight beam passing through the opening, rather than through a single reference point or an internal sensor grid. The main metric developed within this approach is the Sunlight Beam Index (SBI).

1.3.7.1 Sunlight Beam Index (SBI)

The SBI is a metric that quantifies the potential for direct sunlight passing through apertures. This approach is based on an analysis of the cross-section of the sunlight beam passing through the aperture and entering the interior space (Mardaljevic and Roy, 2016).

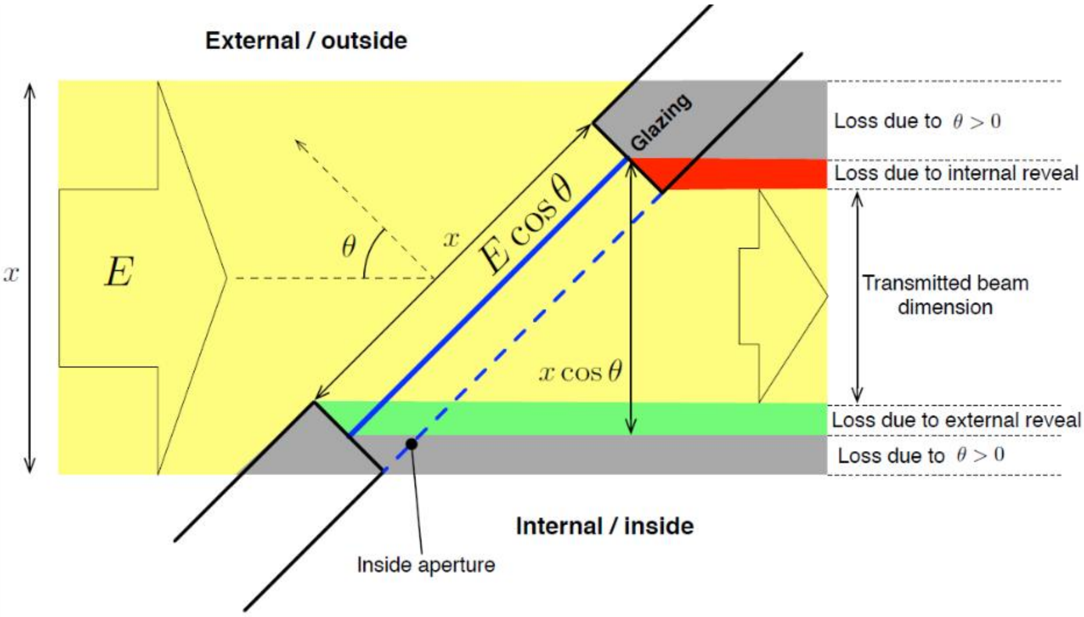

Figure 4 Conceptual sectional diagram of the Sunlight Beam Index (SBI), illustrating the reduction of the effective beam cross-section due to angle of incidence and geometric obstructions at the aperture. Exterior refers to the incoming solar-beam side, while interior refers to the room side after transmission through the aperture (source: Mardaljevic and Roy, 2016).

The conceptual basis of SBI is illustrated in Figure 4. The effective area of the transmitted beam is not constant but depends on the angle of incidence of solar rays. As the angle between the incoming solar ray and the normal to the aperture increases, the projected cross-sectional area of the beam decreases proportionally. This relationship introduces a directional dependency, linking solar access directly to orientation and solar geometry (Mardaljevic and Roy, 2016).

In addition to angular effects, the transmitted beam is further reduced by geometric constraints at the aperture. Internal and external reveals, glazing thickness, and surrounding obstructions limit the portion of the beam that can pass through the opening. As shown in Figure 4, these factors reduce the effective beam dimension before it enters the interior space, meaning that SBI captures not only solar position but also the impact of architectural detailing and urban context (Mardaljevic and Roy, 2016).

This formulation allows SBI to represent sunlight access as a geometric interaction between solar rays and built form. Unlike interior-based metrics, it does not depend on room configuration or sensor placement but instead reflects how aperture design and external obstruction influence the availability of direct sunlight.

The metric is evaluated for all time steps in which direct sunlight is present and can be aggregated over time. This enables SBI to capture seasonal and diurnal variations in solar exposure while maintaining a direct relationship between geometric input and resulting values (Mardaljevic and Roy, 2016).

As a result, SBI provides a consistent approach for analysing how changes in aperture geometry, orientation, and surrounding context affect access to direct sunlight.

Compared with EN 17037 sunlight exposure and ASH, SBI is not limited to identifying whether direct sunlight is available for a given duration. It quantifies the effective beam area passing through the aperture over time. Cases with the same exposure duration may therefore produce different SBI values if they differ in aperture area, angle of incidence, reveal depth, or partial obstruction. This makes SBI directly relevant to the geometric parameters examined in this study.

1.3.7.2 SBI – airmass

SBI-airmass extends the SBI formulation by introducing an atmospheric correction. The purpose of this modification is to reduce the contribution of low-altitude sun positions, where the sunlight beam travels through a longer atmospheric path before reaching the aperture.

SBI – airmass is an extension of the SBI metric, modified to include the influence of the atmosphere. The introduction of this variant was motivated by the need to represent solar ray propagation, which is weakened as it passes through the Earth's atmosphere (Mardaljevic and Brembilla, 2021).

The quantity of the sunrays reaching the aperture is not constant; their intensity depends on the distance the beam travels through the atmosphere. This phenomenon is described by the airmass factor, which determines the relative thickness of the atmosphere through which the sunbeams pass (Mardaljevic and Brembilla, 2021; Liu, Brembilla and Rafiee, 2026).

Consequently, a modification has been introduced to the SBI index by adding an airmass-dependent attenuation factor, namely SBI-airmass. In this form, the metric accounts for both the aperture geometry and shading conditions (Mardaljevic and Roy, 2016), as well as the reduction of sunlight resulting from atmospheric conditions, particularly for low angles of incidence. The result is a reduction in the influence of rays at low solar elevations, which might otherwise be overestimated in the SBI.

SBI-airmass preserves the aperture-based structure of SBI while modifying the weighting of different sun positions. This is relevant in annual analyses, where low solar elevations can contribute substantially to exposure duration but may not represent the same effective sunlight contribution as higher sun positions. In this study, SBI and SBI-airmass are analysed together to evaluate how the airmass correction changes the interpretation of aperture-based sunlight access.

1.3.8 Research gap and scope of the present study

Existing methods for assessing sunlight access provide useful but partial information. EN 17037 sunlight exposure assesses compliance with required exposure duration, ASE identifies the risk of excessive indoor exposure, and ASH describes annual sunlight availability. However, these methods do not fully describe how direct sunlight passes through an aperture as a geometric surface, or how the result changes with aperture size, shape, orientation, reveal depth, and external obstruction.

SBI and SBI-airmass provide a continuous and geometry-based approach to sunlight access assessment. However, their relationship with established metrics has not yet been systematically examined within the controlled geometric and urban-context comparison developed in this thesis. In particular, there is limited evidence on how these metrics respond to controlled changes in aperture geometry and how they perform in real-case urban models.

This study addresses this gap by comparing SBI and SBI-airmass with EN 17037 sunlight exposure, ASH, and ASE. The analysis is based on a controlled shoebox model and a set of existing multi-family residential models in urban contexts. This enables an assessment of whether aperture-based metrics provide additional information relevant to early design decisions and to the evaluation of sunlight access in dense residential developments.

2 Methods

2.1 Research workflow

An overview of the research workflow, covering the stages from the preparation of computational tools to the analysis of results, is presented in Figure 5.

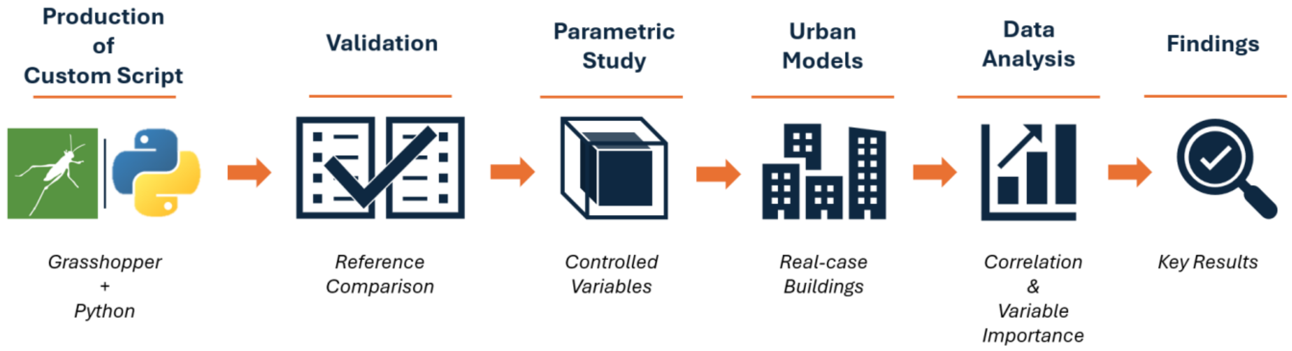

Figure 5 Simplified thesis workflow of methods.

2.2 Custom script

The custom script was developed to calculate sunlight access from aperture geometry, solar position, and external obstruction. The script consists of linked Grasshopper Python components that first test whether direct solar rays reach the aperture, then calculate the sunlit aperture area for each timestep, and finally produce annual SBI and SBI-airmass values. Figure 6 summarises and simplifies the overall structure of the script, including the main input data, the aperture-based calculation sequence, and the parallel extraction for EN17037 sunlight exposure and ASH.

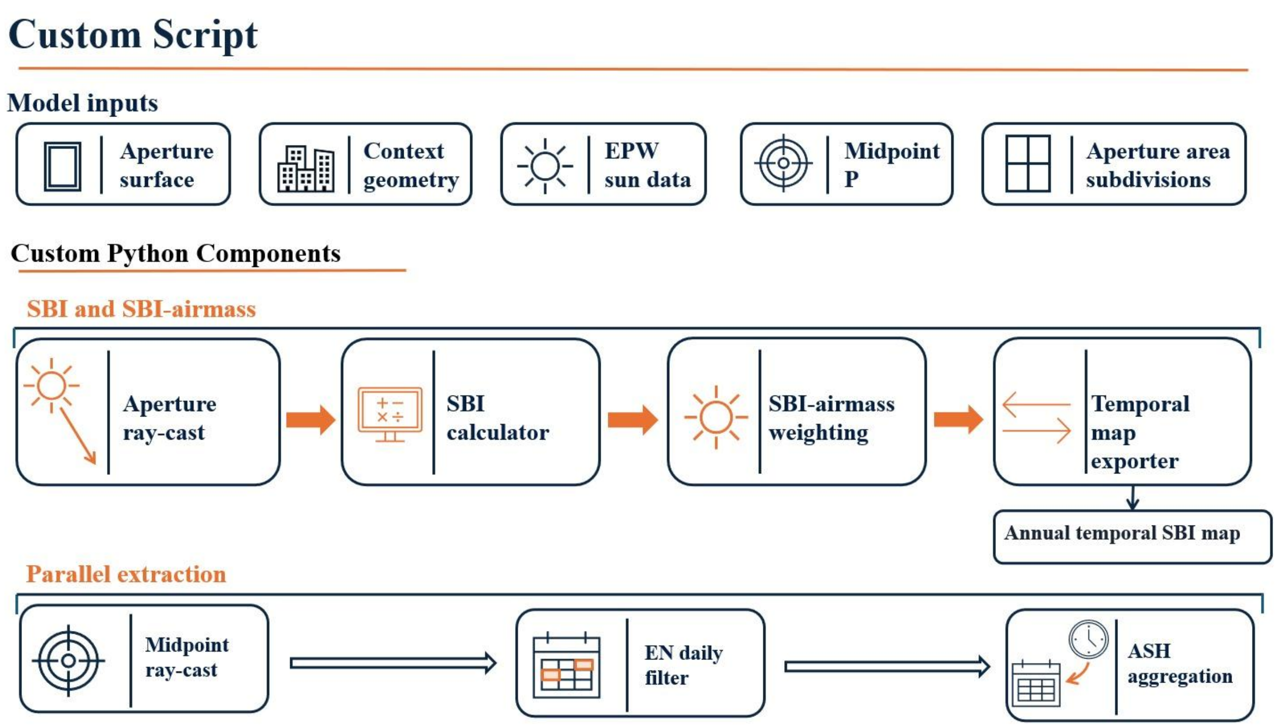

Figure 6 Workflow of the custom Grasshopper Python script used to calculate aperture-based and point-based sunlight access indicators.

The calculation begins with point-based sampling of the aperture surface. Each aperture is divided into a 3 × 3 grid, producing nine equal subsurfaces. One evaluation point is placed at the centre of each subsurface, and each point represents the area weight of its assigned subsurface. For each timestep, a ray is cast from every evaluation point towards the sun direction. If the ray is not blocked by surrounding geometry, the corresponding area weight is counted as sunlit. The sum of these weights gives the sunlit aperture area for that timestep.

A separate midpoint-based component was used for EN 17037 sunlight exposure and ASH evaluation. This component tests sunlight visibility at a single reference point and records a Boolean result for each timestep. The output is then filtered by date range and converted into daily sunlight hours. This allows the point-based results to be compared with the area-based SBI results.

SBI and SBI-airmass were calculated from the timestep sunlit aperture area. SBI uses the sunlit aperture area, the cosine of the solar incidence angle, and the timestep duration. SBI-airmass applies an additional airmass correction based on solar altitude. This reduces the contribution of low-elevation sunlight without changing the geometric basis of SBI.

The final component reconstructs the timestep results into a continuous annual sequence. This produces daily data structures and full-year arrays for temporal mapping. The annual SBI and SBI-airmass totals can then be interpreted together with their seasonal and hourly distribution. The detailed description of the individual script components is provided in Appendix A.

2.3 Validation of the script

The original SBI formulation by Mardaljevic and Roy (2016) was used as the basis for validation. An identical geometric configuration was reconstructed, and SBI was evaluated using the developed script under the same orientation conditions. The reference definition of SBI provided in the original study was treated as the ground truth.

The reference cases followed orientation-dependent evaluations at London latitude, with identical geometric configurations. Solar input was derived from a London EPW file, replacing the analytical sun path used in the original work. The evaluation used 15-minute timesteps, corresponding to a temporal resolution of four timesteps per hour.

The validation assessed percent differences in SBI and SBI-airmass calculated with the custom script and the original work by Mardaljevic and Roy (2016).

2.4 Parametric and urban model studies

The simulations included two levels of geometric modelling: a reference ‘shoebox’ model used for an initial parametric study and real-case models in an urban context.

2.4.1 Parametric study

2.4.1.1 ’Shoebox’ reference model

The analysis was based on a simplified ‘shoebox’ reference model (Figure 7), commonly used in sunlight and solar access studies to enable controlled parametric analysis.

The model represented a single room with fixed geometry (4.0 m × 4.0 m × 2.5 m), in which one of the external walls contained the analysed aperture. The purpose of using this model was not to represent a specific building, but to isolate and evaluate the influence of individual geometric parameters on sunlight access under controlled conditions.

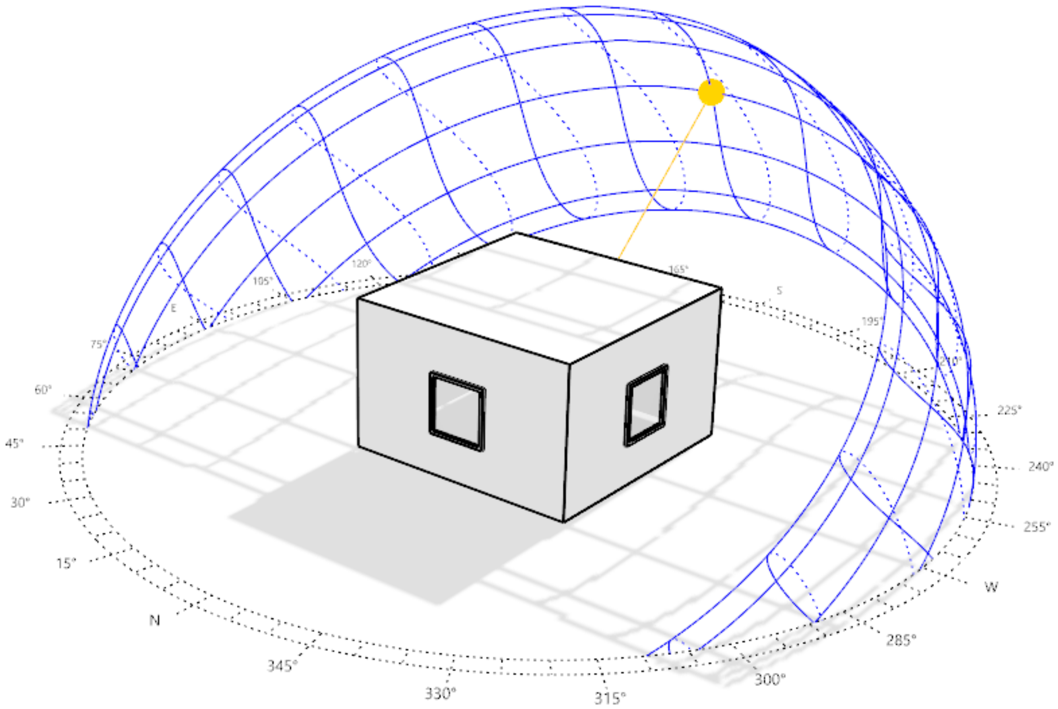

Figure 7 'Shoebox' reference model.

All variables not directly related to the analysis were kept constant, including the room geometry, the sill height (0.8 m), and the window frame thickness (0.05 m). The aperture was positioned centrally within the wall, equidistant from the left and right edges. This allowed changes in the results to be attributed to modifications of aperture-related parameters, such as orientation, area, depth of embedding, or the presence of shading elements.

The base geometry of the shoebox model was created in Rhinoceros 3D, where the room envelope was defined by floor and wall surfaces forming the spatial boundary. Apertures were modelled as planar sub-surfaces within the façade.

The geometry was referenced in Grasshopper, where parametric operations and simulation procedures were implemented. The aperture geometry functioned as the primary variable element, enabling systematic modification across simulation cases.

For each aperture, a set of evaluation points was generated across its surface. These points were used for the calculation of SBI and SBI-airmass, allowing the metrics to respond to spatial variation within the aperture. For EN 17037 sunlight exposure and ASH, a single central point of the aperture was used as the evaluation location.

The ASE index was calculated using a grid of points distributed across the working surface inside the room. For each point, the number of hours per year during which the intensity of direct solar radiation exceeded the specified threshold, as defined by the index, was analysed (Table 1).

Table 1 Input parameters for ASE calculations.

ClimateStudio ASE input	Value / setting
Interior surface material	Wall LM83
Material type	Matte
Reflectance	50.00%
Diffuse	50.00%
RGB reflectance	R 0.500, G 0.500, B 0.500
Glazing material	Optigray
Visible light transmittance (VLT)	63.00%
Visible light reflectance (VLR)	6.00% / 6.00%
Weather file	GBR_ENG_London.City.AP.037683_TMYx.2004-2018
Sensor grid spacing	0.50 m
Sensor grid inset from room boundary	0.35 m
Workplane height	0.80 m

Sunlight access was evaluated using a custom Python component implemented in Grasshopper. Sun position vectors generated with Ladybug Tools were combined with aperture evaluation points and surrounding geometry. For each timestep, rays were cast towards the sun direction, and intersections with geometry were tested to determine whether direct sunlight reached the aperture.

Within this workflow, Rhinoceros 3D defined the fixed geometric configuration of the model, while Grasshopper managed parametric variation and performed sunlight evaluation.

2.4.1.2 Independent, dependent and controlled variables based on 'shoebox'

2.4.1.2.1 Independent variables

The independent variables were defined as follows:

- Aperture orientation, defined by a vector normal to the window plane (case ID: S 1.1 – S 1.16),
- Aperture size, i.e. the active area of the window opening (S 2.1 – S 2.4),
- Proportions and shape of the aperture, i.e. comparison of different geometries while maintaining the same or very similar area (S 3.1 – S 3.3, S 4.1 – S 4.3),
- Depth of the window recess (aperture setback), affecting the degree of window shading (S 5.1 – 5.4),
- Aperture inclination, deviation of the window plane from the vertical (S 6.1 – S 6.3),
- The presence and geometry of shading elements, such as eaves (S 7.1 – S 7.4).
- The external context, i.e. the surrounding neighbouring buildings that shade the aperture (S 8.1 – S 8.3). Four obstruction scenarios were tested: the Reference Case, without external obstruction, 7.50 m Obstruction, 15.00 m Obstruction, and 30.00 m Obstruction across a 15.00 m street canyon,
- Two apertures with different orientations: S + S, S + E, S + W and S + S (S 9.1 – S 9.4),
- Climate data represented by Typical Meteorological Year (TMYx) EPW files specific to the analysed location [GU14.1].

These variables were analysed parametrically within a structured series of simulations (Table 2), allowing their impact on the analysed indicators to be observed in an isolated and comparable manner.

2.4.1.2.2 Dependent variables

The following dependent variables were analysed in the study:

- Sunlight Beam Index (SBI),
- Sunlight Beam Index – airmass (SBI-airmass),
- Sunlight access assessment result in accordance with EN 17037 sunlight exposure,
- Annual Sunlight Exposure (ASE 1000,250),
- Annual Sunlight Hours (ASH) as an auxiliary indicator.

The values of these variables were analysed in both absolute and comparative terms, with emphasis on differences in the response of individual indicators to identical geometric changes.

2.4.1.2.3 Controlled variables

The controlled variables included:

- The height of the windowsill, set at 0.80 m,
- The height of the opening axis relative to the ground, set at 3.00 m,
- The width of the window frame, set at a geometric value of 0.05 m
- The geometry and dimensions of the "shoebox" test room, which did not change in the simulations,
- The material parameters of the partition and glazing, including light transmission,
- The calculation parameters of the simulation, such as the time range and scope of analysis.

By excluding these parameters from the range of variability, the analysis was focused exclusively on the relationship between aperture geometry, its spatial context, and the resulting direct sunlight access indicators.

Table 2 Input parameters of analysed cases.

Case ID	Aperture width (m)	Aperture height (m)	Aperture area (m^2)	Orientation	Number of apertures	Aperture setback (m)	External obstruction (Y/N)
S 1.1	1.0	1.0	1.0	N	1.0	0.0	N
S 1.2	1.0	1.0	1.0	NE	1.0	0.0	N
S 1.3	1.0	1.0	1.0	E	1.0	0.0	N
S 1.4	1.0	1.0	1.0	SE	1.0	0.0	N
S 1.5	1.0	1.0	1.0	S	1.0	0.0	N
S 1.6	1.0	1.0	1.0	SW	1.0	0.0	N
S 1.7	1.0	1.0	1.0	W	1.0	0.0	N
S 1.8	1.0	1.0	1.0	NW	1.0	0.0	N
S 1.9	1.0	1.0	1.0	N	1.0	0.2	N
S 1.10	1.0	1.0	1.0	NE	1.0	0.2	N
S 1.11	1.0	1.0	1.0	E	1.0	0.2	N
S 1.12	1.0	1.0	1.0	SE	1.0	0.2	N
S 1.13	1.0	1.0	1.0	S	1.0	0.2	N
S 1.14	1.0	1.0	1.0	SW	1.0	0.2	N
S 1.15	1.0	1.0	1.0	W	1.0	0.2	N
S 1.16	1.0	1.0	1.0	NW	1.0	0.2	N
S 2.1	1.0	1.0	1.0	S	1.0	0.0	N
S 2.2	2.0	1.0	2.0	S	1.0	0.0	N
S 2.3	3.0	1.0	3.0	S	1.0	0.0	N
S 2.4	2.0	2.0	4.0	S	1.0	0.0	N
S 3.1	1.2	1.5	1.8	S	1.0	0.0	N
S 3.2	1.8	1.0	1.8	S	1.0	0.0	N
S 3.3	2.0	0.9	1.8	S	1.0	0.0	N
S 4.1	Triangle		~1.0	S	1.0	0.0	N
S 4.2	Hexagon		~1.0	S	1.0	0.0	N
S 4.3	Circle		~1.0	S	1.0	0.0	N
S 5.0	1.0	1.0	1.0	S	1.0	0.0	N
S 5.1	1.0	1.0	1.0	S	1.0	0.2	N
S 5.2	1.0	1.0	1.0	S	1.0	0.3	N
S 5.3	1.0	1.0	1.0	S	1.0	0.4	N
S 6.1	1.0	1.0	1.0	S	1.0	0.0	N
S 6.2	1.0	1.0	1.0	S	1.0	0.0	N
S 6.3	1.0	1.0	1.0	S	1.0	0.0	N
S 7.1	1.0	1.0	1.0	S	1.0	0.0	Y
S 7.2	1.0	1.0	1.0	S	1.0	0.0	Y
S 7.3	1.0	1.0	1.0	S	1.0	0.0	Y
S 7.4	1.0	1.0	1.0	S	1.0	0.0	Y
S 8.1	1.0	1.0	1.0	S	1.0	0.0	Y
S 8.2	1.0	1.0	1.0	S	1.0	0.0	Y
S 8.3	1.0	1.0	1.0	S	1.0	0.0	Y
S 9.1	1.0	1.0	2.0	S+N	2.0	0.0	N
S 9.2	1.0	1.0	2.0	S+E	2.0	0.0	N
S 9.3	1.0	1.0	2.0	S+W	2.0	0.0	N
S 9.4	1.0	1.0	2.0	S+S	2.0	0.0	N

2.4.2 Real-case models with urban context

The analysis was extended from the shoebox model to a set of real-case models representing urban conditions. These models, provided by the project's main supervisor, represented typical residential developments with varying densities and spatial configurations (Figures 8–13, Table 3). The aerial reference images were based on Google Earth imagery accessed in May 2026.

Figure 8 Örebro - high-rise multi-apartment building.

Figure 9 Göteborg - large courtyard block.

Figure 10 Stockholm – multi-apartment building.

Figure 11 Stockholm – point tower.

Figure 12 Stockholm – postmodern block.

Figure 13 Stockholm - semi-closed courtyards.

Six building models, representing different building types, locations, and levels of urban density, were selected to evaluate the analysed metrics under varying spatial conditions. The models were originally developed as part of the Moderniserad dagsljusstandard project (Rogers et al., 2018) and were later revised and adapted by Jin et al. (2025). The models originated from three locations in Sweden: Stockholm, Göteborg, and Örebro. The inclusion of multiple locations made it possible to consider different climatic data and represent a range of building typologies, including high-rise, point, block and semi-closed multi-family developments.

For each case, the orientation of the apertures, building type, number of storeys and nature of the urban context were considered. A summary of the analysed models is presented in Table 3.

In contrast to the shoebox models, where parameters were systematically varied to generate controlled datasets, the urban models were treated as fixed inputs. No geometric or parametric changes were applied. The analysis consisted of extracting indicator responses from predefined conditions.

The same simulation workflow was applied as in the shoebox analysis. Geometry was processed within the existing Rhinoceros 3D–Grasshopper environment, and the SBI and SBI-airmass calculations were carried out using the same Python-based implementation. The calculation logic and timestep resolution remained unchanged.

Climate data were selected based on the location of each model. Weather files corresponding to each city were used so that solar conditions reflected the geographic context of each case.

Within this setup, the influence of the urban context was introduced exclusively through obstruction. Surrounding buildings affected the visibility of the sky and sun, which in turn modified the sunlit portion of the aperture at each timestep. No additional parameters or adjustments were introduced beyond this geometric condition.

The purpose of this stage was to observe how EN 17037 sunlight exposure, ASH, SBI and SBI-airmass responded under real obstruction patterns. This included conditions where sunlight was partially available across the aperture, varied over time, and was affected by multiple surrounding surfaces. These effects were not present in the shoebox models and therefore required separate evaluation. At this stage, ASE analysis was excluded, as it represents a different type of metric focused on excessive direct sunlight exposure. Furthermore, the varying internal layouts and partition wall configurations of the analysed buildings would have introduced inconsistencies, making direct comparison between cases less reliable.

The real-case models introduced spatial and temporal complexity that could not be represented under isolated conditions. Obstruction occurred from multiple directions, varied with solar position, and produced non-uniform exposure across the aperture surface.

Urban density was defined as an indicator describing the intensity of development in the surroundings of the analysed building. The urban density factor was calculated as the ratio of the total building volume to the area of the site under analysis.

The building volume was calculated using Rhinoceros 3D as the sum of the volumes of all buildings located within the site under analysis, within a 100-metre radius of the central point of the defined building:

$$Urban\ density = \frac{\sum V}{A_{site}}\ (\mathrm{m^3/m^2}) \qquad (1)$$

where:
V – refers to the volume of the building,
A_{site} – refers to the area of the site under analysis.

Table 3 Input parameters of analysed real-case models.

Case ID	Location	Building type	Urban density (m^3/m^2)	Floors	Aperture orientation
ID_5	Gothenburg	large courtyard block	3.02	3	S, E, N, W
ID_18	Stockholm	multi-apartment building	0.76	3	ENE, SSE, WSW, NNW
ID_29	Stockholm	point tower	3.96	6	S, E, N, W
ID_52	Stockholm	postmodern blocks	3.57	6	S, E, N, W
ID_60	Stockholm	semi-closed courtyard	2.57	4	SSE, SW, SSW, NW, NE, WSW
ID_75	Örebro	high-rise multi-apartment building	1.25	9	E, W

The analysis was carried out at two levels:

- *Single-aperture based* - where each opening was evaluated independently based on geometry and exposure conditions,
- *Room-based* - where results were aggregated for all apertures associated with the same interior space.

2.4.3 Simulation workflow

The simulation framework enabled controlled and comparable evaluation of sunlight access metrics under identical computational conditions, isolating their response to geometric variation. Two modelling contexts were employed: a parametric shoebox model with systematic variation of aperture geometry, orientation and shading, and three-dimensional models of existing urban environments analysed without modification.

Geometry was defined by apertures and surrounding obstructions, which determined solar access. Climate data were introduced through EPW files, enabling annual simulation with continuous evaluation of solar position at a fixed temporal resolution of four times per hour – 15.00-minute timesteps. All calculations were performed within a unified Python–Grasshopper environment.

The procedure was based on time-resolved sun vectors and ray casting from defined evaluation points. Each ray was tested against the surrounding geometry to determine obstruction at each timestep, producing a binary representation of solar access. For the EN 17037 sunlight exposure evaluation, a solar altitude cut-off angle of 7.50° was applied in accordance with the standard requirements.

From this shared basis, SBI and SBI-airmass were computed as continuous, weighted measures, while EN 17037 sunlight exposure and ASH were derived as time-based accumulations. ASE was evaluated using an illuminance threshold and exposure duration, based on the same time-resolved simulation data. This ensured comparison of the results and attributed observed differences solely to geometric variation.

2.5 Data analysis

The results of all simulations were exported to an external spreadsheet in a standardised format, allowing for further statistical and comparative analysis. The values for each geometric configuration were recorded for each analysed indicator, enabling direct comparison of the responses of individual assessment methods to the same input parameters.

The next step was data cleaning and export to CSV format, followed by import into a Jupyter Notebook environment running in Visual Studio Code, where analysis was carried out using Python-based calculation scripts.

The data analysis consisted of five components: correlation and cluster analysis, distribution analysis, relationship analysis, relative performance analysis, and predictive variable-importance analysis.
Correlation analysis was performed between all analysed metrics and geometric parameters. Pearson correlation coefficients (r) were calculated to evaluate the strength and direction of linear relationships between variables.

Pearson correlation analysis was selected because all analysed variables were continuous numerical variables and the study focused on identifying relationships between geometric parameters and simulation outcomes. Correlation coefficients range from −1 to +1, where values close to ±1 indicate strong positive or negative relationships, while values close to 0 indicate weak or no linear dependency (Schober et al., 2018).

The correlation coefficients were visualised using correlation matrices and hierarchically clustered correlation matrices, or clustermaps. In the clustermaps, hierarchical clustering was applied to group variables according to the similarity of their correlation patterns across the dataset. Variables joined by shorter branches in the dendrogram exhibit more similar correlation structures with the remaining analysed variables, while variables connected at greater distances show less similar patterns. The clustering was used to identify groups of metrics and parameters with comparable response behaviour. It was treated as an exploratory ordering method and was not interpreted as evidence of causality or equivalence between metrics.

The distribution of selected metrics was analysed using histograms and violin plots combined with kernel density estimation (KDE). To enable comparison between metrics expressed in different units, selected metrics were normalised relative to their maximum values. Distribution analysis was used to evaluate value ranges, variability, and data spread within the simulation dataset. The KDE curves provided a smoothed approximation of the data distribution, where peaks indicated the value ranges with the highest concentration of observations.

Relationships between variables were analysed using scatter plots. Extended visualisations, including bubble charts, were used to incorporate additional parameters, such as aperture area and urban density, through marker size and colour. Quadrant plots were additionally employed to classify cases according to selected compliance criteria and performance thresholds.

Bar plots were used to evaluate the influence of selected parameters, such as aperture area and urban density, on metric values. These error bar visualisations supported comparison of average values and identification of general trends. Radar plots were additionally applied to analyse variations in metric values across different orientations, enabling comparative assessment of directional performance.

Relative performance analysis was conducted to evaluate the response of the analysed metrics to geometric modifications. For comparative analyses, a reference case was defined and assigned a baseline value of 1.0. All remaining cases were calculated relative to this reference condition. The resulting deviations were visualised using bar plots, enabling comparison of the relative sensitivity of the analysed metrics to changes in geometric parameters.

Random Forest models were used as a supplementary analysis to rank the variables associated with EN 17037 sunlight exposure in the urban-context datasets. Separate models were applied to the single-aperture and room-based analyses, with EN 17037 sunlight exposure defined as the target variable. The predictors included SBI, SBI-airmass, ASH, urban density, and orientation, supplemented by aperture area in the single-aperture model and by total aperture area and number of apertures in the room-based model. The extracted feature-importance values were compared with the results of the correlation and relationship analyses.

This structured workflow enabled evaluation of relationships between geometry and simulation outcomes, as well as consistent comparison of different sunlight access metrics. The combination of statistical methods and graphical analysis supported the interpretation of the results and the identification of dependencies between variables.

2.5.1 CSV export component for SBI temporal map data

Timestep-organised SBI data were exported from a Grasshopper DataTree to a CSV file, where each branch represented a day and each column corresponded to a day in the temporal map (Figure 14). The inputs consisted of a DataTree (data) containing day-structured timestep values and a file path (path, string). The outputs included the resolved CSV path (csv_path), the number of rows (rows), and the number of columns (cols).

The input tree was validated to confirm that it was not empty and that the file path was defined as a non-empty string. The number of columns was obtained from data.BranchCount, where each branch represented one day in the temporal structure.

The number of rows was determined as the length of the first branch:

$$rows=len(data.Branch(0)) \quad (2)$$

This corresponded to the number of timesteps per day. A consistency check was performed to verify that all branches had identical length. Any mismatch resulted in the termination of execution.

The output directory was extracted from the file path. If the directory did not exist, it was created before writing the file.

The CSV file was written using Python's csv.writer. Data were written row-wise. For each timestep index i, values were extracted across all branches:

```
writer.writerow([data.Branch(j)[i] for j in range(cols)])
```

This produced a matrix with dimensions:
rows × cols

where rows represented intra-day timesteps and columns represented days across the annual sequence.

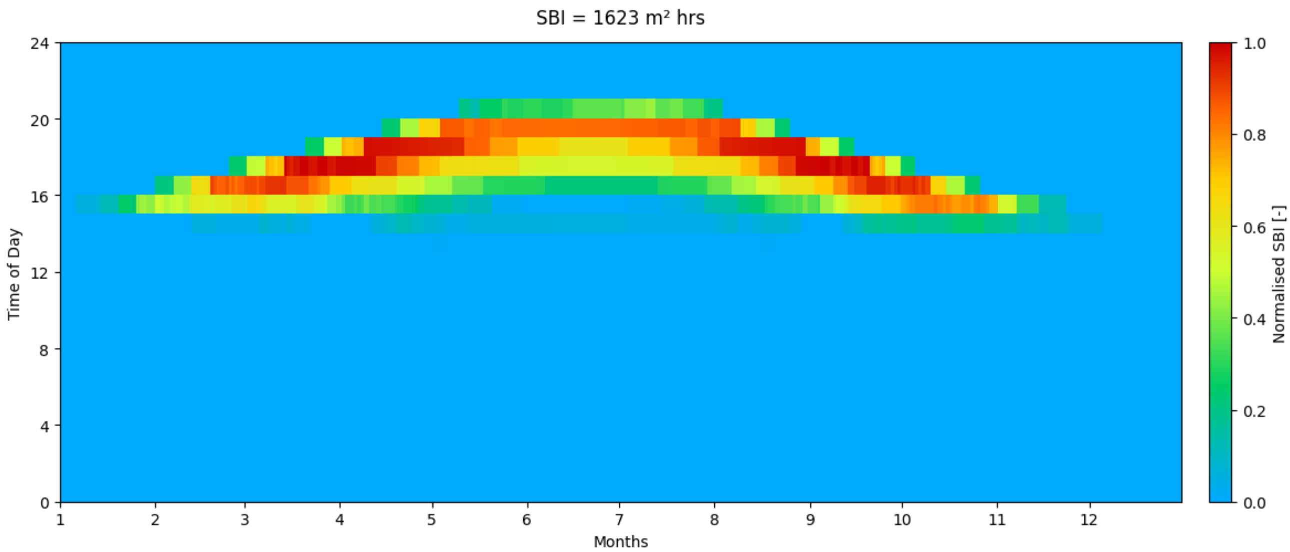

Figure 14 Example temporal map of normalised SBI values by months and time of day

3 Results

3.1 Script validation SBI and SBI-airmass

The custom script used to calculate the SBI and SBI-airmass metrics was verified prior to commencing the shoebox-based parametric analysis. The evaluation includes eight aperture orientations, with paired SBI values reported for each case (Table 4).

Table 4 Validation of SBI results against reference values.

Aperture orientation	SBI (m^2·hrs)		Absolute difference (%)
	J. Mardaljevic	Script	
N	204.00	220.17	7.93
NE	608.00	623.47	2.54
E	1 348.00	1 370.47	1.67
SE	1 826.00	1 845.04	1.04
S	1 927.00	1 947.38	1.06
SW	1 822.00	1 846.34	1.34
W	1 345.00	1 373.66	2.06
NW	604.00	625.26	3.52

The results were consistent for models without a window reveal. The reference SBI values range from 204 m^2·hrs (N) to 1 927 m^2·hrs (S), while the corresponding script outputs range from 220 m^2·hrs (N) to 1 947 m^2·hrs (S). The percentage differences between the two datasets range from 1.04% to 7.93%. The maximum deviation is observed for the north-facing orientation (7.93%), while the minimum deviation occurs for the south-east orientation (1.04%). For the remaining orientations, the differences lie between 1.06% and 3.52% (Table 4). The distribution of values as a function of orientation remained identical, with a maximum for south-facing directions and a minimum for north-facing ones.

3.2 Reference 'shoebox' model

The reference shoebox model was used to examine how individual geometric parameters affect the evaluated sunlight metrics under controlled conditions. The results are summarised in Table 5, which reports the full set of outputs for aperture orientation, aperture surface area, aperture aspect ratio, aperture geometry, aperture setback, shading elements, and aperture inclination.

The following subsections scrutinise the response of SBI, SBI-airmass, EN 17037 sunlight exposure, ASH, and ASE to each tested parameter. The table is used as the numerical basis for the section, and the figures are used to show the relative response of the metrics across the tested configurations.

Table 5 "Shoebox" reference model results.

Case ID	SBI (m²·hrs)	SBI-airmass (m²·hrs)	EN17037 (hrs)	ASH (hrs)	ASE (%)
S 1.1	220.17	32.28	0.00	837.25	0.00
S 1.2	623.47	169.61	3.50	1 310.75	0.00
S 1.3	1 370.47	469.49	6.00	2 222.75	0.00
S 1.4	1 845.04	750.54	8.50	3 148.00	14.30
S 1.5	1 947.38	853.84	12.00	3 621.00	16.30
S 1.6	1 846.34	750.59	8.50	3 147.50	14.30
S 1.7	1 372.66	469.55	6.00	2 235.50	8.20
S 1.8	625.26	169.65	3.50	1 310.25	0.00
S 1.9	107.39	12.04	0.00	288.50	0.00
S 1.10	500.66	119.05	2.00	860.50	0.00
S 1.11	1 219.06	386.91	5.00	1 777.75	0.00
S 1.12	1 593.90	623.48	7.25	2 541.00	10.70
S 1.13	1 593.12	667.77	8.50	2 908.00	11.20
S 1.14	1 596.63	624.55	7.25	2 541.50	11.20
S 1.15	1 221.86	387.6	5.00	1 782.50	6.10
S 1.16	502.74	119.31	2.00	862.50	0.00
S 2.1	1 947.38	853.84	12.00	3 621.00	16.30
S 2.2	3 894.76	1 707.68	12.00	3 621.00	32.10
S 2.3	5 842.14	2 561.51	12.00	3 621.00	51.00
S 2.4	7 789.52	3 415.35	12.00	3 621.00	64.80
S 3.1	3 505.28	1 536.91	12.00	3 621.00	18.70
S 3.2	3 505.28	1 536.91	12.00	3 621.00	18.70
S 3.3	3 505.28	1 536.91	12.00	3 621.00	18.70
S 4.1	1 947.38	853.84	12.00	3 621.00	8.70
S 4.2	1 947.38	853.84	12.00	3 621.00	16.80
S 4.3	1 947.93	854.08	12.00	3 621.00	0.00
S 5.0	1 947.38	853.84	12.00	3 621.00	16.30
S 5.1	1 593.12	667.77	8.50	2 908.00	11.20
S 5.2	1 345.45	550.83	7.50	2 315.25	10.70
S 5.3	1 118.73	437.69	6.25	1 770.00	8.20
S 6.1	2 314.86	1 078.42	12.00	3 767.25	23.50
S 6.2	2 535.91	1 233.65	12.00	3 870.75	26.80
S 6.3	2 592.85	1 307.45	12.00	3 979.00	27.30
S 7.1	1 798.30	743.36	12.00	3 621.00	13.80
S 7.2	1 698.79	679.35	12.00	3 323.25	11.70
S 7.3	1 591.69	609.48	12.00	3 010.25	11.20
S 7.4	1 498.44	551.38	12.00	2 843.25	11.20
S 8.1	1 802.61	841.86	12.00	3 393.50	15.80
S 8.2	1 134.17	635.44	12.00	2 563.75	7.10
S 8.3	708.79	379.74	5.50	1 877.00	3.10
S 9.1	2 167.55	886.11	12.00	4 458.25	16.30
S 9.2	3 317.85	1 323.33	12.00	5 843.75	16.30
S 9.3	3 320.04	1 323.39	12.00	5 856.50	29.10
S 9.4	3 894.76	1 707.68	12.00	7 242.00	33.70

3.2.1 Impact of aperture orientation

All metrics vary with aperture orientation (Figure 15, Tables 2 and 5). The analysis includes eight orientations without reveal and the same eight orientations with a 0.20 m reveal depth. Values increase from the north-facing orientation towards the south-facing orientation and decrease again towards the west and northwest.

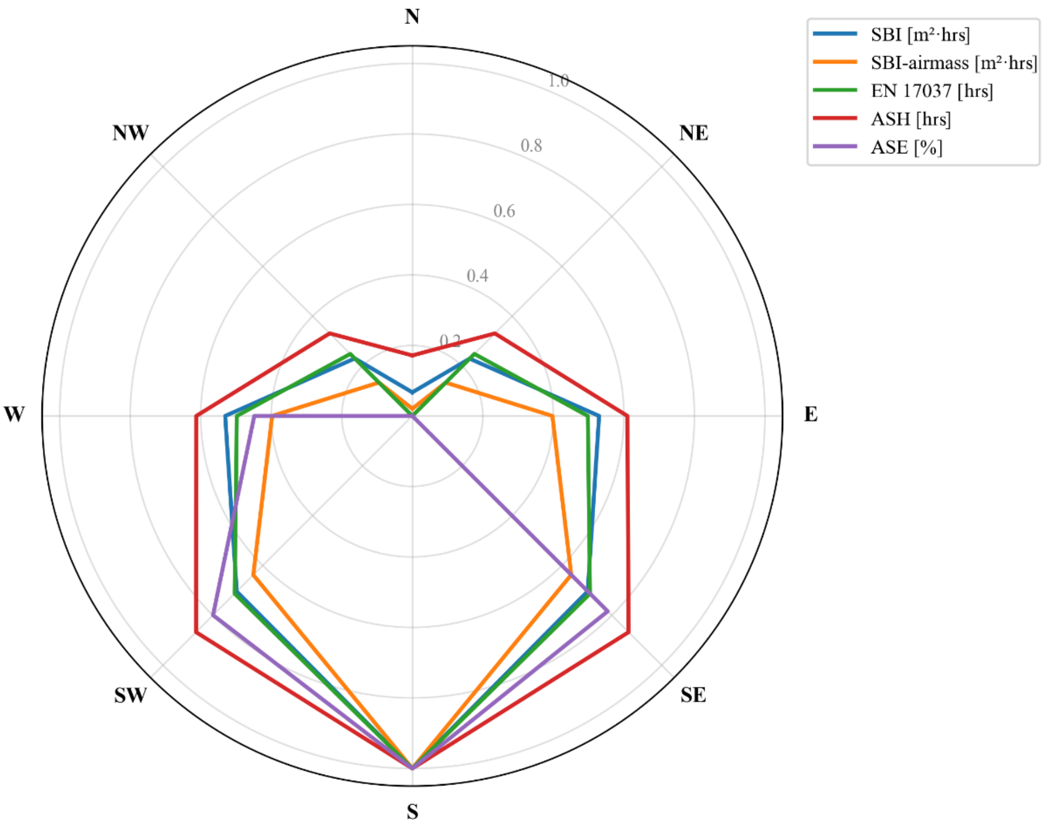

Figure 15 Radar chart of aperture orientation effects across SBI, SBI-airmass, EN 17037 sunlight exposure, ASH, and ASE.

SBI and SBI-airmass follow the same directional pattern. Values increase from N through NE and E, reach a maximum at S, and decrease through SW and W towards NW. SE and SW produce similar values, while N represents the minimum across both metrics.

EN 17037 sunlight exposure and ASH follow a comparable progression. Values increase from N to S, with intermediate orientations forming a stepwise transition. Maximum values occur at S, while reduced values are observed towards N, E and W orientations produce similar values within each metric.

ASE is limited to a subset of orientations. Non-zero values are observed between SE and W, with a maximum at S, N, NE, and NW do not register any ASE values. This pattern reflects the threshold-based definition of ASE, where orientations below the annual direct-sunlight exceedance threshold are recorded as 0, and the London weather file appears to produce stronger qualifying exposure towards the western orientations than the eastern orientations.

Across all metrics, S corresponds expectedly to the maximum solar access and N to the minimum, with intermediate orientations defining the transition between these extremes under the climatic conditions represented by the London weather file.

3.2.2 Impact of aperture surface area

All metrics are evaluated across four aperture sizes (1.00 m² to 4.00 m²), using direct values obtained from the simulations (Figure 16, Tables 2 and 5). SBI and SBI-airmass vary proportionally with aperture area, ASE increases progressively, and EN 17037 sunlight exposure and ASH remain unchanged across the tested range.

SBI increases from 1 947.38 to 7 789.52 m²·hrs across the tested range, while SBI-airmass increases from 853.84 to 3 415.35 m²·hrs. The increments between successive area steps are uniform for both metrics, with equal differences observed between each configuration.

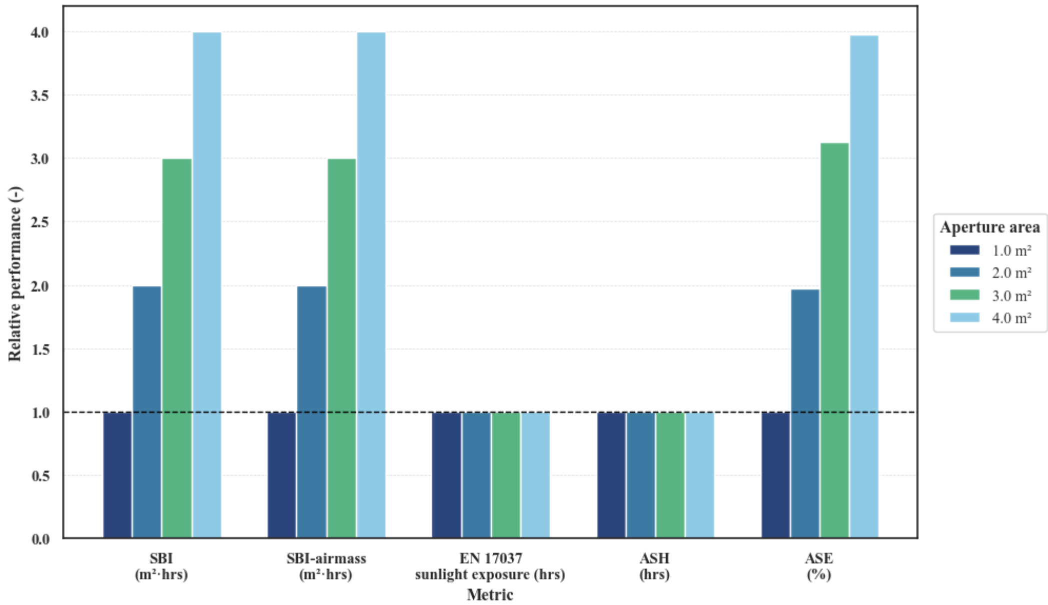

Figure 16 Relative performance chart – Impact of aperture area on sunlight access metrics.

The graphical representation compares the relative change in each metric across the four tested aperture areas: 1.00 m², 2.00 m², 3.00 m², and 4.00 m². SBI and SBI-airmass show an approximately proportional response to aperture area, increasing from the 1.00 m² case to 4.00 m² case at the largest aperture size.

EN 17037 sunlight exposure remain constant at 12.00 hours for all aperture sizes. ASH also remains constant at 3 621.00 hours across the full range.

ASE, which is the only indoor metric in this study, and which is based on a weather file, increases from 5.92 to 23.69, with intermediate values of 11.85 and 17.77. The increase is stepwise across all steps, with slightly smaller increments between the higher area configurations.

3.2.3 Impact of aperture proportions and geometry

Under the same aperture area conditions, none of the evaluated metrics vary with aperture aspect ratio, defined here as the width-to-height ratio of the aperture. Four aperture configurations were tested: one reference case with dimensions of 1.00 × 1.00 m and three additional configurations with different aperture aspect ratios: 1.20 × 1.50, 1.80 × 1.00 and 2.00 × 0.90. Identical values are observed across all configurations in aspect ratio for SBI, SBI-airmass, EN 17037 sunlight exposure, ASH, and ASE (Figure 17, Tables 2 and 5). Across all aspect ratio cases, SBI remains at 3 505.28 m²·h, SBI-airmass remains at 1 536.91 m²·h, EN 17037 sunlight exposure remains at 12.00 h, ASH remains at 3 621.00 h, and ASE remains at 18.70%.

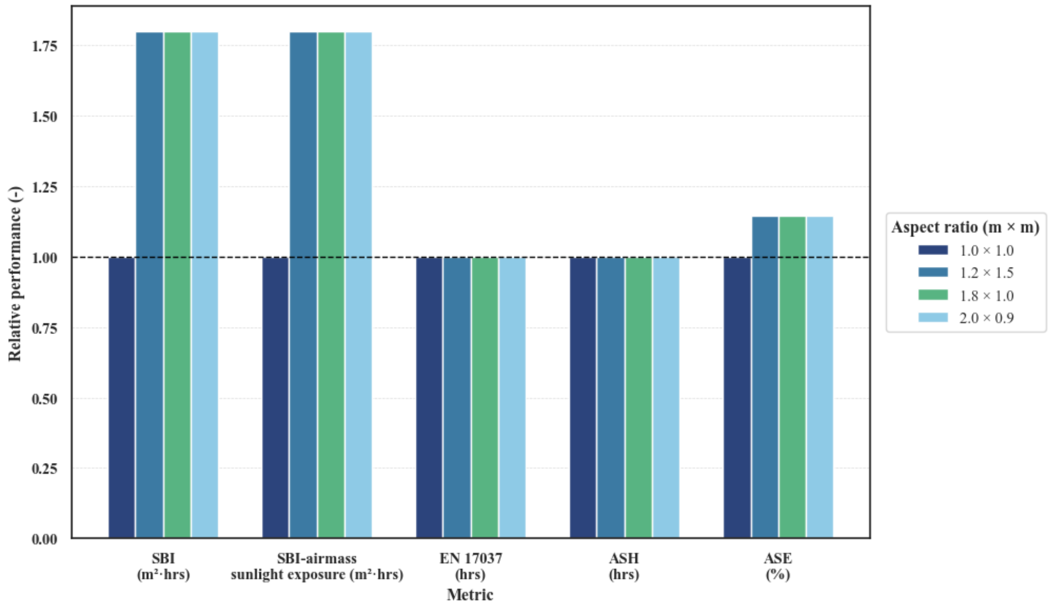

Figure 17 Relative performance chart – Impact of aperture aspect ratio on sunlight access metrics.

Across all tested shapes with the same aperture area conditions (Figure 17), SBI, SBI-airmass, EN 17037 sunlight exposure and ASH remain nearly unchanged, with almost identical values recorded for square, triangular, hexagonal, and circular apertures. For the triangular and hexagonal apertures, SBI records 1 947.38 m²·h and SBI-airmass records 853.84 m²·h. The circular aperture records a slightly higher SBI of 1 947.93 m²·h and an SBI-airmass value of 854.08 m²·h. EN 17037 sunlight exposure remains at 12.00 h and ASH remains at 3 621.00 h across all tested shapes. This is reflected in the graphical representation, where no separation between configurations is visible for SBI, SBI-airmass, EN 17037 sunlight exposure, and ASH (Figures 18 and 19, Tables 2 and 5).

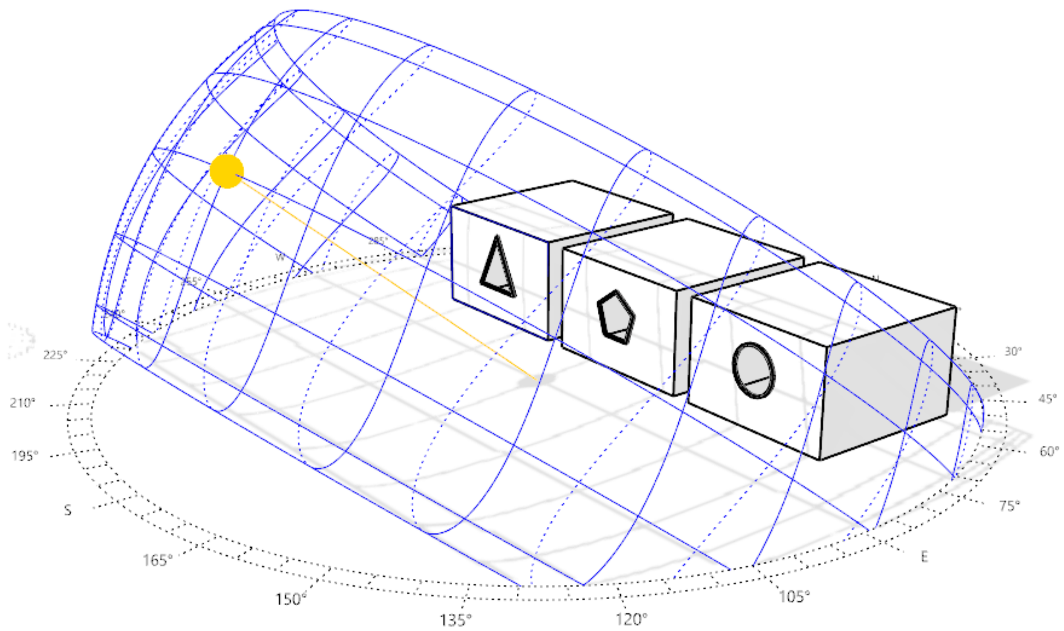

Figure 18 Aperture shape variations shown against the annual sun-path diagram for the London weather file.

ASE varies across shapes, with lower values for the triangular case, a higher value for the hexagonal case, and a value of zero for the circular case. ASE records 8.70% for the triangular aperture, 16.80% for the hexagonal aperture, and 0.00% for the circular aperture. This variation is visible in the graphs as distinct separation between geometric configurations.

This indicates that most metrics depend on total aperture area rather than its distribution, while ASE remains sensitive to geometric configuration.

EN 17037 sunlight exposure and ASH also remain unchanged across all geometric configurations, with identical values reported in Table 2 and overlapping values in the graphs.

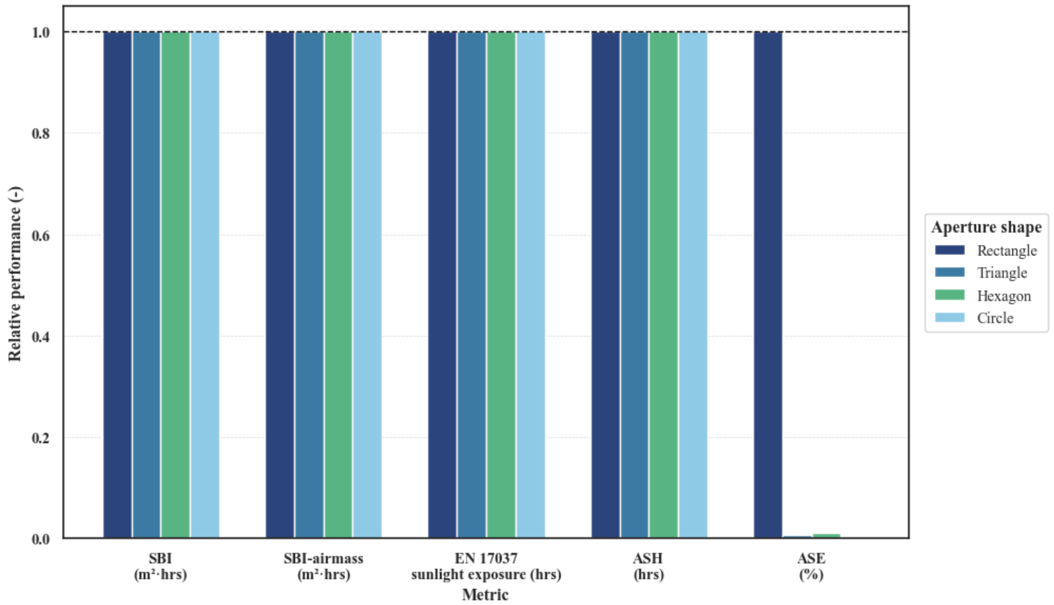

Figure 19 Relative performance chart – Comparison of metrics across different aperture shapes.

3.2.4 Impact of aperture setback

Aperture setback is evaluated at four depths (0.00 m, 0.20 m, 0.30 m, and 0.40 m) (Figures 20 and 21, Tables 2 and 5), with all metrics reported relative to the reference case configuration.

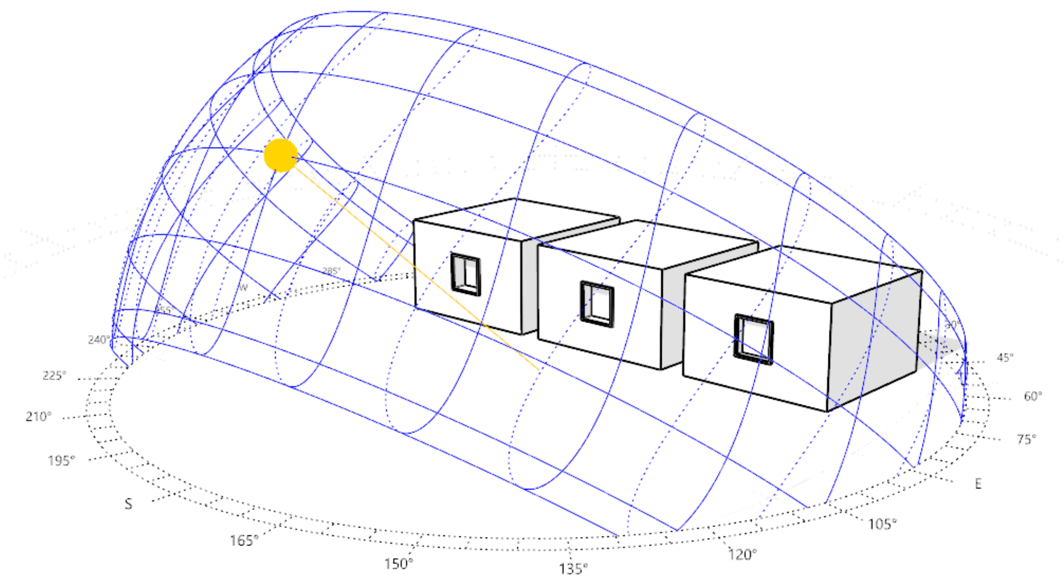

Figure 20 Aperture setback variations shown against the annual sun-path diagram for the London weather file. From right: 0.20 m, 0.30 m, and 0.40 m setback depth.

SBI decreases from 1 947.38 at 0.00 m to 1 118.73 m²·hrs at 0.40 m, with intermediate values of 1 593.12 at 0.20 m and 1 345.45 at 0.30 m, showing a stepwise reduction at each increase in setback.

SBI-airmass follows a similar pattern, decreasing from 853.84 to 437.69 m²·hrs, with intermediate values of 667.77 and 550.83, maintaining a consistent decline across all steps.

EN 17037 sunlight exposure decrease from 12.00 to 6.25 hours, with intermediate values of 8.50 and 7.50, indicating a continuous reduction in sunlight exposure as setback increases.

ASH decreases from 3 621.00 to 1 770.00 hours, with intermediate values of 2 908.00 and 2 315.25, following the same stepwise reduction pattern observed in the other metrics.

ASE decreases from 5.92 to 2.64, with intermediate values of 5.02 and 2.98, showing a monotonic decline across all setback conditions.

The relative values indicate a consistent reduction across all metrics, with values at 0.40 m ranging between 0.49 and 0.57 of the baseline condition.

At a setback of 0.20 m, the relative values range from 0.69 to 0.82, while at 0.30 m they range from 0.62 to 0.69, indicating reduction with each increase in depth.

At the maximum tested setback of 0.40 m, ASH reaches the lowest relative value (0.49), while SBI retains the highest relative value (0.57) among the evaluated metrics.

Across all metrics, the reduction remains monotonic but stepwise rather than linear with increasing setback, and the decrease in values is consistently visible across all configurations in the graphical representation.

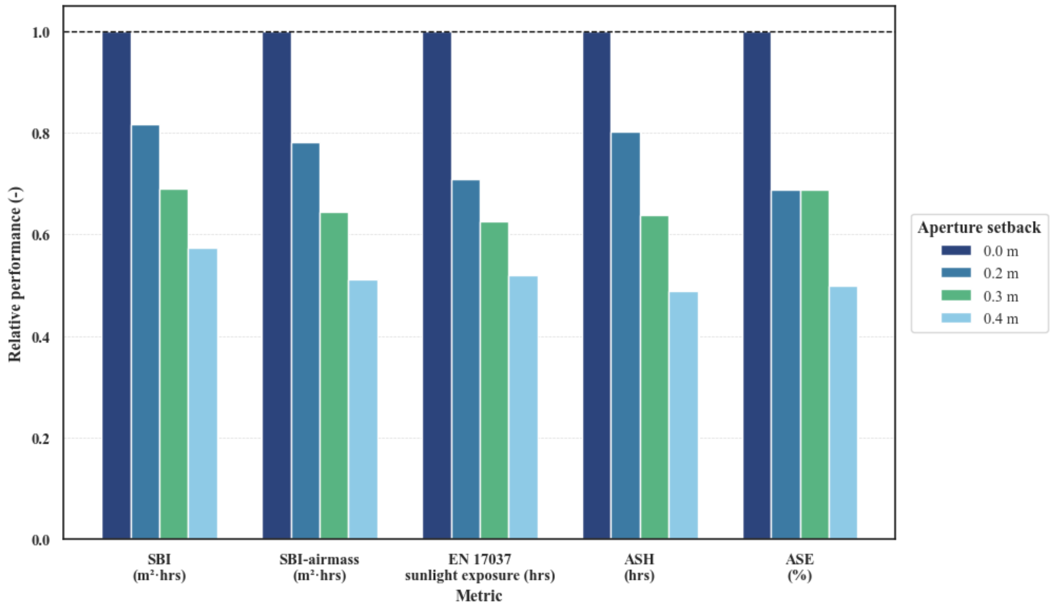

Figure 21 Relative performance chart – Impact of glazing setback on sunlight access metrics.

3.2.5 Impact of shading elements

Shading elements are evaluated using two configurations: overhang depth and opposing building obstruction within a street canyon setup (Figures 22 - 25, Tables 2 and 5), both assessed using the same set of performance metrics.

For the overhang case (Figures 22 and 23), four depths were tested (0.20 m, 0.30 m, 0.40 m, and 0.50 m), together with a reference case without shading. Increasing overhang depth reduced SBI from 1 798.30 to 1 498.44 m^2·hrs and SBI-airmass from 743.36 to 551.38 m^2·hrs. ASH also decreased, from 3 621.00 to 2 843.25 hrs. ASE decreased from 5.92 to 4.47, with the largest reduction occurring at the first depth increment. Further increases in overhang depth produced only minor changes, as most high-angle direct sunlight had already been obstructed. In contrast, EN 17037 sunlight exposure remained constant at 12.00 hrs across all cases.

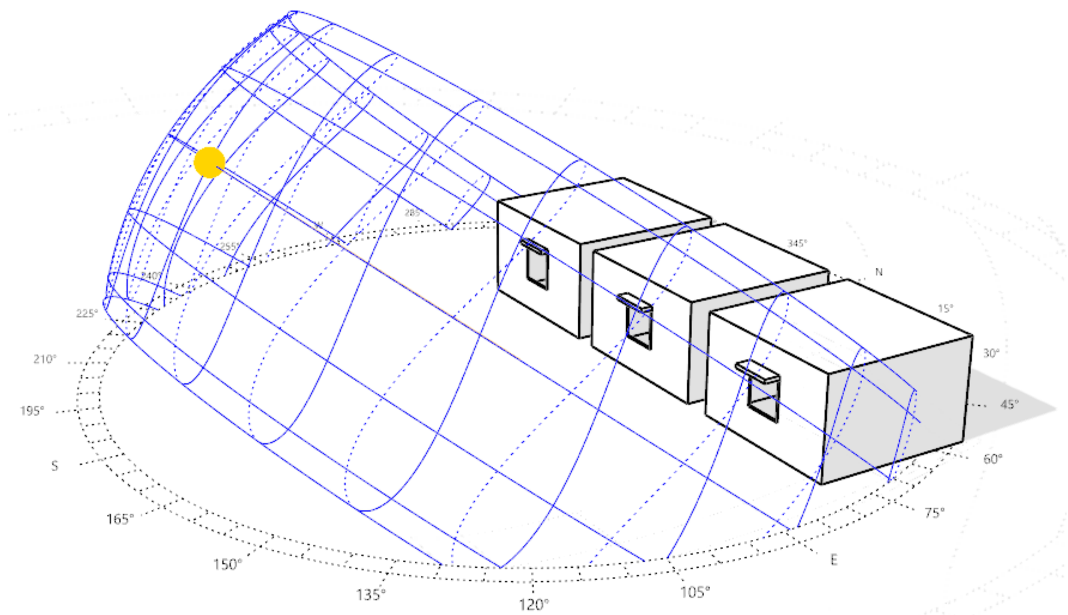

Figure 22 Overhang variations shown against the annual sun-path diagram for the London weather file. From left: 0.20 m, 0.30 m, and 0.50 m horizontal overhang depth.

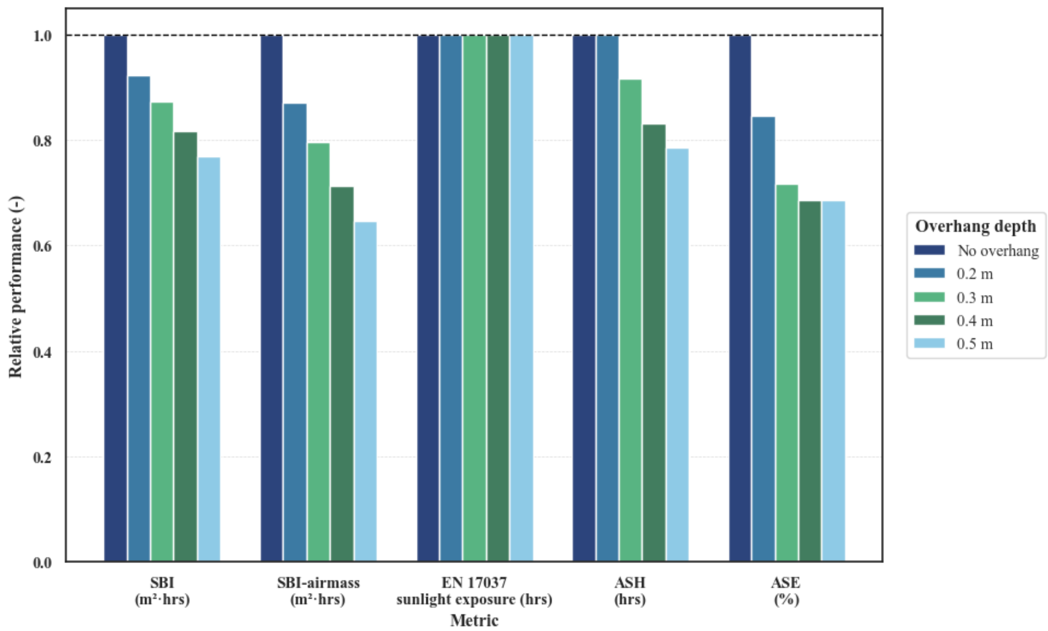

Figure 23 Relative importance chart – Sunlight access metrics comparison across different overhang depths.

For the street canyon configuration (Figures 24 and 25), opposing building heights of 7.50 m, 15.00 m, and 30.00 m were evaluated across a 15.00 m street canyon to represent increasing levels of external obstruction. All metrics decreased as obstruction height increased, although the magnitude of reduction differed between metrics. SBI decreased from 1 802.61 to 708.79 m^2·hrs, while SBI-airmass decreased from 841.86 to 379.74 m^2·hrs, both showing a progressive reduction across successive obstruction heights. EN 17037 sunlight exposure decreased from 12.00 to 5.50 hrs, with the reduction becoming more apparent at higher obstruction levels. ASH decreased from 3 393.50 to 1 877.00 hrs. ASE showed the largest proportional reduction, decreasing from 5.92 to 1.75 as obstruction height increased.

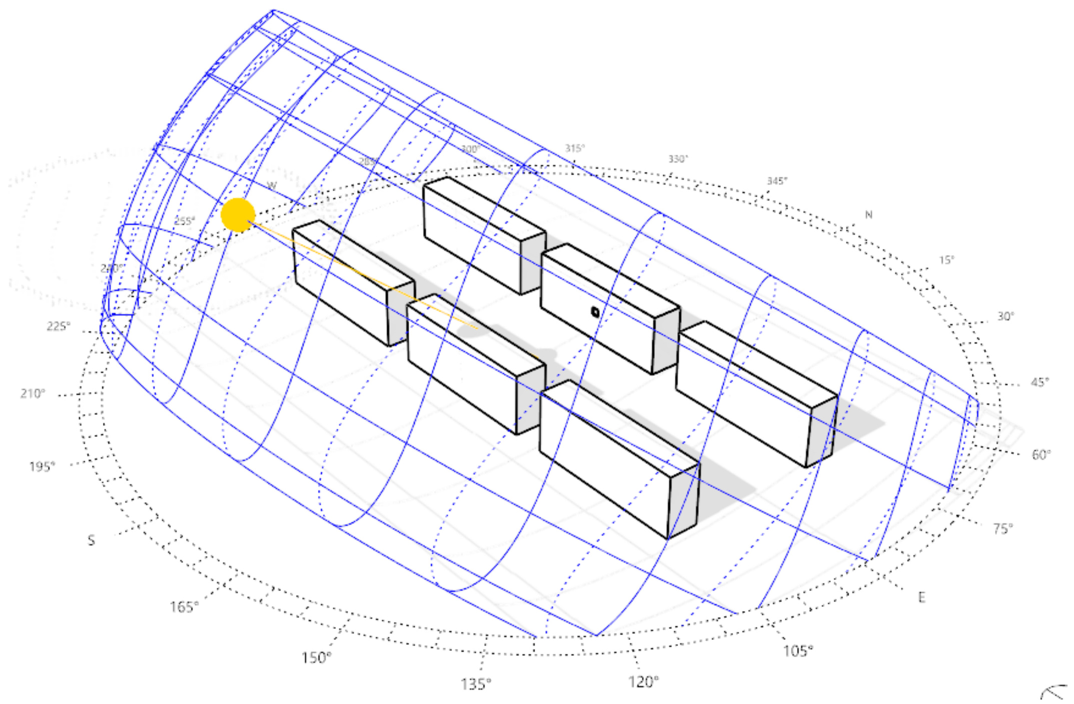

Figure 24 Street canyon obstruction variations shown against the annual sun-path diagram for the London weather file, illustrating the 7.50 m external obstruction case.

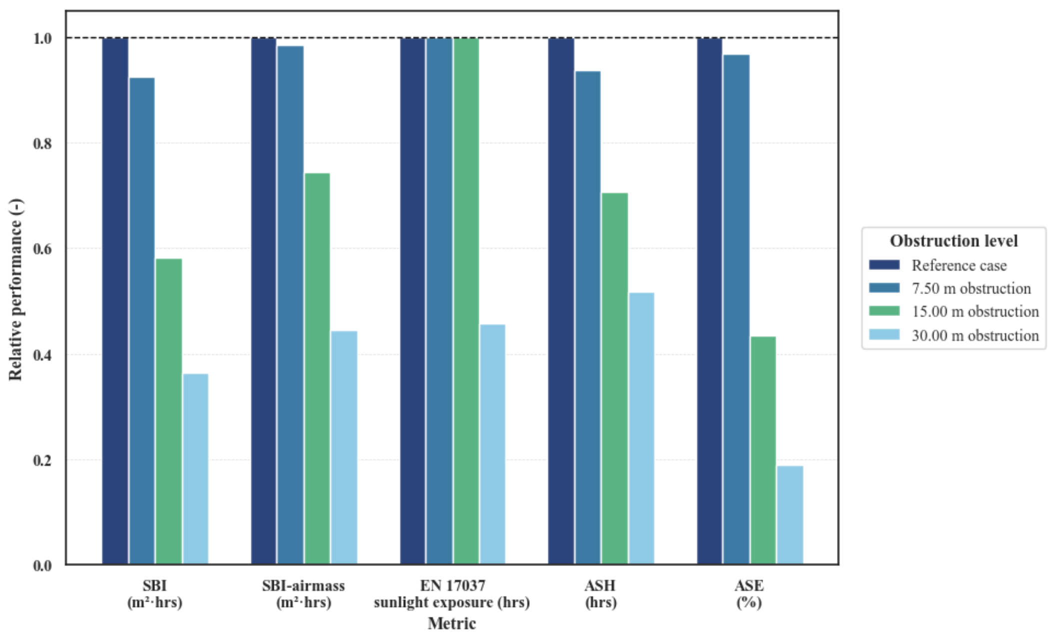

Figure 25 Relative performance of evaluated sunlight access metrics under increasing external obstruction levels.

3.2.6 Impact of aperture inclination

Aperture inclination is evaluated at four tilt angles (0°, 15°, 30°, and 45°), with all values normalised to the 0° baseline (Figure 26 and 27, Tables 2 and 5). All metrics increase with increasing tilt angle, except EN 17037 sunlight exposure. The progression remains monotonic but non-linear in the tested inclination range.

SBI increased from 2 314.86 at 0° to 2 535.91 at 15° and 2 592.85 at 30°, with only minor changes at higher inclination angles. SBI-airmass showed a stronger increase over the same range, rising from 1 078.42 to 1 307.45.

EN 17037 sunlight exposure remained constant at 12.00 hrs across all inclination angles, indicating no sensitivity to aperture inclination. ASH increased more moderately, from 3 767.25 to 3 979.00 hrs, while ASE increased from 6.97 to 7.61, with the largest change occurring between 0° and 15°.

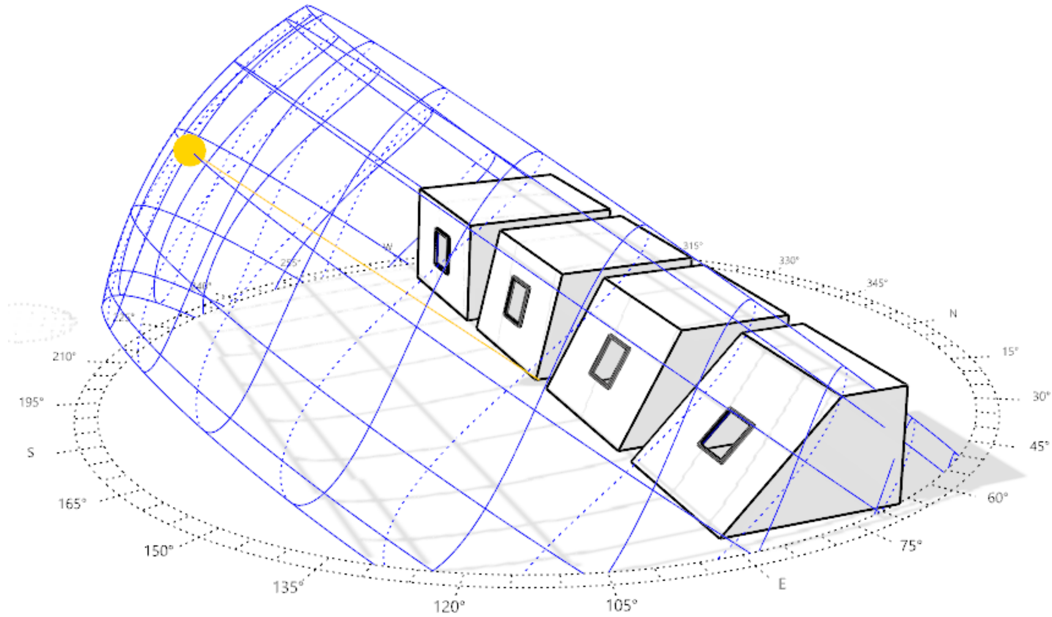

Figure 26 Shoebox aperture inclination variations shown against the annual sun-path diagram for the London weather file.

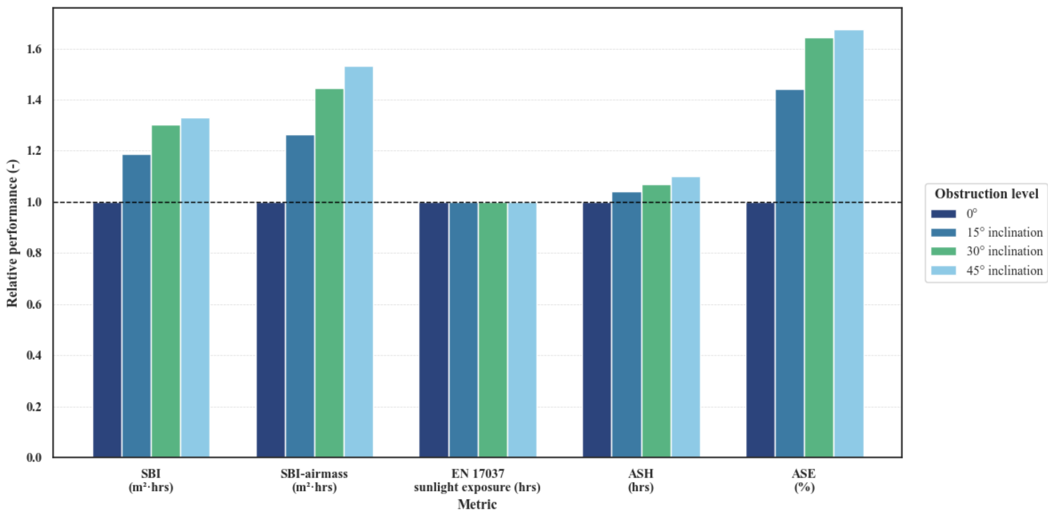

Figure 27 Relative performance chart – Comparison of sunlight access metrics across different tilt angles.

Overall, ASE and SBI-airmass showed the strongest response to increasing inclination, whereas ASH showed a more limited variation and EN 17037 sunlight exposure remained unchanged.

3.2.7 Comparative analysis of SBI / SBI-Airmass / EN 17037 / ASE / ASH

The comparison was performed across the tested parameters, including orientation, aperture area, aspect ratio, geometry, setback, inclination, and shading configurations (Table 2 and 5). The analysis examined how the normalised values of SBI, SBI-airmass, EN 17037 sunlight exposure, ASH, and ASE were distributed across the tested cases.

SBI and SBI-airmass varied in 36 cases and remained identical in eight cases. This indicates that both metrics responded to most tested geometric parameters. EN 17037 sunlight exposure and ASH remained unchanged across aperture size, overhang, and inclination configurations, and varied only under changes in orientation, aperture setback, and external obstruction. ASE showed a discontinuous response, including zero values in eight cases associated with different orientations and the circular aperture shape.

Figure 28 summarises the distribution of normalised metric values across the tested parameters. SBI and SBI-airmass show similar distributions, with values spread across a wide part of the normalised range. EN 17037 sunlight exposure shows a narrower distribution, with many values concentrated near the upper end of the scale.

This reflects the repeated EN 17037 sunlight exposure results recorded for aperture area, aspect ratio, shape, overhang, and inclination cases.

ASH shows a distribution centred around intermediate values, with a smaller spread than SBI and SBI-airmass. ASE shows the most discontinuous distribution, with values extending from 0.00% to the maximum normalised value. The zero values occur in several north-oriented and highly obstructed cases, while higher values occur under changes in aperture area, inclination, and obstruction.

The results show clear differences in metric sensitivity across the tested parameters. SBI and SBI-airmass respond to a broader range of geometric changes, while EN 17037 sunlight exposure produces repeated values because of its point-based and threshold-based formulation. ASE changes abruptly between cases, and ASH remains between the aperture-based metrics and EN 17037 sunlight exposure in its overall distribution.

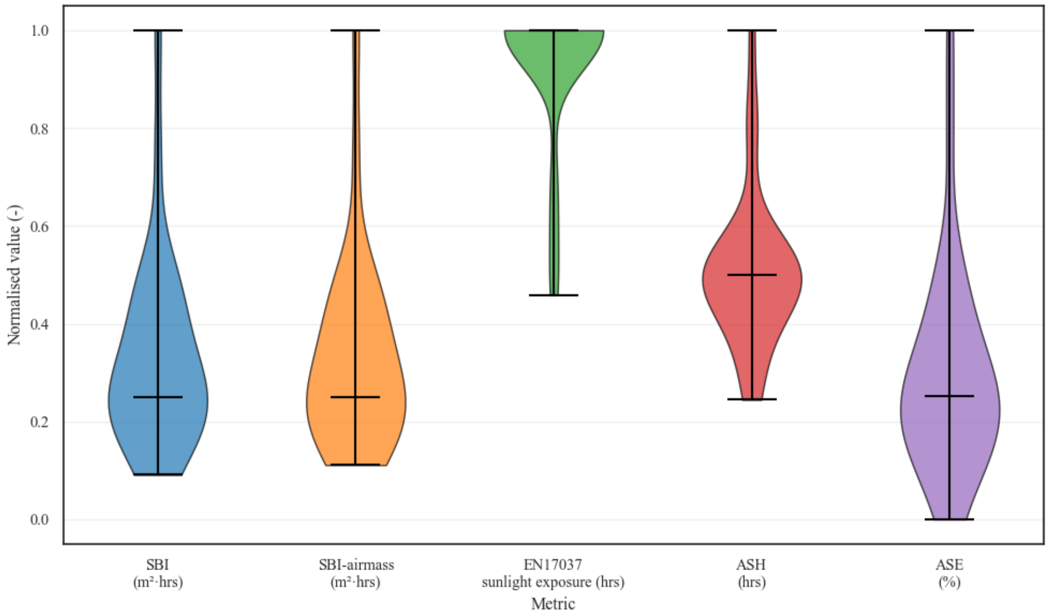

Figure 28 Distribution of normalised sunlight access metric values across the 'shoebox' reference model test matrix.

3.2.8 Analysis of correlation between metrics

Pairwise correlations were calculated to examine the degree of association between SBI, SBI-airmass, EN 17037 sunlight exposure, ASH, and ASE across the shoebox test matrix (Figure 29). The analysis evaluates similarities in metric response to the tested geometric variations.

SBI shows moderate correlations with EN 17037 sunlight exposure (r = 0.63) and ASH (r = 0.64). These relationships indicate that the metrics capture related aspects of sunlight access, while responding differently to geometric variation.

The lower correlation values are primarily associated with configurations where EN 17037 sunlight exposure and ASH remain invariant, including aperture area, aspect ratio, shape, and some inclination cases. In contrast, SBI and SBI-airmass continue to respond continuously across these configurations.

ASH shows a stronger correlation with EN 17037 sunlight exposure (r = 0.83), reflecting their constrained and point-based behaviour. ASE presents positive correlations with all other metrics. The strongest correlations occur with SBI (r = 0.94) and SBI-airmass (r = 0.95), followed by ASH (r = 0.62) and EN 17037 sunlight exposure (r = 0.61). This indicates that ASE follows the aperture-based metrics more closely in the correlation matrix, although its response remains discontinuous across individual cases due to its threshold-based formulation. Changes become visible only after specific threshold conditions are exceeded.

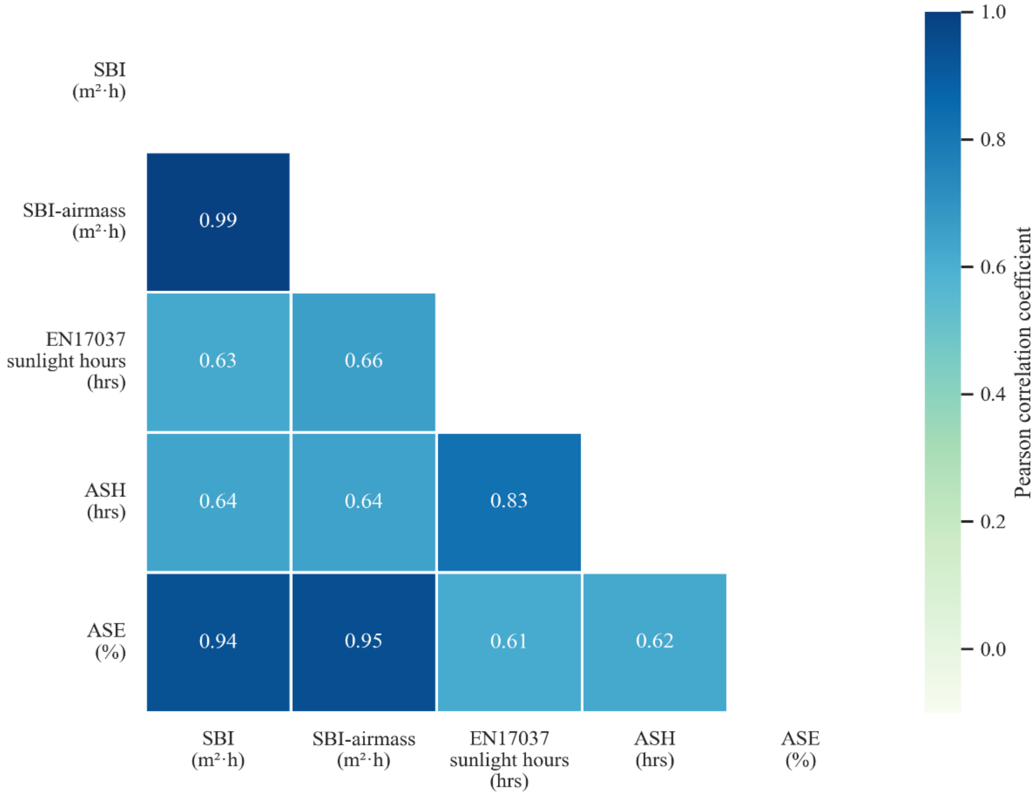

Figure 29 Correlation matrix of performance metrics based on 'shoebox' reference model.

Overall, the correlation analysis indicates that the evaluated metrics describe the same sunlight access phenomenon but differ in their sensitivity and representation of geometric variation.

3.2.9 Sensitivity of metrics to changes in aperture geometry

Figure 30 presents the Pearson correlation coefficients between the sunlight metrics and the tested design parameters in the shoebox study. Positive coefficients indicate that the metric value increases with the parameter value. Negative coefficients indicate that the metric value decreases with the parameter value. Values closer to 1 or -1 indicate stronger linear association, while values near 0 indicate weaker linear association. The coefficients describe relationships across the full parametric dataset, so each value must be read together with the controlled parameter tests.

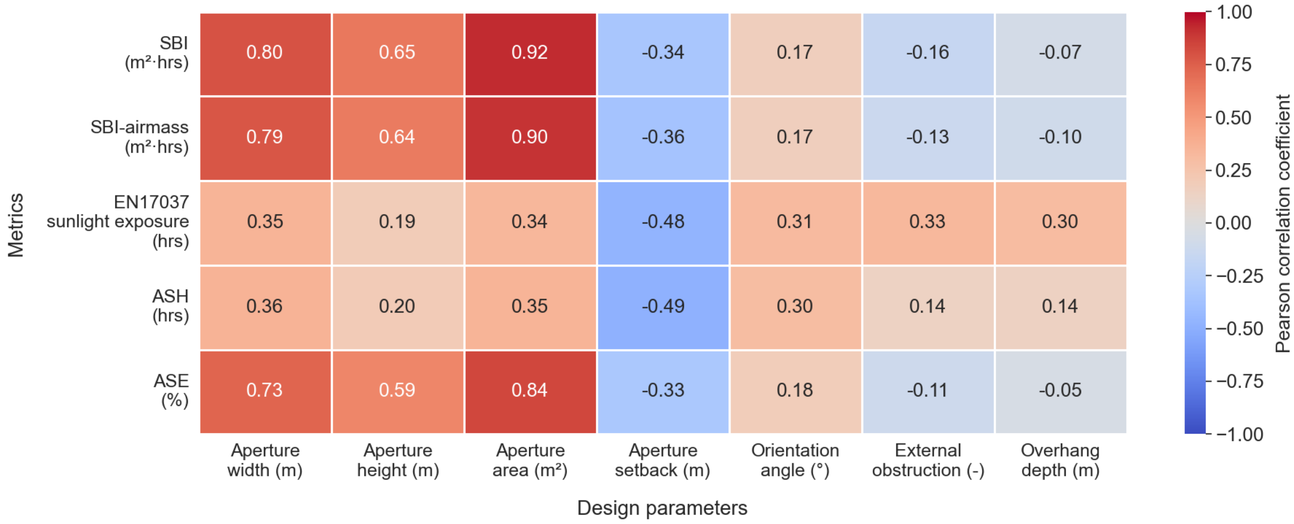

Figure 30 Correlation matrix illustrating the sensitivity of sunlight access metrics to variations in aperture geometry and contextual design parameters.

Aperture width and aperture height show the separation between area-sensitive and point-based metrics. SBI, SBI-airmass, and ASE show positive correlations with aperture width, with coefficients of 0.80, 0.79, and 0.73.

The same order appears for aperture height, with coefficients of 0.65, 0.64, and 0.59. EN 17037 sunlight exposure and ASH show weaker correlations with width and height, ranging from 0.19 to 0.36. In the controlled width and height tests, EN 17037 sunlight exposure and ASH remained unchanged because their evaluation point stayed in the same relative aperture position. The remaining Pearson values come from the combined structure of the full dataset.

Aperture area produces the strongest positive correlations for SBI and SBI-airmass. The coefficients are 0.92 for SBI and 0.90 for SBI-airmass. This follows from the formulation of both metrics, because sunlit aperture area is included in their calculation. ASE also shows a strong positive correlation with aperture area, with a coefficient of 0.84. This response reflects the area-based indoor grid used by ASE, because larger apertures increase the potential for more sensor points to exceed the direct sunlight threshold. EN 17037 sunlight exposure and ASH remain lower, with coefficients of 0.34 and 0.35, because their reference-point evaluation does not scale with aperture area in the controlled aperture-size tests.

Aperture setback produces negative correlations for all metrics. EN 17037 sunlight exposure and ASH show the strongest negative values, with coefficients of -0.48 and -0.49. SBI, SBI-airmass, and ASE show lower negative values, with coefficients of -0.34, -0.36, and -0.33. This pattern reflects the binary response of the midpoint-based metrics under reveal obstruction. If the reference point loses direct sun visibility, the timestep is removed from the EN 17037 sunlight exposure and ASH result. SBI and SBI-airmass can still record partial sunlit aperture area when only part of the opening remains exposed. ASE follows a similar direction because setback can reduce indoor direct sun exposure, although its output still depends on the threshold condition at the sensor grid.

Orientation angle on the correlation matrix (Figure 30), defined as the aperture azimuth measured clockwise from north (0°–360°), shows weak to moderate positive correlations across the metrics. EN 17037 sunlight exposure and ASH show the highest orientation correlations, with coefficients of 0.31 and 0.30. SBI, SBI-airmass, and ASE remain lower, with coefficients of 0.17, 0.17, and 0.18. Orientation changes the timing and availability of direct sunlight, but the full-year aperture-based metrics distribute this effect across many timesteps. The lower SBI and SBI-airmass coefficients should be read with the metric range in mind, because these metrics can still assign sunlight exposure to orientations with limited sun access. EN 17037 sunlight exposure and ASH can move from zero exposure to high exposure between orientations, while SBI and SBI-airmass record a graded change across the tested orientations.

External context and overhang depth produce weak correlations for most metrics. SBI, SBI-airmass, and ASE show weak negative correlations with external context, with coefficients of -0.16, -0.13, and -0.11. The same pattern appears for overhang depth, with coefficients of -0.07, -0.10, and -0.05. EN 17037 sunlight exposure shows positive correlations with external context and overhang depth, with coefficients of 0.33 and 0.30. ASH also shows positive values for these parameters, with coefficients of 0.14 and 0.14. These positive values indicate interaction with the full parametric dataset, especially for metrics that can remain unchanged across obstruction cases until the reference point gains or loses sun visibility.

ASE forms a separate case in the matrix. It shows high positive correlations with aperture width, height, and area, with the strongest value under aperture area at 0.84. It also shows negative correlations with setback, external context, and overhang depth. This places ASE close to SBI and SBI-airmass for aperture-size sensitivity. Its response still depends on an indoor illuminance threshold, so changes appear only when the threshold exceedance condition changes. This behaviour is consistent with the discontinuous ASE response observed throughout the shoebox analysis. Changes become visible only after specific threshold conditions are exceeded.

The correlation matrix separates the metrics into distinct sensitivity patterns. SBI and SBI-airmass are most closely associated with aperture extent, especially aperture area. EN 17037 sunlight exposure and ASH show weaker associations with aperture dimensions and stronger responses to conditions that affect reference-point visibility, such as aperture setback. ASE combines area sensitivity with threshold-driven behaviour. The same geometric change can produce different coefficient patterns because the metrics use different spatial units, temporal scopes, and evaluation conditions.

3.3 Models in urban context

3.3.1 Single-aperture based analysis

The single-aperture based analysis is based on 508 apertures extracted from the urban-context models (Table 1 in appendix B). The analysed values include annual SBI, SBI-airmass, ASH, and EN 17037 sunlight exposure. This analysis describes how the metrics are distributed across individual apertures.

The single-aperture based distributions do not show a uniform pattern across all metrics. SBI, SBI-airmass, and EN 17037 sunlight exposure are concentrated at low values and extend through right-sided tails (Figures 31 and 32). ASH is also concentrated in the lower range, with a wider spread across the middle values and a smaller upper group. The lines overlaid on the histograms represent Kernel Density Estimation (KDE), showing the smoothed approximation of data distribution values across each metric range. The reported concentration values refer to KDE peaks.

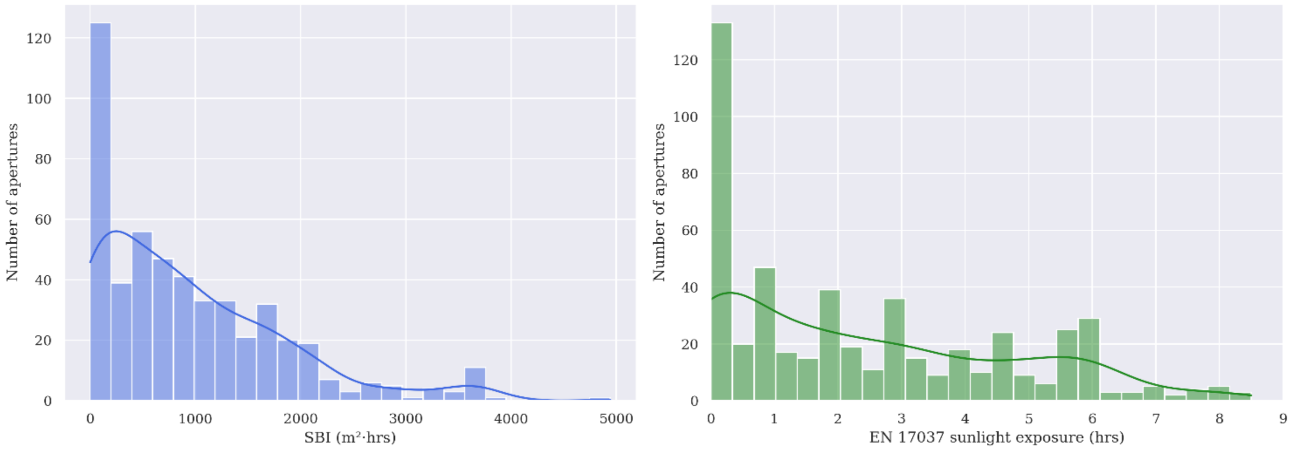

Figure 31 Left side - distribution of SBI, right side - distribution of EN 17037 sunlight exposure; single-aperture based analysis.

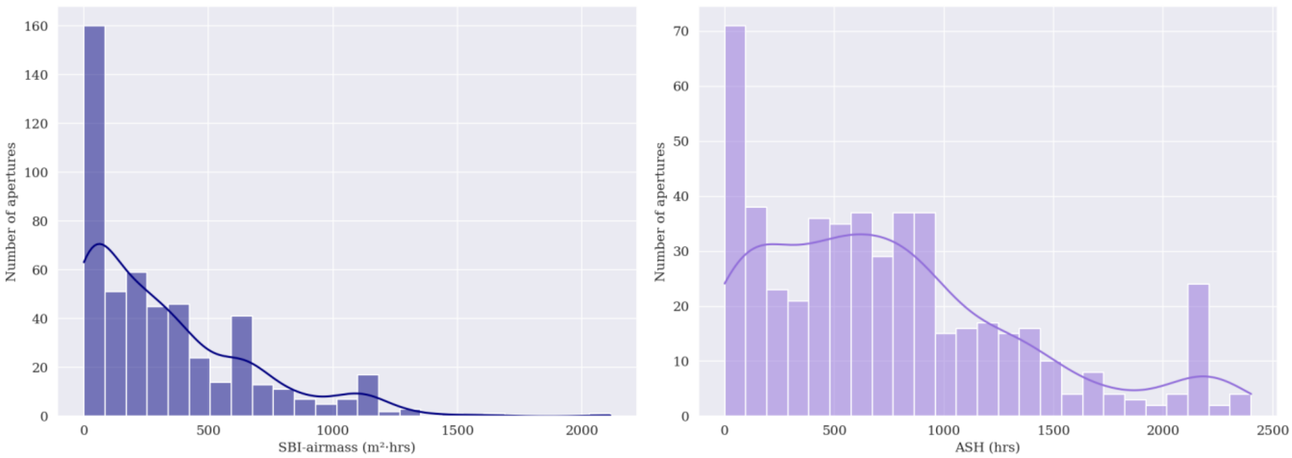

Figure 32 Left side - distribution of SBI-airmass, right side - distribution of ASH; single-aperture based analysis.

Single-aperture SBI values are concentrated at the lower end of the distribution, with the main KDE peak located around 207.82 m^2h. The distribution is asymmetric, with many apertures below approximately 1 000 m^2h and a gradual tail towards higher SBI values (Figure 31). A secondary KDE peak appears around 3 587.41 m^2h, with a much lower density. The high-value tail reflects apertures with larger sunlit area, longer direct sunlight exposure, or more favourable orientation and obstruction conditions.

EN 17037 sunlight exposure is strongly concentrated near zero, with the main KDE peak located around 0.30 h. The histogram shows a large group of apertures in the lowest exposure range and smaller groups distributed between approximately 1 h and 6 h (Figure 31). A secondary KDE peak appears around 5.48 h, with lower density. This pattern indicates that many individual apertures receive short qualifying sunlight exposure under the EN 17037 sunlight exposure evaluation conditions, while fewer apertures reach longer exposure durations.

SBI-airmass follows the same general distributional structure as SBI, with the main KDE peak located around 55.04 m^{2}h. The distribution is concentrated at low values and extends through a thin right-sided tail (Figure 32). A secondary KDE peak appears around 1 090.12 m^{2}h, with lower density. The reduced numerical scale reflects the airmass correction, which lowers the contribution of sunlight at low solar elevations.

ASH values are concentrated in the lower annual-hour range, with the main KDE peak located around 211.48 h. The distribution spreads across a broader range than EN 17037 sunlight exposure, with many apertures between approximately 0 h and 1 000 h and a smaller group above 2 000 h (Figure 32). A secondary KDE peak appears around 2 182.06 h, with lower density. This indicates that annual sunlight availability varies across individual apertures, with a smaller subset receiving substantially longer sunlight duration.

Overall, the single-aperture based analysis shows that the evaluated metrics share a lower-value concentration but differ in spread and upper-range behaviour. SBI and SBI-airmass produce long-tailed aperture-based distributions. EN 17037 sunlight exposure remains concentrated near short exposure durations. ASH spreads across a wider annual-hour range.

3.3.1.1 SBI approach against EN 17037 and ASH in urban context

The single-aperture distributions show how each metric behaves individually. The following comparisons examine the relationship between aperture-based cumulative exposure and duration-based sunlight access. This step examines how SBI, SBI-airmass, EN 17037 sunlight exposure, and ASH differ due to their structures in spatial units, time periods, and categorisations.

Figure 33 compares SBI with EN 17037 sunlight exposure for the single-aperture dataset. Each point represents one aperture. The horizontal axis gives the SBI value, and the vertical axis gives EN 17037 sunlight exposure value in hours. Bubble size represents aperture area. The horizontal lines and the colour mark the EN 17037 sunlight exposure threshold categories at 1.5 h, 3 h, and 4 h.

Figure 33 Relationship between SBI and EN 17037 sunlight exposure categories, with bubble size representing aperture area.

Figure 33 shows an ordered relationship between SBI and EN 17037 sunlight exposure at the lower and upper ranges. Apertures with low SBI values are mainly located within the fail and low EN 17037 sunlight exposure categories. Medium and high EN 17037 sunlight exposure categories become more frequent as SBI increases. The intermediate range remains dispersed, with several EN 17037 sunlight exposure categories appearing across similar SBI intervals. This means that higher cumulative aperture exposure is generally associated with longer sunlight exposure, although EN 17037 sunlight exposure categories do not form separate SBI bands. The bubble sizes also show that larger apertures tend to move further along the SBI axis, since SBI includes aperture area in its calculation.

Figure 34 compares SBI-airmass with EN 17037 sunlight exposure. The plot uses the same EN 17037 sunlight exposure category structure as Figure 33. The horizontal axis uses SBI-airmass instead of SBI, and bubble size again represents aperture.

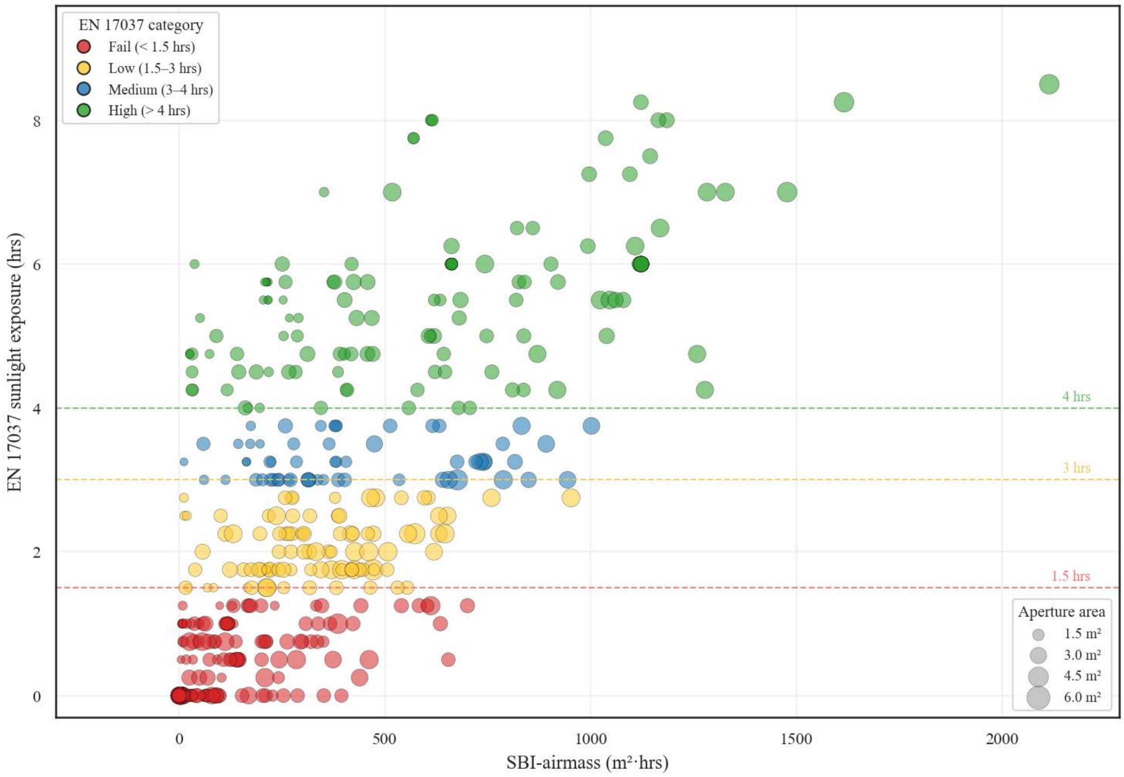

Figure 34 Relationship between SBI-airmass and EN 17037 sunlight exposure categories, with bubble size representing aperture area.

Figure 34 shows that the EN 17037 sunlight exposure category overlap remains after applying the airmass correction. Fail and low EN 17037 sunlight exposure cases are concentrated at lower SBI-airmass values. Medium and high EN 17037 sunlight exposure cases extend across a wider SBI-airmass range. The horizontal scale is compressed compared with SBI, because low-elevation sunlight receives a reduced contribution in SBI-airmass. The category structure still does not translate into fixed SBI-airmass intervals. The airmass correction reduces the numerical scale of SBI-airmass. The EN 17037 sunlight exposure categories still overlap across the SBI-airmass range.

Figure 35 compares SBI with ASH for the single-aperture dataset. The horizontal axis gives SBI, and the vertical axis gives annual sunlight hours. Bubble size represents aperture area. The figure compares cumulative aperture exposure with annual sunlight duration without the airmass correction.

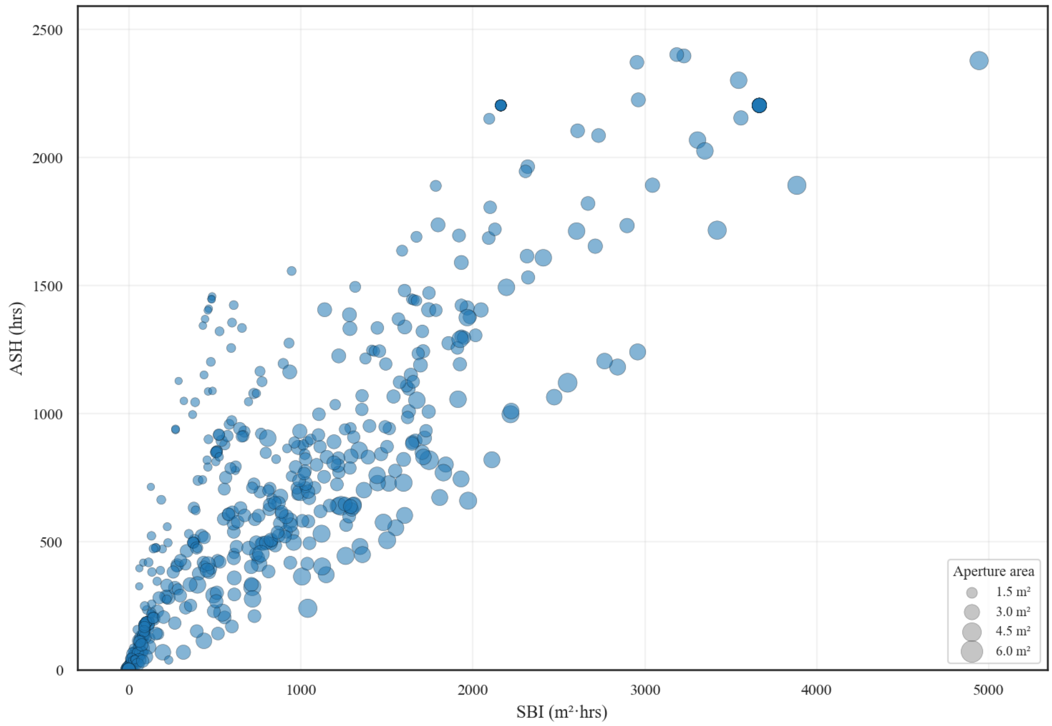

Figure 35 Relationship between SBI and ASH values, with bubble size representing aperture area.

Figure 35 shows a stronger continuous pattern than the EN 17037 sunlight exposure comparisons. Low SBI values are mostly associated with low ASH values. Higher SBI values generally appear with higher ASH values. The spread increases in the middle and upper ranges. This indicates that annual sunlight duration is a major contributor to SBI, although it does not define SBI alone. Apertures with similar ASH can still produce different SBI values because SBI also includes sunlit aperture area and incidence effects

Figure 36 compares SBI-airmass with ASH for the same single-aperture dataset. The horizontal axis gives the SBI-airmass value, and the vertical axis gives annual sunlight hours. Bubble size represents aperture area. The figure compares an airmass-weighted aperture-based metric with an annual duration-based metric.

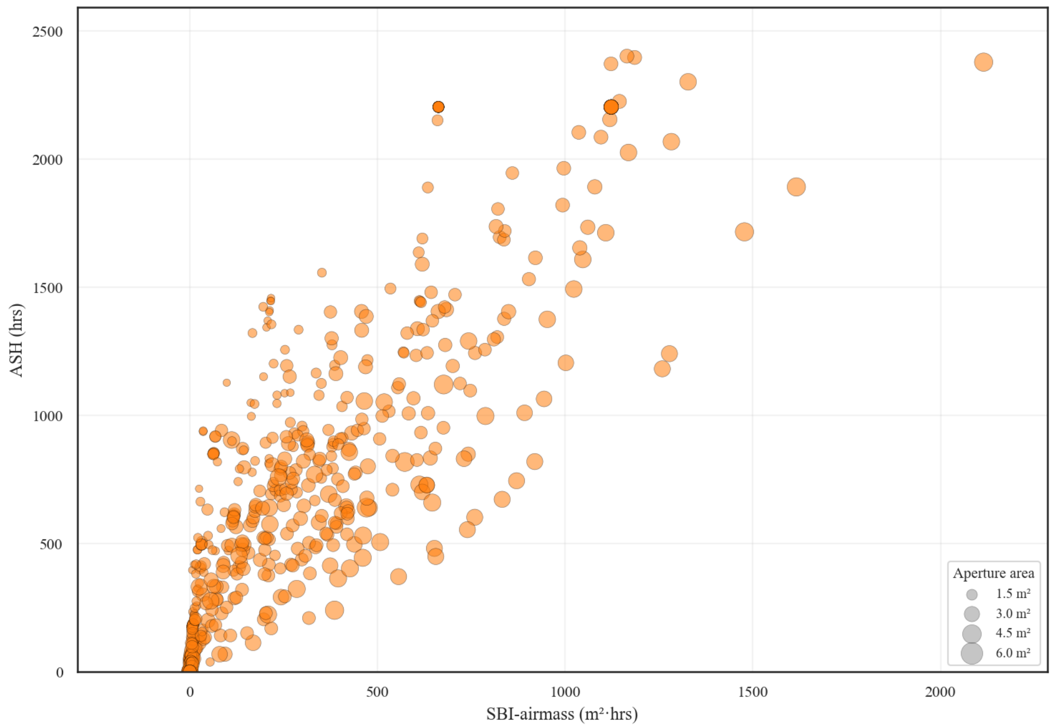

Figure 36 Relationship between SBI-airmass and ASH values, with bubble size representing aperture area.

Figure 36 shows a positive relationship between SBI-airmass and ASH. Apertures with low SBI-airmass generally have low ASH values. Higher ASH values appear more often as SBI-airmass increases. The middle range remains scattered, which shows that similar ASH values can correspond to different SBI-airmass values. This spread follows from the metric definitions. ASH counts annual sunlight duration, and SBI-airmass combines duration with sunlit aperture area, incidence angle, and airmass weighting. Larger bubbles appear more often in the higher SBI-airmass range, showing that aperture area has an influence on SBI-airmass values.

Figure 37 compares SBI and SBI-airmass across urban density scenarios. The bars show the metric values for each density group. The error bars indicate variation within each group. The figure is used to examine how SBI and SBI-airmass change across urban volumetric density scenarios.

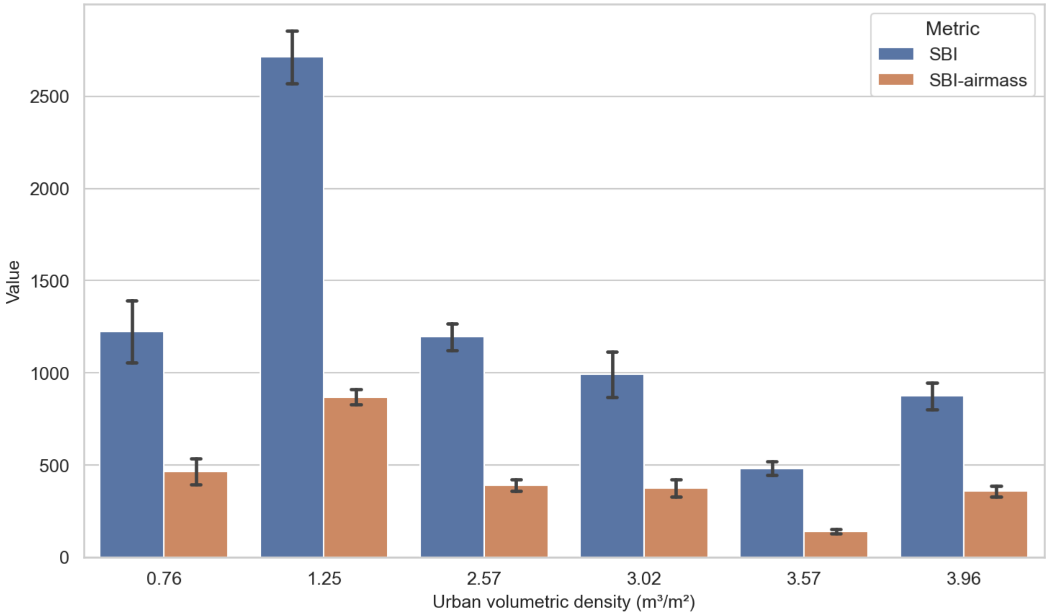

Figure 37 SBI and SBI-airmass values across different urban volumetric density scenarios based on the single-aperture analysis.

Figure 37 shows how SBI and SBI-airmass change across urban volumetric density scenarios. Both metrics reach their highest values at the 1.25 m^3/m^2 scenario and decrease under higher density conditions. The lowest density scenario does not produce the highest values. This indicates that density alone does not determine aperture-based sunlight exposure. The pattern reflects the combined influence of density, aperture placement, orientation, and obstruction geometry.

Figure 38 compares SBI with EN 17037 sunlight exposure and adds urban volumetric density as a colour scale. Each point represents one aperture. The dashed horizontal lines show the EN 17037 sunlight exposure threshold categories. The figure is used to examine whether apertures from different urban volumetric density scenarios form separate groups in the SBI and EN 17037 sunlight exposure relationship.

Figure 38 Relationship between SBI and EN 17037 sunlight exposure at the single-aperture level. Colours represent urban volumetric density [m³/m²], while dashed lines indicate EN 17037 sunlight exposure threshold categories.

Figure 38 shows that urban volumetric density does not separate the EN 17037 sunlight exposure categories into distinct groups. Fail and low EN 17037 sunlight exposure outcomes appear across several density values. High EN 17037 sunlight exposure outcomes also occur across different density values. Similar SBI and EN 17037 sunlight exposure combinations are found under different density scenarios. This means that density affects the general sunlight condition, but the final aperture result also depends on local aperture position, orientation, and obstruction. The figure also confirms the category overlap seen in Figure 33. Similar SBI values can correspond to different EN 17037 sunlight exposure categories, and similar EN 17037 sunlight exposure categories can occur across different SBI values.

Overall, Figures 33 to 38 show that SBI, SBI-airmass, EN 17037 sunlight exposure, and ASH are related without producing equivalent readings of single-aperture sunlight access. Low SBI and SBI-airmass values usually correspond to low EN 17037 sunlight exposure and low ASH values. High SBI and SBI-airmass values are more frequently associated with higher EN 17037 sunlight exposure and higher ASH values. The middle range contains the largest EN 17037 sunlight exposure category overlap and the widest scatter against ASH. Aperture area contributes to SBI and SBI-airmass values. Urban density affects the general exposure pattern, although it does not group the EN 17037 sunlight exposure outcomes into separate density classes. The section therefore shows that SBI and SBI-airmass relate to EN 17037 sunlight exposure and ASH through the general sunlight-exposure pattern; aperture area, angular weighting, airmass weighting, and the restricted temporal scope of EN 17037 sunlight exposure explain the remaining separation between aperture cases.

3.3.1.2 Consistencies and inconsistencies between SBI and EN 17037 in urban context

This dispersion was further examined in relation to aperture-level geometric and urban-context effects using the hierarchically clustered correlation matrix presented in Figure 39. The analysis was used to identify whether the differences observed between SBI and EN 17037 sunlight exposure were associated with aperture area, orientation, or surrounding urban obstruction.

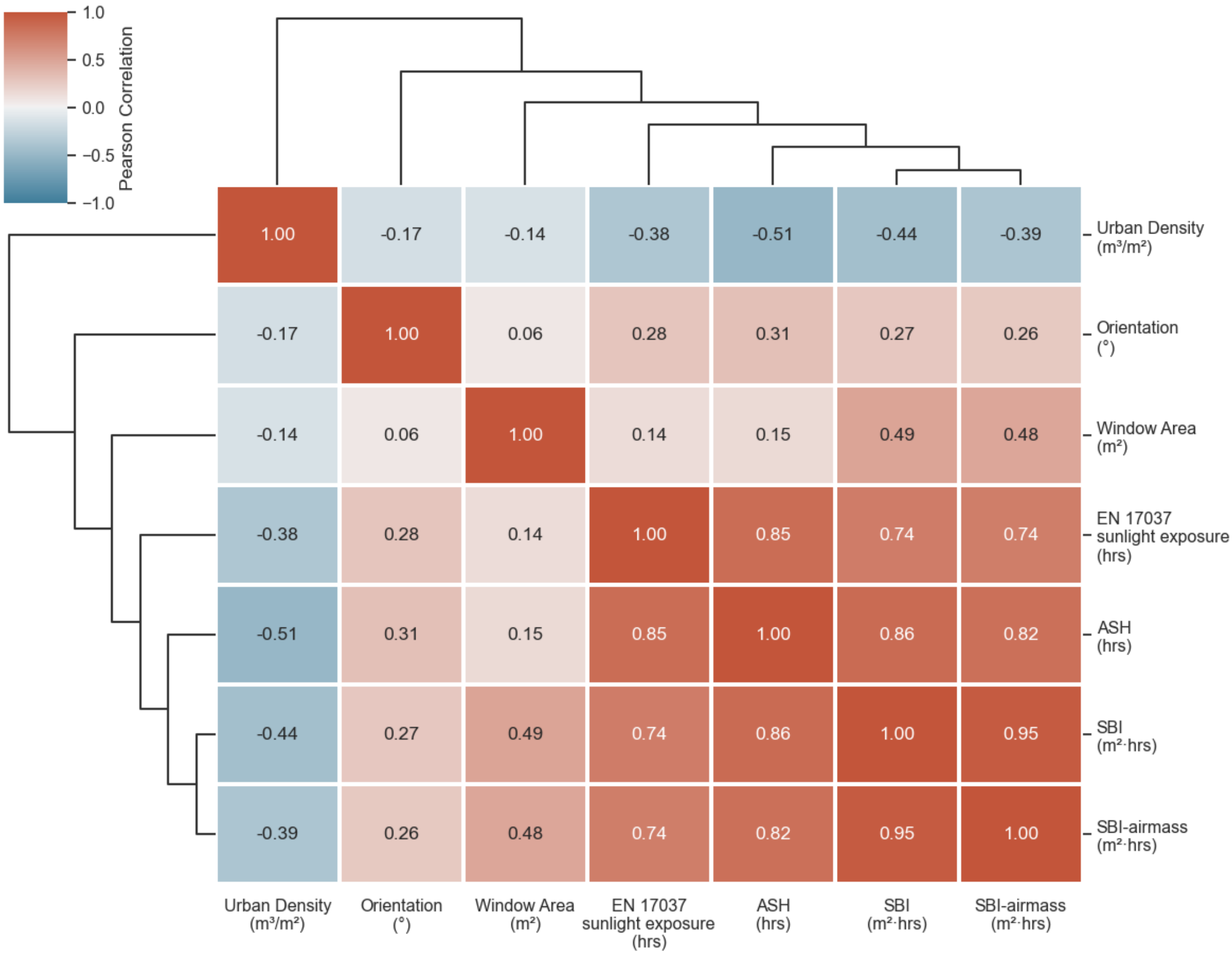

Figure 39 Hierarchically clustered correlation matrix showing relationships between sunlight metrics and selected urban and aperture design parameters in the single-aperture analysis.

Among the analysed sunlight metrics, the strongest correlation is observed between SBI and SBI-airmass (r = 0.95). SBI is also strongly correlated with ASH (r = 0.86), while its correlation with EN 17037 sunlight exposure is lower (r = 0.74). EN 17037 sunlight exposure is strongly correlated with ASH (r = 0.85) and shows the same correlation coefficient with SBI and SBI-airmass (r = 0.74).

The hierarchical clustering places SBI and SBI-airmass as the closest pair of variables. ASH is grouped with these metrics at the next level, followed by EN 17037 sunlight exposure. The clustered arrangement therefore shows that SBI, SBI-airmass, ASH, and EN 17037 sunlight exposure form one broader group within the analysed dataset, with the closest similarity observed between the two aperture-based indicators.

Window area shows a moderate positive correlation with SBI (r = 0.49) and SBI-airmass (r = 0.48). In comparison, its relationships with EN 17037 sunlight exposure (r = 0.14) and ASH (r = 0.15) are weaker. This difference is visible in the correlation matrix, where window area is more closely associated with SBI and SBI-airmass than with the two duration-based metrics.

Orientation shows weak positive correlations with all sunlight metrics. The correlation coefficient is highest for ASH (r = 0.31), followed by EN 17037 sunlight exposure (r = 0.28), SBI (r = 0.27), and SBI-airmass (r = 0.26). The limited variation between these values shows a similar correlation level between orientation and each of the analysed sunlight metrics in the single-aperture dataset.

Urban density shows negative correlations with all sunlight metrics. The strongest negative correlation is recorded for ASH (r = −0.51), followed by SBI (r = −0.44), SBI-airmass (r = −0.39), and EN 17037 sunlight exposure (r = −0.38). Urban density is also negatively correlated with orientation (r = −0.17) and window area (r = −0.14), although these relationships are weaker than those observed for the sunlight metrics.

The relationship between SBI and EN 17037 sunlight exposure remains positive but non-equivalent. Low SBI values occur together with low EN 17037 sunlight exposure values, while higher SBI values are generally associated with higher EN 17037 sunlight exposure values. However, variation remains within the intermediate range, where similar SBI values correspond to different EN 17037 sunlight exposure durations.

Overall, the single-aperture results show that SBI and EN 17037 sunlight exposure follow a similar general tendency across the analysed urban-context cases, while differences remain in the distribution of values. SBI is more strongly correlated with SBI-airmass and ASH than with EN 17037 sunlight exposure. Among the analysed parameters, window area shows a stronger relationship with SBI and SBI-airmass, whereas urban density is negatively correlated with all sunlight metrics.

To further examine the relationships observed in the single-aperture dataset, a Random Forest model was applied to predict EN 17037 sunlight exposure using the analysed sunlight-access metrics and selected design parameters. The variable-importance ranking was used to identify which input variables had the highest importance values within the predictive model. The results of this analysis are presented in Figure 40.

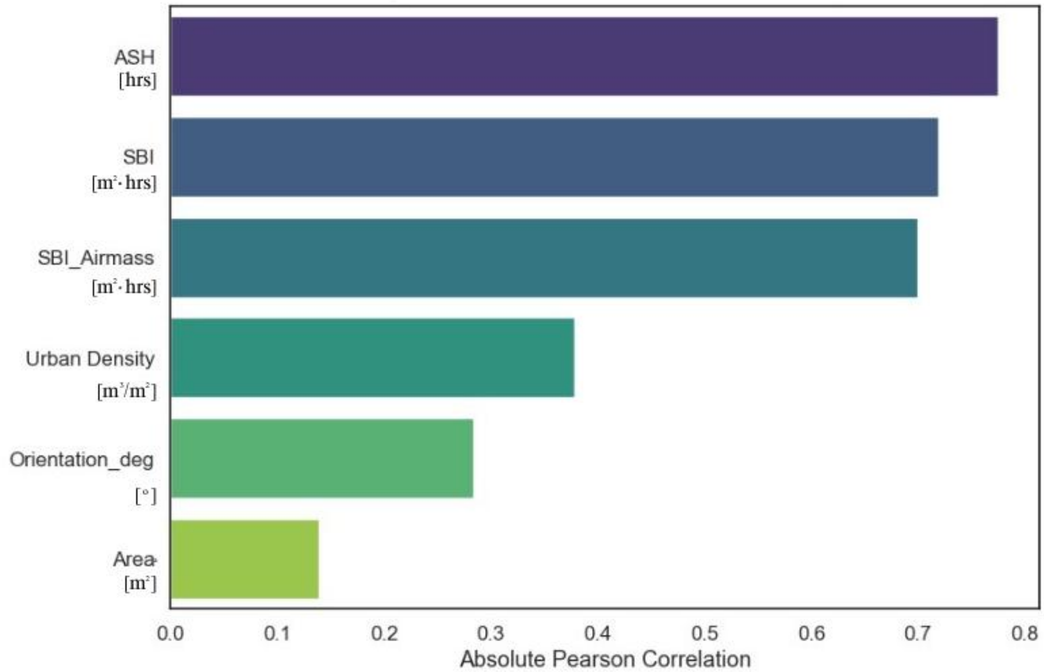

Figure 40 Feature-importance ranking derived from the Random Forest model predicting EN 17037 sunlight exposure at the single-aperture level, based on sunlight-access metrics and selected design parameters.

The Random Forest feature-importance analysis shows that ASH has the highest importance value in the model (0.78), followed by SBI (0.72) and SBI-airmass (0.70). The selected design parameters rank lower: urban density reaches an importance value of 0.38, orientation reaches 0.28, and aperture area reaches 0.14. The three sunlight-access metrics therefore occupy the highest-ranking positions in the prediction of EN 17037 sunlight exposure in the single-aperture dataset. Among the selected design parameters, urban density has the highest importance value, while aperture area records the lowest value among all variables included in the model.

3.3.2 Room-based analysis

The room-based analysis includes 365 rooms extracted from the urban-context models (Table 1 in appendix C). Of these, 251 rooms contain one aperture, 78 contain two apertures, 29 contain three apertures, 6 contain four apertures, and 1 room contains five apertures. Room-based values are derived by aggregating aperture-based results within each room. SBI and SBI-airmass are summed across apertures, whereas EN 17037 sunlight exposure and ASH are calculated through temporal merging of sunlight periods.

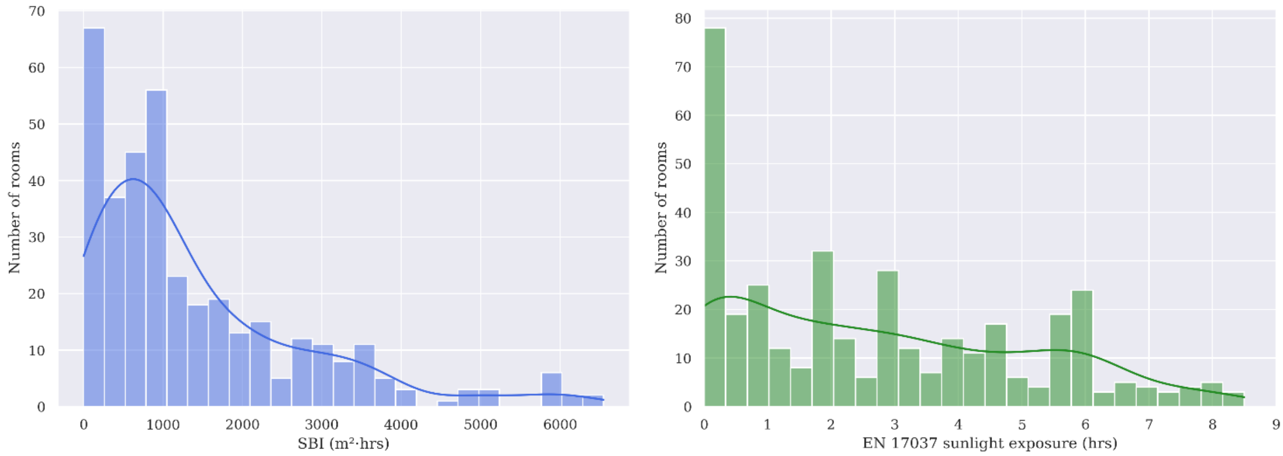

Figure 41 Left side - distribution of SBI, right side - distribution of EN 17037 sunlight exposure; room-based analysis.

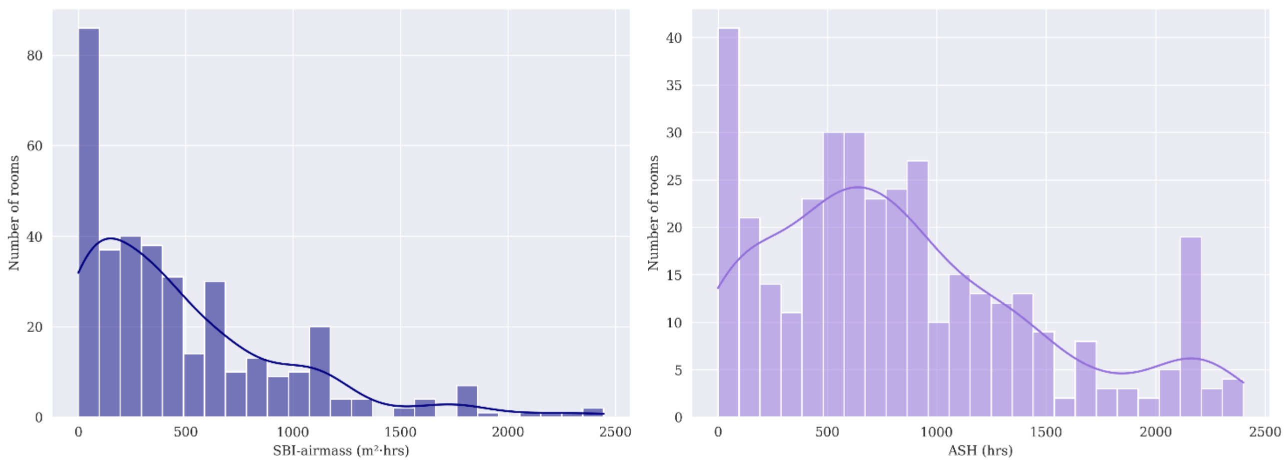

Figure 42 Left side - distribution of SBI-airmass, right side - distribution of ASH; room-based analysis.

The room-based distributions do not show a uniform pattern across all metrics. SBI, SBI-airmass, and EN 17037 sunlight exposure are concentrated at low values and extend through long right-sided tails (Figures 41 and 42). ASH is more widely distributed, with a broad middle range and a secondary concentration at higher values. The lines overlaid on the histograms represent Kernel Density Estimation (KDE), showing the smoothed concentration of values across each metric range. The reported concentration values refer to the KDE peak. This difference shows that the room-based results are influenced by both sunlight availability and the type of metric used to describe it.

Room-based SBI values range from 0.00 to 6 548.47, with the KDE peak located around 960.57. The distribution remains asymmetric, with many rooms below approximately 1 000 and a gradual tail towards higher SBI ranges (Figure 41). The high-value tail reflects rooms where several aperture contributions are combined, or where larger openings receive longer periods of direct sunlight. The small number of very high values should be treated as a distinct upper-end group.

EN 17037 sunlight exposure ranges from 0.00 to 11.25 h, with the KDE peak located around 2.00 h. A total of 57 rooms record EN 17037 sunlight exposure values equal to 0.00 h. The distribution is concentrated near zero, with several smaller peaks between approximately 1 h and 6 h and a limited tail towards higher exposure durations (Figure 41). This pattern indicates that many rooms receive little or no qualifying sunlight exposure, while a smaller group reaches longer durations through a wider spread of sunlit periods.

The effect of room aggregation becomes visible when rooms with different numbers of apertures are compared. Rooms with two apertures show higher SBI values than rooms with a single aperture. The KDE peak for SBI shifts from 910.34 for one-aperture rooms to 1 915.12 for two-aperture rooms. SBI-airmass follows the same pattern, with the KDE peak shifting from 312.49 to 786.02.

EN 17037 sunlight exposure also increases in rooms with multiple apertures, although the increase is smaller and non-proportional. The KDE peak for EN 17037 sunlight exposure shifts from 1.75 h for one-aperture rooms to 2.88 h for two-aperture rooms. Unlike SBI, the increase depends on whether sunlight periods from different apertures occur at different times of the day and extend the total sunlight duration at point P within the room. Aperture count affects EN 17037 sunlight exposure indirectly.

ASH shows a different room-based response. The KDE peak for ASH shifts downward from 706.63 for one-aperture rooms to 585.75 for two-aperture rooms. The ASH distribution is not concentrated only at the lower end; many rooms occur between approximately 400 h and 1 000 h, and a smaller group appears above 2 000 h (Figure 42). The lower KDE peak for the two-aperture subset indicates that the additional apertures in this subset do not necessarily add distinct annual sunlight hours. Orientation, obstruction, and temporal overlap can outweigh aperture count in time-based room results.

Overall, the room-based analysis increases the separation between cumulative aperture-based metrics and point- and duration-based metrics. Aperture count alone cannot explain room-based sunlight performance. SBI and SBI-airmass describe cumulative aperture exposure, whereas EN 17037 sunlight exposure and ASH describe distinct periods of sunlight availability. The distributions show this separation clearly: SBI and SBI-airmass produce long-tailed cumulative results, EN 17037 sunlight exposure remains concentrated near short exposure durations, and ASH spreads across a wider annual-hour range. A room can gain cumulative exposure without gaining equivalent sunlight duration.

3.3.2.1 SBI approach against EN 17037 and ASH in urban context

The room-based comparison repeats the single-aperture metric comparison using room-level aggregation. SBI and SBI-airmass are summed across the apertures belonging to each room. EN 17037 sunlight exposure and ASH are calculated from room-level sunlight periods. The figures, therefore, test whether the metric relationships observed at the aperture level remain visible after aggregation.

Figures 43 and 44 compare room-based SBI and SBI-airmass with EN 17037 sunlight exposure. Each point represents one room. The horizontal axes give SBI and SBI-airmass values, and the vertical axis gives EN 17037 sunlight exposure in hours. Bubble size represents room area. The horizontal lines and colour categories mark the EN 17037 sunlight exposure threshold levels at 1.5 h, 3 h, and 4 h.

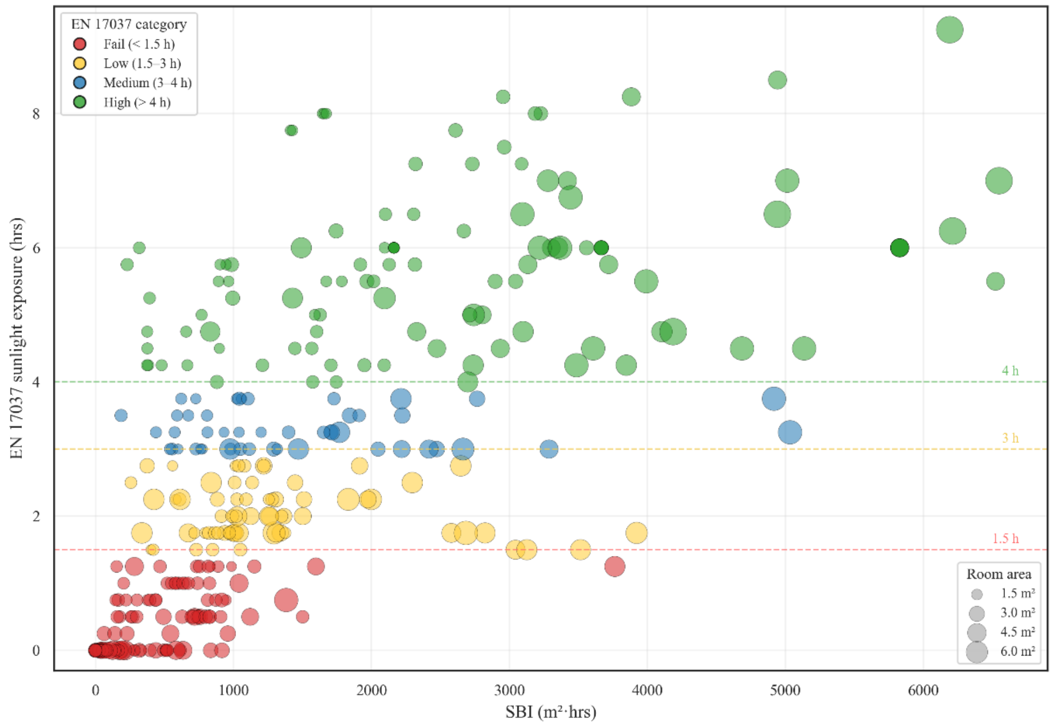

Figure 43 Relationship between SBI and EN 17037 sunlight exposure categories, with bubble size representing aperture area.

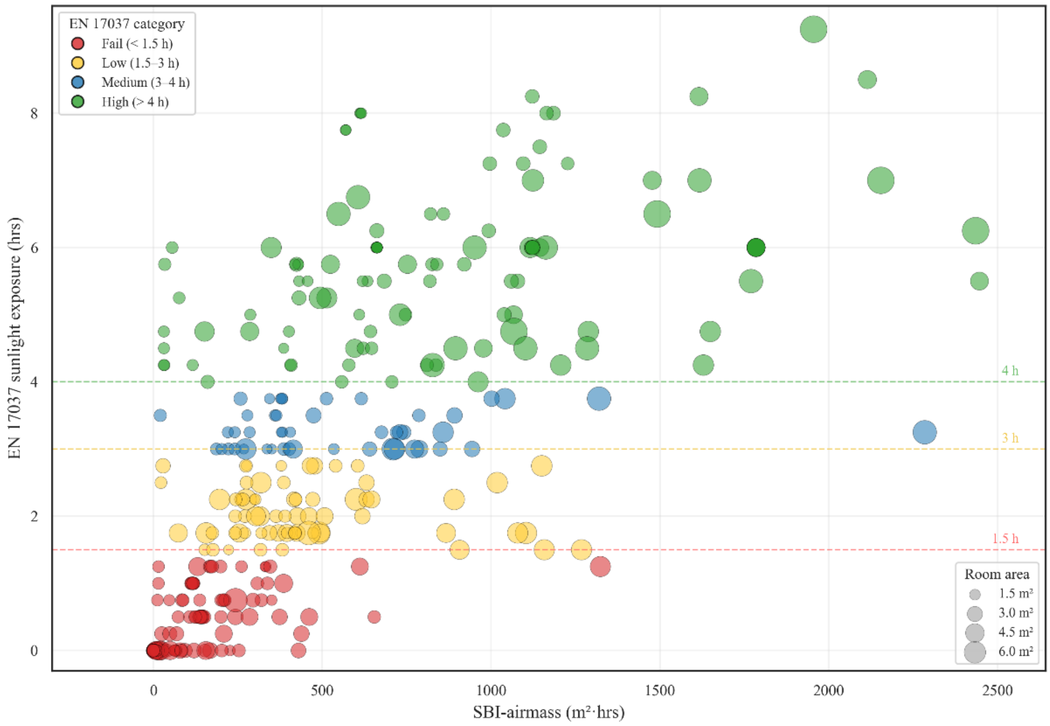

Figure 44 Relationship between SBI-airmass and EN 17037 sunlight exposure categories, with bubble size representing aperture area.

Figures 43 and 44 show that the room-based results keep the same ordered tendency observed at the aperture level. Low SBI and SBI-airmass values are mostly located in the fail and low EN 17037 sunlight exposure categories, while medium and high EN 17037 sunlight exposure categories become more frequent at higher metric values. The categories still overlap across the middle range. The airmass correction compresses the horizontal scale, but it does not produce separate EN 17037 sunlight exposure bands.

Figures 45 and 46 compare room-based SBI and SBI-airmass with ASH. The horizontal axes give SBI and SBI-airmass values, and the vertical axis gives annual sunlight hours. Bubble size represents room area.

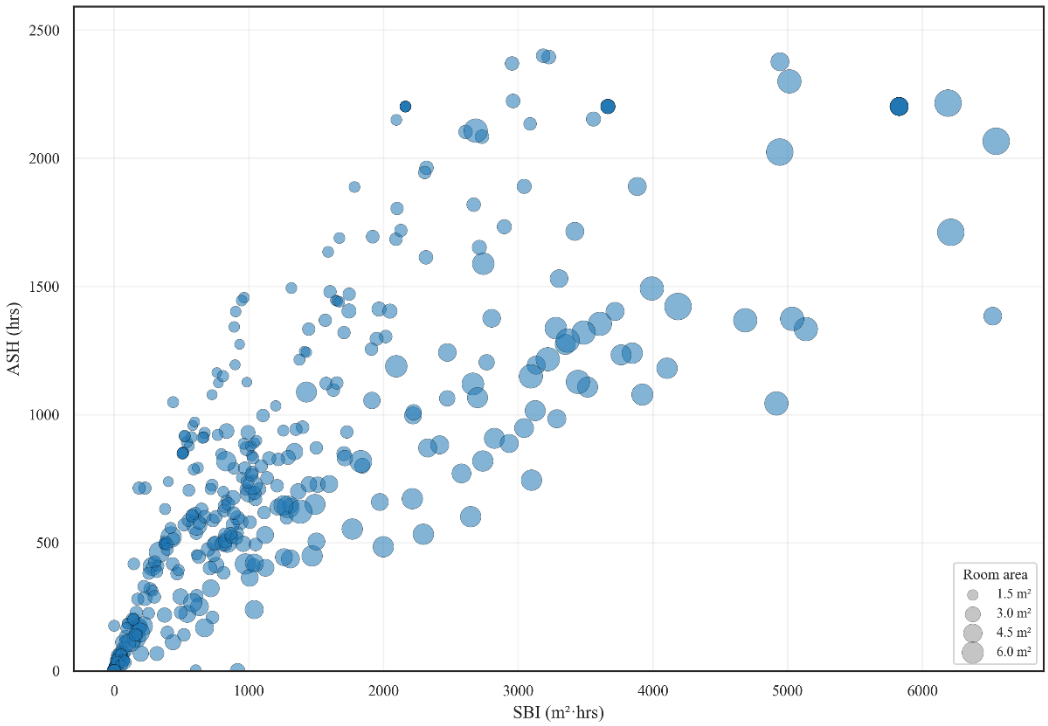

Figure 45 Relationship between SBI and ASH, with bubble size representing aperture area.

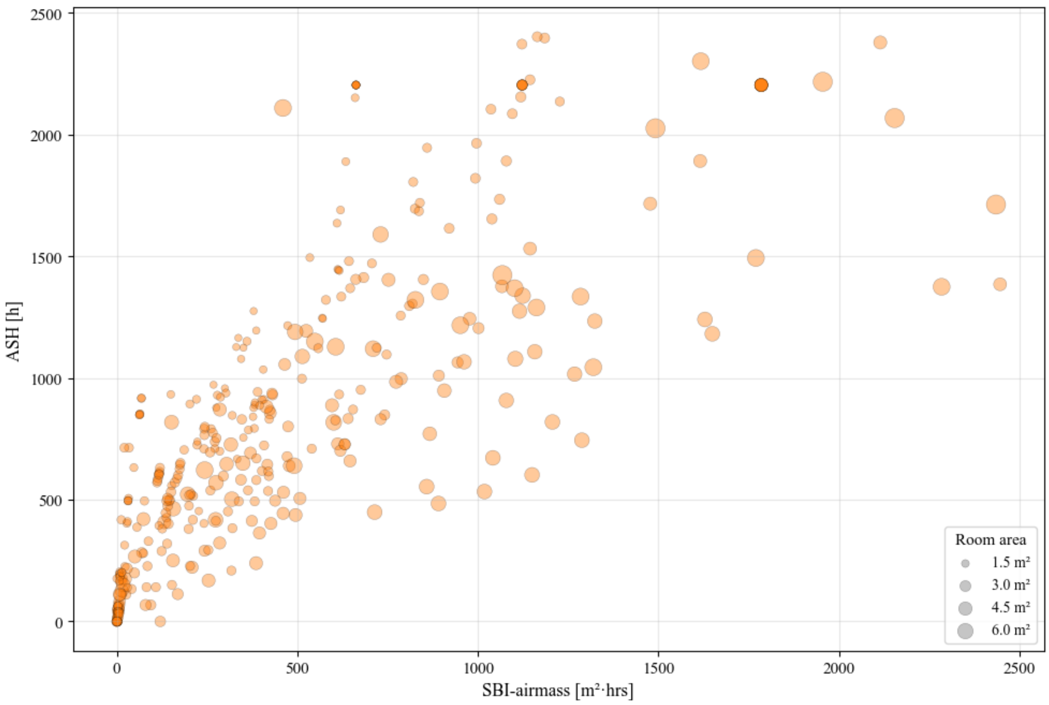

Figure 46 Relationship between SBI-airmass and ASE, with bubble size representing aperture area.

Figures 45 and 46 show a positive relationship between the aperture-based metrics and ASH. Low SBI and SBI-airmass values mostly correspond to low ASH values. Higher ASH values appear more often as SBI and SBI-airmass increase. The middle and upper ranges remain scattered, showing that annual sunlight duration and cumulative aperture exposure do not produce equivalent room-level readings.

Figure 47 compares SBI and SBI-airmass across urban density scenarios. The bars show the room-based metric values for each density group. The error bars show variation within each group.

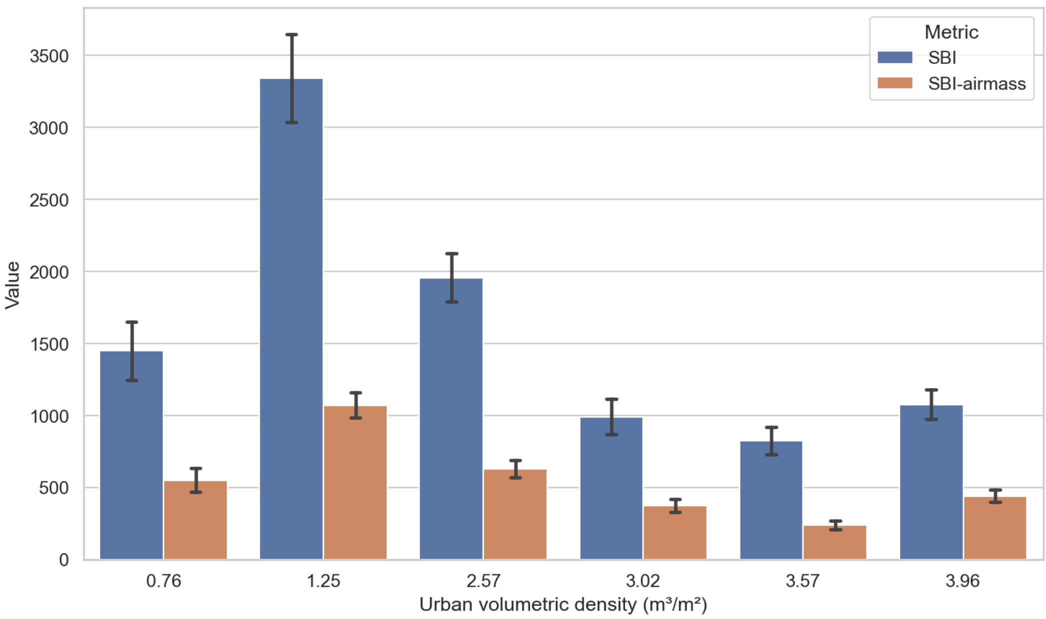

Figure 47 SBI and SBI-airmass values across different urban volumetric density scenarios based on the room analysis.

Figure 47 shows that both metrics follow the same density-related pattern. The highest values occur at the 1.25 m^3/m^2 urban density scenario. Values decrease under higher density conditions, although the 3.96 m^3/m^2 urban density scenario increases again compared with the preceding density group. SBI remains higher than SBI-airmass in every density group due to the reduced contribution of low-elevation sunlight in SBI-airmass.

Figure 48 compares room-based SBI with EN 17037 sunlight exposure and adds urban density as a colour scale. Each point represents one room. The dashed horizontal lines show the EN 17037 sunlight exposure threshold categories.

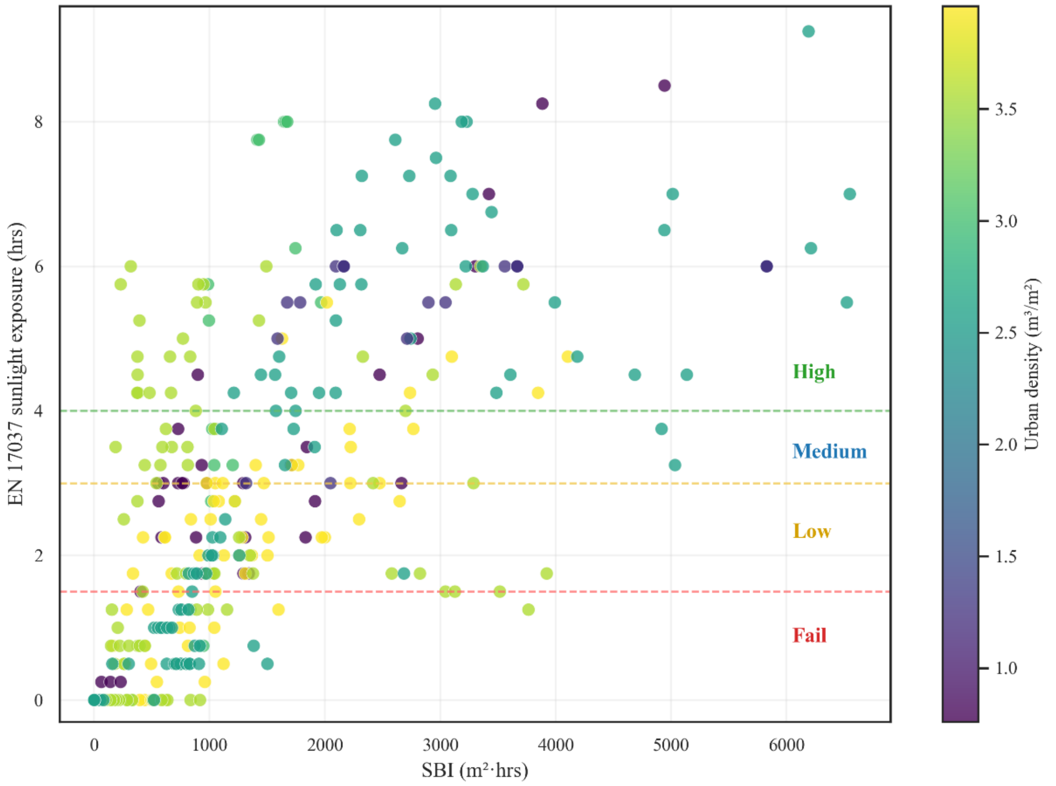

Figure 48 Relationship between SBI and EN 17037 sunlight exposure at the single-aperture level. Colours represent urban volumetric density [m³/m²], while dashed lines indicate EN 17037 sunlight exposure threshold categories.

Figure 48 shows that urban density does not separate the EN 17037 sunlight exposure categories into distinct groups. Fail, low, medium, and high EN 17037 sunlight exposure outcomes appear across several density values. Similar SBI values can also correspond to different EN 17037 sunlight exposure categories.

Compared with the single-aperture analysis, the room-based plots show wider scatter. This is caused by the aggregation method: SBI and SBI-airmass add aperture contributions, while EN 17037 sunlight exposure and ASH are based on sunlight periods within the room. The room-based analysis, therefore, keeps the same general relationships as single aperture analysis, but shows stronger separation between SBI and SBI-airmass and ASH and EN 17037 sunlight exposure after aperture aggregation.

3.3.2.2 Consistencies and inconsistencies between SBI and EN 17037 sunlight exposure in urban context

The greater dispersion observed at room level was further examined in relation to room-level aggregation parameters and urban-context conditions. Figure 49 presents the hierarchically clustered correlation matrix for the room-based dataset, including the sunlight metrics, total aperture area, number of apertures, orientation, and urban density.

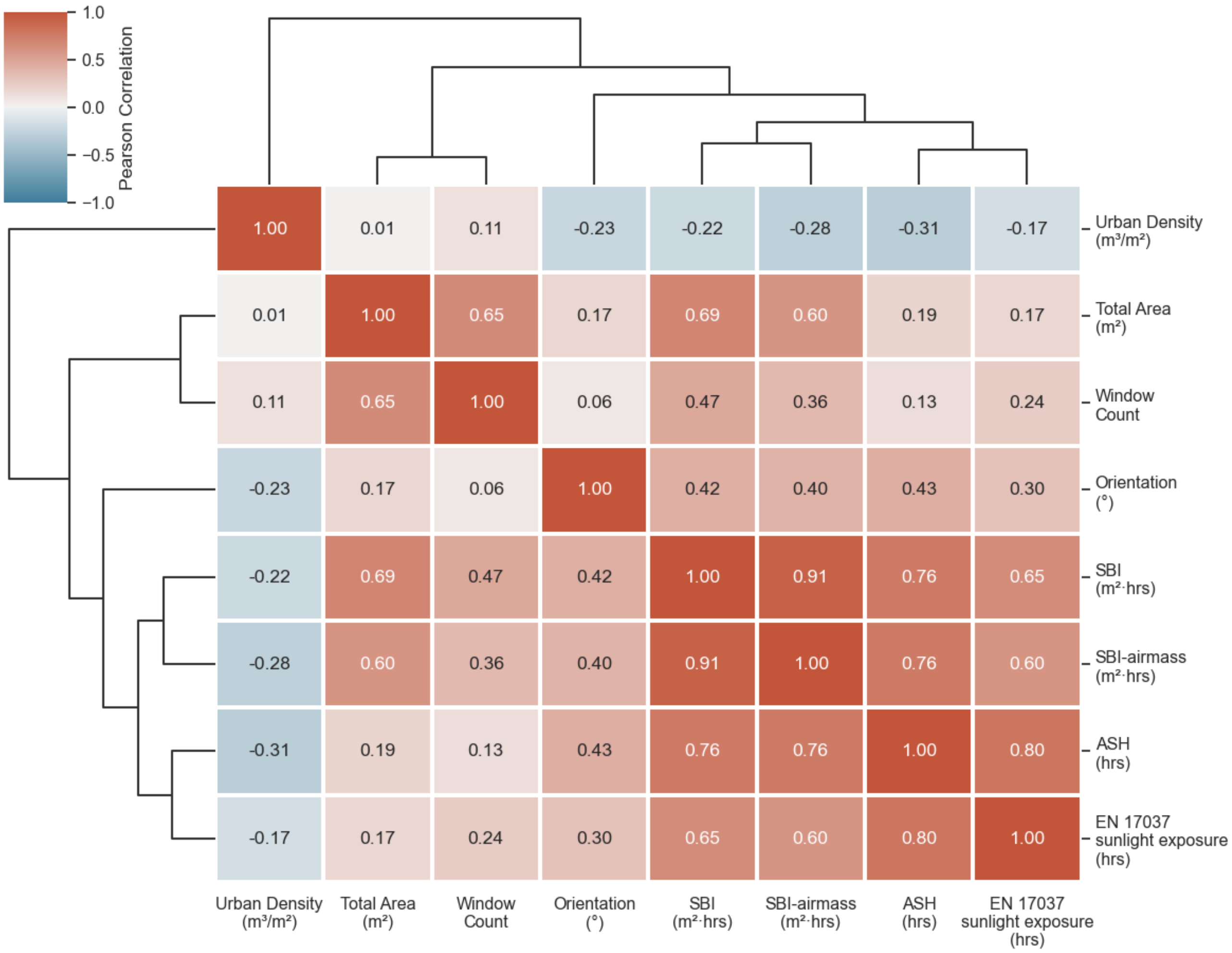

Figure 49 Hierarchically clustered correlation matrix showing relationships between sunlight metrics and selected urban and aperture design parameters in the room analysis.

At room level, the strongest relationship among the analysed sunlight metrics is observed between SBI and SBI-airmass (r = 0.91). ASH and EN 17037 sunlight exposure also show a strong correlation (r = 0.80). SBI correlates with ASH at r = 0.76 and with EN 17037 sunlight exposure at r = 0.65, while SBI-airmass correlates with ASH at r = 0.76 and with EN 17037 sunlight exposure at r = 0.60.

The hierarchical clustering reflects these relationships. SBI and SBI-airmass form one closely grouped pair, while ASH and EN 17037 sunlight exposure form a second pair. These two pairs are subsequently joined within a broader cluster of sunlight metrics. The clustered arrangement shows that the room-based dataset contains two closely related metric groupings: the two aperture-based indicators, and the two duration-based indicators.

Among the room-level aperture parameters, total aperture area shows a strong positive correlation with SBI (r = 0.69) and a moderate positive correlation with SBI-airmass (r = 0.60). Its correlations with ASH (r = 0.19) and EN 17037 sunlight exposure (r = 0.17) are substantially lower. The number of apertures shows a moderate relationship with SBI (r = 0.47) and a weaker relationship with SBI-airmass (r = 0.36). Its correlations with EN 17037 sunlight exposure (r = 0.24) and ASH (r = 0.13) remain lower. Total aperture area and number of apertures are themselves correlated at r = 0.65 and form a separate pair within the clustered matrix.

Orientation shows positive correlations with all analysed sunlight metrics. The highest correlation is observed with ASH (r = 0.43), followed by SBI (r = 0.42), SBI-airmass (r = 0.40), and EN 17037 sunlight exposure (r = 0.30). The values show a similar correlation pattern across the four-sunlight metrics, with the lowest relationship recorded for EN 17037 sunlight exposure.

Urban density shows negative correlations with all analysed sunlight metrics. The strongest negative correlation is observed for ASH (r = −0.31), followed by SBI-airmass (r = −0.28), SBI (r = −0.22), and EN 17037 sunlight exposure (r = −0.17). Urban density is also negatively correlated with orientation (r = −0.23), while its relationships with total aperture area (r = 0.01) and number of apertures (r = 0.11) are weak.

Compared with the single-aperture analysis, the room-based correlation matrix shows a lower relationship between SBI and EN 17037 sunlight exposure, decreasing from r = 0.74 at aperture level to r = 0.65 at room level. At the same time, total aperture area and number of apertures show stronger relationships with SBI than with EN 17037 sunlight exposure. The room-based results therefore show that SBI and EN 17037 sunlight exposure remain positively related, while their correlation is reduced after results are aggregated across multiple apertures.

To further examine the relationships observed in the room-based dataset, a Random Forest model was applied to predict EN 17037 sunlight exposure using the analysed sunlight-access metrics and selected room-level and urban-context parameters. The feature-importance ranking obtained from the model is presented in Figure 50.

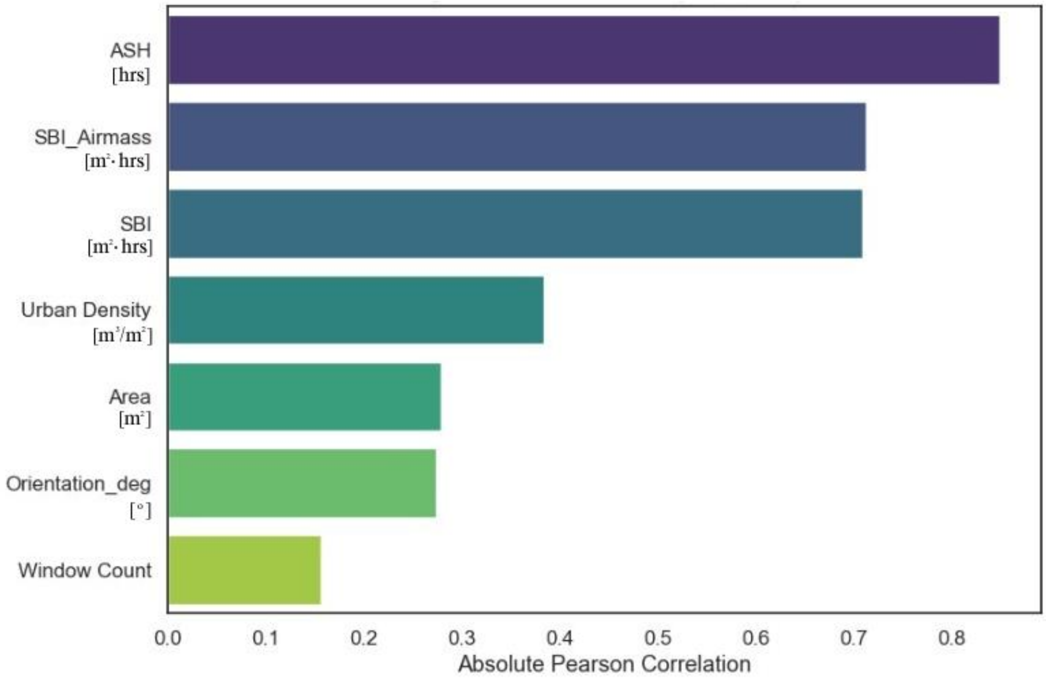

Figure 50 Feature-importance ranking derived from the Random Forest model predicting EN 17037 sunlight exposure at the room level, based on sunlight-access metrics and selected room-level and urban-context parameters.

The Random Forest feature-importance analysis shows that ASH has the highest importance value in the room-level model (0.86). SBI-airmass and SBI follow with similar importance values, both reaching approximately 0.72. The remaining variables rank lower: urban density reaches an importance value of 0.38, total aperture area and orientation each reach approximately 0.28, and number of apertures records the lowest importance value, at approximately 0.16.

The ranking identifies ASH, SBI-airmass, and SBI as the three highest-ranked variables in the model predicting EN 17037 sunlight exposure at room level. Among the selected room-level and urban-context parameters, urban density has the highest importance value, followed by total aperture area and orientation, while number of apertures has the lowest value among all variables included in the model.

4 Discussion

4.1 Interpretation of results in relation to research questions

4.1.1 RQ: How are SBI, SBI-airmass, and other traditional sunlight metrics affected by aperture size, geometry, orientation, and surrounding obstructions?

As presented in Table 5 and figures 15, 16, 17, 19, 21, 23, 25, and 27, SBI and SBI-airmass respond directly to geometric parameters, while EN 17037 sunlight exposure and ASH are governed by exposure duration. This difference is reflected in the continuous variation of SBI and SBI-airmass with aperture size, orientation, and obstruction, whereas EN 17037 sunlight exposure and ASH remain unchanged or respond only under specific conditions. The observed behaviour indicates that SBI-type metrics reflect geometric modification in their values, while traditional metrics do not consistently represent these geometric variations.

A shown in Figure 30, aperture area is the primary determinant of SBI and SBI-airmass. Increases in aperture size lead to proportional increases in accumulated sunlight access, which establishes a direct relationship between opening extent and metric value. Orientation modifies the timing and distribution of exposure, although variability within identical orientations shows that orientation alone does not determine sunlight access.

EN 17037 sunlight exposure and ASH show limited sensitivity to changes in aperture size and geometry, while ASE does not respond consistently to geometric variation within the analysed scope. EN 17037 sunlight exposure and ASH rely on point-based visibility of direct sunlight, whereas ASE is defined through threshold exceedance within the interior space and depends on factors beyond aperture geometry, including interior conditions and material properties. As a result, changes in aperture size or form do not produce proportional or predictable changes in ASE.

SBI and SBI-airmass quantify the extent of direct sunlight passing through an opening over time, EN 17037 sunlight exposure and ASH represent the duration of direct sunlight visibility, and ASE captures conditions of excessive interior exposure based on threshold criteria. This difference in definition leads to divergent interpretations under identical geometric conditions.

SBI and SBI-airmass provide a direct and continuous response to geometric variation, which supports their use in design analysis. The consistent relationship between geometric input and metric output allows changes in aperture configuration to be reflected in the results. In contrast, the limited response of EN 17037 sunlight exposure and ASH, and the dependence of ASE on interior conditions, restrict their ability to capture the effect of geometric modification in such analyses.

4.1.2 SQ.1: How do SBI and SBI-Airmass compare with the sunlight access metrics in EN 17037, ASE and ASH?

SBI and SBI-airmass differ from EN 17037 sunlight exposure, ASH, and ASE because they quantify direct sunlight access through aperture area and time. EN 17037 sunlight exposure and ASH use point-based sunlight duration, so their values can remain unchanged under changes in aperture geometry.

ASH is closer to SBI than EN 17037 sunlight exposure because it uses an annual evaluation period. It records the duration of direct sunlight across the year and therefore follows several of the same directional trends as SBI. Its response remains lower because it does not account for the sunlit area of the aperture and the angular incidence of direct sunlight.

ASE has a different basis. It measures interior illuminance threshold exceedance and depends on room geometry, surface reflectance, sensor-grid configuration, and aperture properties. Its results are therefore not directly comparable with the aperture-based metrics.

The metrics produce different result structures for the same geometric inputs (Figure 28). SBI and SBI-airmass change with orientation, aperture area, setback, slope, and shading. EN 17037 sunlight exposure behaves as a bounded criterion-based metric, as it responds mainly through point-based sunlight duration. ASH shows annual duration-based variation. ASE responds only in cases where the illuminance threshold is exceeded.

The comparison shows that SBI and SBI-airmass are not equivalent to EN 17037 sunlight exposure, ASH, or ASE (Figure 29 and 30). The aperture-based metrics make use of sunlit aperture area and exposure time. EN 17037 sunlight exposure and ASH describe sunlight duration at a point. ASE describes interior threshold exceedance. These differences explain why the same shoebox configurations produce different metric responses across the analysed cases.

4.1.2.1 Individual comparison cases and Temporal maps of SBI

4.1.2.1.1 Similar annual SBI with different EN 17037 sunlight exposure results

Figures 51 and 52 present the SBI and SBI-airmass temporal maps for Room_1 and Room_2. Room_1 has one south-oriented aperture and Room_2 has one east-oriented aperture. This comparison examines how two rooms with small annual SBI and SBI-airmass differences can show different seasonal and hourly sunlight patterns.

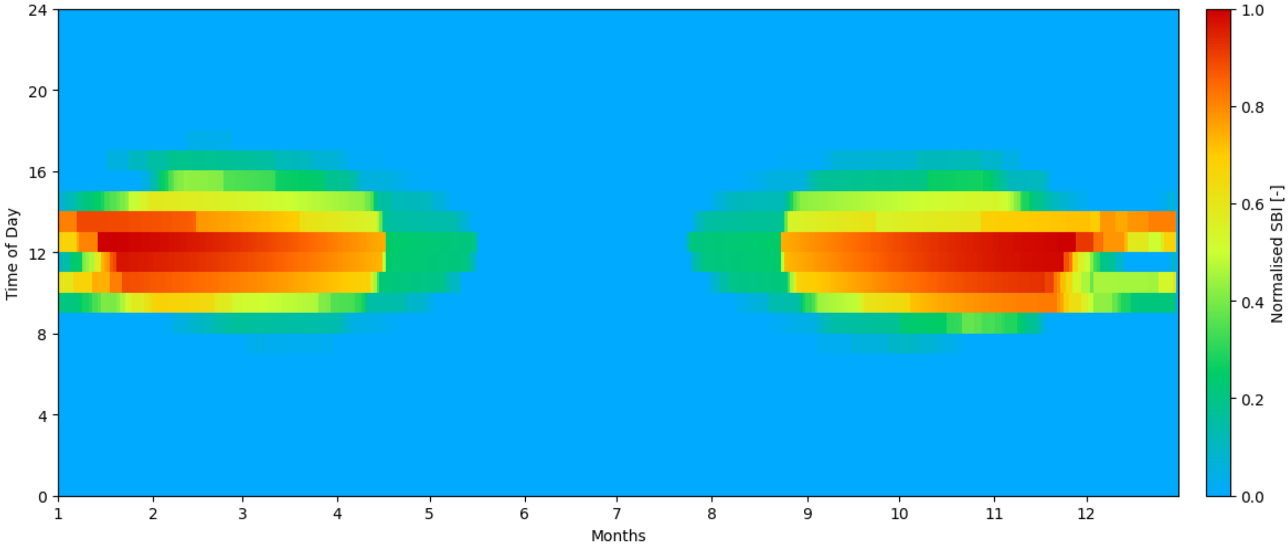

Figure 51 Temporal map distribution of normalised SBI values across the year - Room 1.

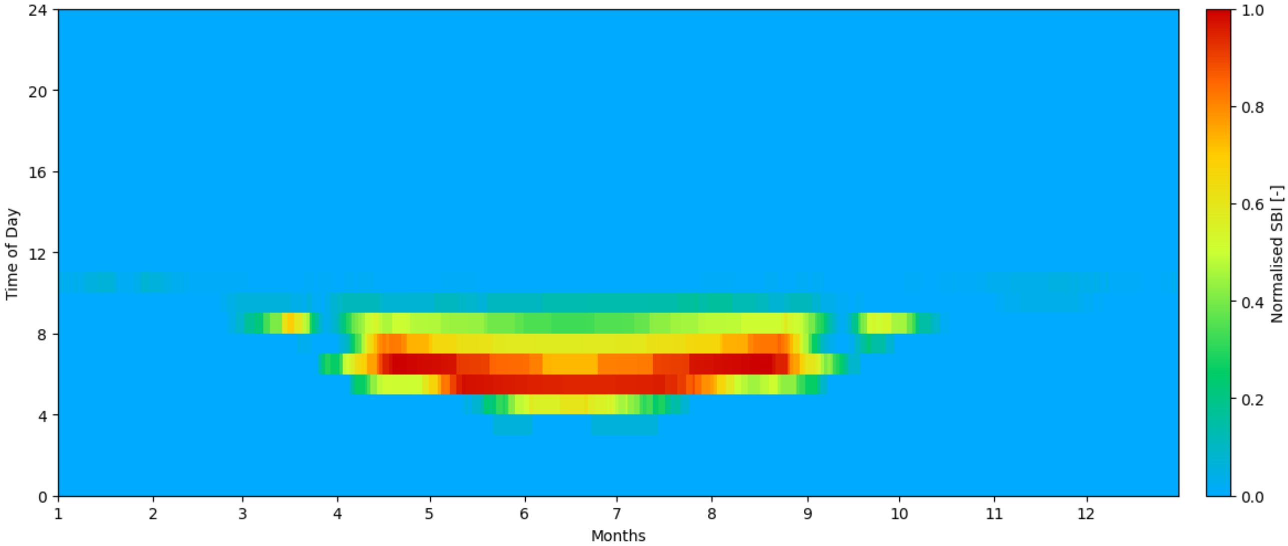

Figure 52 Temporal map distribution of normalised SBI values across the year - Room 2.

Room_1 records an SBI of 1 656.83 m²·h and an SBI-airmass value of 613.72 m²·h, and Room_2 records an SBI of 1 597.26 m²·h and an SBI-airmass value of 611.56 m²·h. The difference is 59.57 m²·h for SBI and 2.16 m²·h for SBI-airmass.

Room_1 and Room_2 have different EN 17037 sunlight exposure results. Room_1 records 8.00 h, and Room_2 records 1.25 h, producing a difference of 6.75 h between the two cases. Room_2 remains below the 1.5 h minimum threshold, despite having annual SBI and SBI-airmass totals with small numerical differences from Room_1.

The per-area values show that annual values with small numerical differences can still come from different aperture efficiencies. Room_1 has approximately 184.09 h for SBI and 68.19 h for SBI-airmass, and Room_2 has approximately 63.89 h for SBI and 24.46 h for SBI-airmass. The smaller aperture therefore receives more direct sunlight per unit area.

The temporal maps show the monthly and hourly distribution behind the normalised SBI values. Room_1 receives direct sunlight mostly from January to April and September to December, with the highest values around late morning to early afternoon. Room_2 receives direct sunlight mostly from April to September, with the strongest values concentrated in the morning period. EN 17037 sunlight exposure evaluates sunlight access within the period from 1 February to 21 March. The difference in seasonal performance can be appreciated from the temporal maps: small differences in annual SBI can correspond to more winter sunlighting in one case and more summer sunlighting in the other. This distinction matters because winter sunlight can support comfort and passive solar gains, but summer sunlight can increase overheating risk. The temporal map therefore acts as a proxy for interpreting seasonal building performance beyond the SBI value.

4.1.2.1.2 Similar SBI per aperture area with different EN 17037 sunlight exposure categories

Figures 53 and 54 present the SBI and SBI-airmass temporal maps for Aperture_1 and Aperture_2. This comparison examines two apertures with similar annual and per-area SBI values, but different EN 17037 sunlight exposure threshold categories.

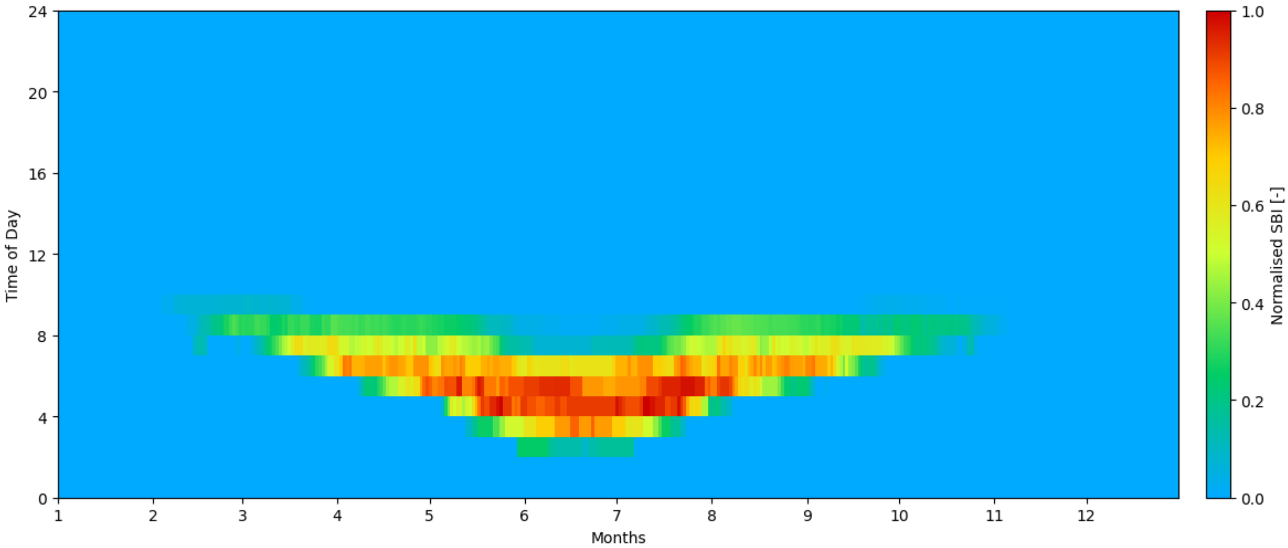

Figure 53 Temporal map distribution of normalised SBI values across the year - Aperture 1.

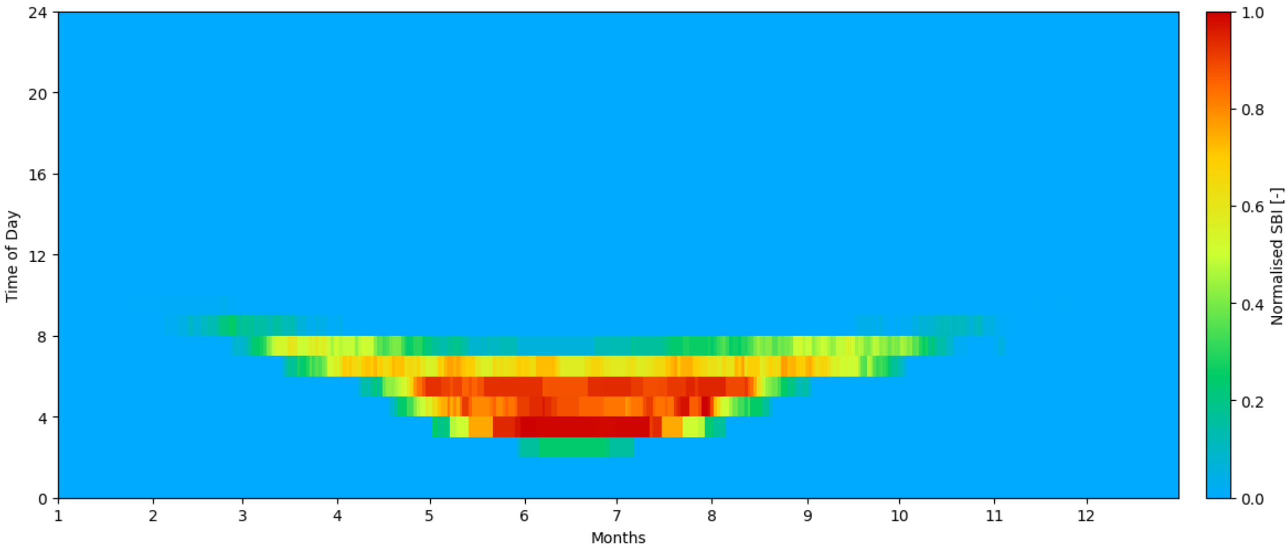

Figure 54 Temporal map distribution of normalised SBI values across the year - Aperture 2.

Aperture_1 and Aperture_2 pairing rank 63rd in similarity within the collected dataset of 128 778 aperture pairings when annual SBI and SBI-airmass totals are evaluated together under percentage difference. Aperture_1 records an SBI of 1 457.30 $m^2 \cdot h$ and an SBI-airmass value of 632.11 $m^2 \cdot h$, and Aperture_2 records an SBI of 1 501.22 $m^2 \cdot h$ and an SBI-airmass value of 654.16 $m^2 \cdot h$. The difference is 43.92 $m^2 \cdot h$ for SBI and 22.05 $m^2 \cdot h$ for SBI-airmass.

Aperture_1 and Aperture_2 have SBI and SBI-airmass values per unit aperture area with percentage differences on the lower side of the collected dataset. Aperture_1 records 697.27 h for SBI and 302.44 h for SBI-airmass, and Aperture_2 records 701.50 h for SBI and 305.68 h for SBI-airmass.

Aperture_1 and Aperture_2 have EN 17037 sunlight exposure results that differ across threshold categories. Aperture_1 records 3.75 h, and Aperture_2 records 0.50 h, producing a difference of 3.25 h between the two cases. Aperture_1 exceeds the 3.0 h good threshold, and Aperture_2 remains below the 1.5 h minimum threshold.

The temporal maps show comparable SBI distributions for Aperture_1 and Aperture_2, with direct sunlight presence from March to April. The EN 17037 sunlight exposure results place the two apertures in different threshold categories. SBI records sunlit aperture area over time, and EN 17037 sunlight exposure computes sunlight access at point P during its reference period. The area-based SBI calculation can register direct sunlight contributions from sunlit aperture regions that are not captured by the point-based EN 17037 sunlight exposure result. One can appreciate that similar annual SBI values, similar SBI values per square metre, and comparable temporal map distributions can still correspond to different EN 17037 sunlight exposure threshold categories. The value of the temporal maps comes from making the seasonal distribution of SBI visible, which clarifies how similar the two aperture-based results are across the year.

4.1.2.1.3 Similar room-level SBI with different EN 17037 sunlight exposure outcomes

Room_3 has one east-facing (Figure 55) and one north-facing aperture, and Room_4 has two north-facing apertures. Figure 55 shows the temporal map of the east-facing aperture in Room_3. This comparison examines a room pair with a small SBI difference and different EN 17037 sunlight exposure threshold outcomes.

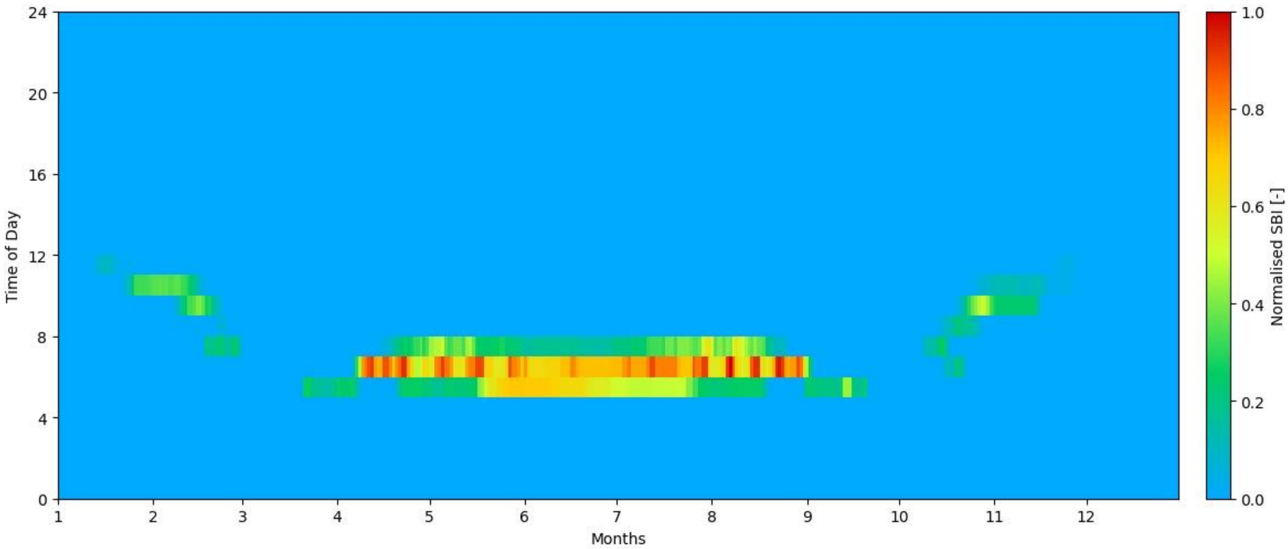

Figure 55 Temporal map distribution of normalised SBI values across the year – east-facing aperture.

Room_3 and Room_4 produce SBI totals separated by 2.67 m²·h. Room_3 records an SBI of 185.31 m²·h, and Room_4 records 182.64 m²·h. The difference between the two rooms is 2.67 m²·h. Room_3 and Room_4 produce different SBI-airmass totals despite the small SBI difference. Room_3 records an SBI-airmass value of 20.41 m²·h, and Room_4 records 13.82 m²·h. The difference between the two rooms is 6.59 m²·h.

Room_3 and Room_4 have different EN 17037 sunlight exposure results. Room_3 records 3.50 h, and Room_4 records 0.00 h. Room_3 exceeds the 3.0 h good threshold, and Room_4 remains below the 1.5 h minimum threshold.

The SBI totals remain close because the metric aggregates sunlit aperture area across both openings over the year. EN 17037 sunlight exposure combines non-overlapping sunlight durations from multiple apertures at point P. In Room_3, the east-facing aperture contributes the recorded sunlight duration, and Room_4 does not produce a corresponding non-overlapping contribution and remains at 0.00 h despite a similar annual SBI total.

The temporal map of the east-facing aperture (Figure 55) shows a short period of direct sunlight during February and March. This period has limited duration and lower normalised SBI values than the stronger annual pattern later in the year. It overlaps with the EN 17037 sunlight exposure reference period and helps contextualise the 3.50 h result for Room_3. By making the seasonal distribution visible, the map shows how Room_3 and Room_4 can produce closely matched room-level SBI values, yet a short point-accessible period within the EN 17037 sunlight exposure evaluation window is enough to place Room_3 in a different threshold category.

4.1.2.1.4 Similar room-level SBI with different aperture orientation patterns

Room_5 has one west-facing (Figure 56) and one north-facing aperture, and Room_6 has one north-west-facing aperture. Figure 56 shows the temporal map of the west-facing aperture in Room_5. This comparison examines a room pair with similar room-level SBI values and different aperture orientation patterns.

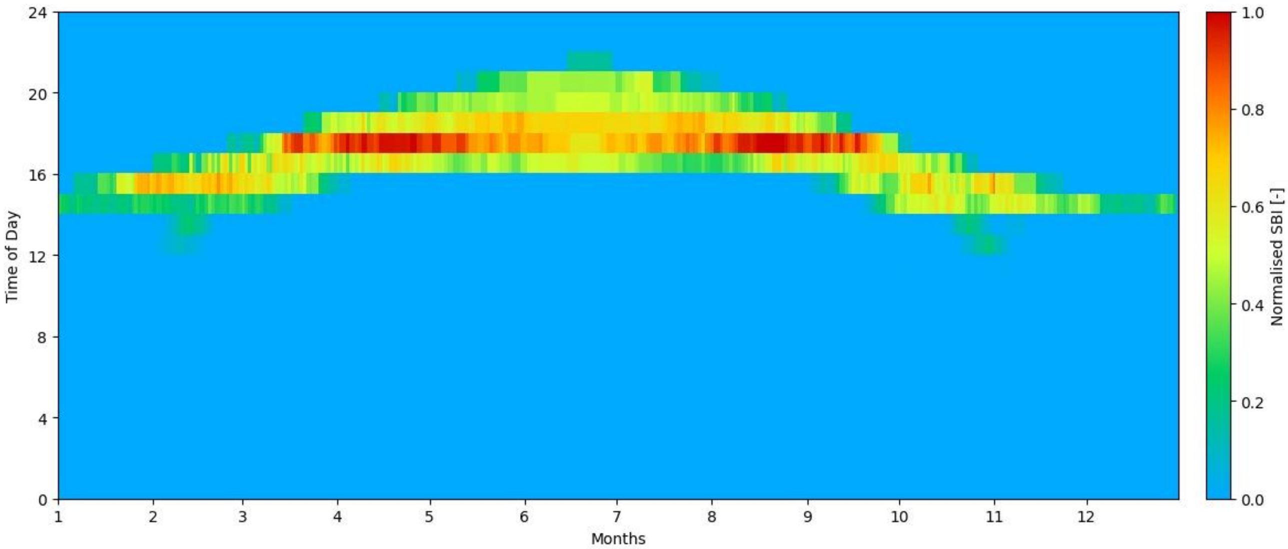

Figure 56 Temporal map distribution of normalised SBI values across the year – west-facing aperture.

Room_5 and Room_6 produce SBI totals with a difference of 5.57 m²·h. Room_5 records an SBI of 831.64 m²·h, and Room_6 records 826.07 m²·h. Room_5 and Room_6 produce SBI-airmass totals with a difference of 1.49 m²·h. Room_5 records an SBI-airmass value of 151.38 m²·h, and Room_6 records 149.89 m²·h.

Room_5 and Room_6 have EN 17037 sunlight exposure results that differ across threshold categories. Room_5 records 4.75 h, and Room_6 records 0.50 h, producing a difference of 4.25 h. Room_5 exceeds the 4.0 h high recommended threshold, and Room_6 remains below the 1.5 h minimum threshold.

The temporal map (Figure 56) shows sunlight presence across the year for the west-facing aperture in Room_5. In the EN 17037 sunlight exposure result, the recorded sunlight duration for Room_5 comes from the west-facing aperture. Room_6 has a single north-west-facing aperture and records 0.50 h, despite producing an annual SBI total close to Room_5.

The temporal map also shows the seasonal and hourly structure behind the west-facing contribution in Room_5. Direct sunlight is distributed across a broad part of the year and occurs mainly in the afternoon. This distribution includes visible early-year exposure, and that period overlaps with the EN 17037 sunlight exposure reference period. The comparison therefore shows how two rooms can produce closely matched SBI values yet differ strongly in EN 17037 sunlight exposure because the point-based duration depends on whether point P receives direct sunlight within the reference period.

4.1.2.1.5 Same EN 17037 sunlight exposure results with different annual SBI values

Figures 57 and 58 present the normalised SBI temporal maps for Aperture_3 and Aperture_4. This comparison examines two apertures that return the same EN 17037 sunlight exposure result but differ in annual SBI, SBI per square metre, and temporal distribution. Aperture_3 and Aperture_4 return the same EN 17037 sunlight exposure result. Both apertures record 6.00 h, resulting in a pair difference of 0.00 h. Both values exceed the 4.0 h high recommendation level.

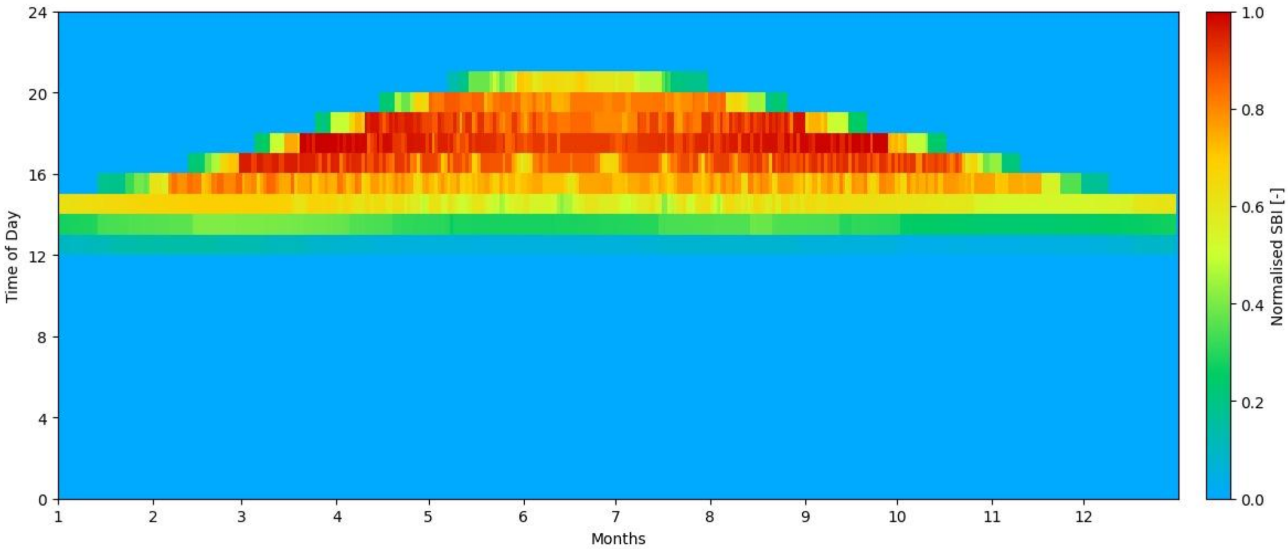

Figure 57 Temporal map distribution of normalised SBI values across the year - Aperture 3.

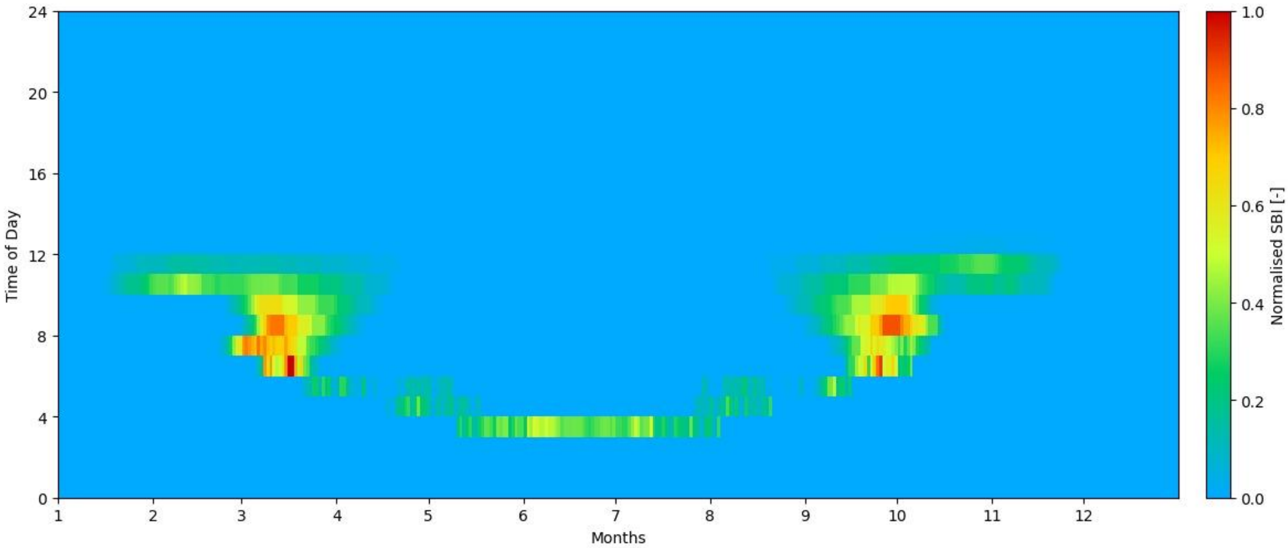

Figure 58 Temporal map distribution of normalised SBI values across the year - Aperture 4.

Aperture_3 and Aperture_4 produce different annual SBI values. Aperture_3 records 183.67 m^2·h. Aperture_4 records 3 665.73 m^2·h. The pair difference is 3 482.06 m^2·h. The difference also appears in the SBI values per unit aperture area. Aperture_3 records 197.49 h, based on an aperture area of 0.93 m^2. Aperture_4 records 1 352.67 h, based on an aperture area of 2.71 m^2.

The temporal maps show different annual distributions of normalised SBI. Aperture_3 shows a broad annual sunlight pattern, extending from the early-year period into late autumn. Aperture_4 shows more limited sunlight presence, concentrated mainly in February and March and again in September and October. The EN 17037 exposure to sunlight assessment uses the early-year reference period from 1 February to 21 March, and both apertures show direct sunlight presence during this part of the year. This overlap helps contextualise why both apertures can record 6.00 h under EN 17037 sunlight exposure, even though their annual SBI distributions are different.

One can appreciate from this case that two apertures can both exceed the 4.0 h high recommendation level under EN 17037 sunlight exposure and still differ in SBI. Aperture_4 records an SBI value 19.96 times higher than Aperture_3. The per-area value of Aperture_4 is 6.85 times higher than the per-area value of Aperture_3. The temporal maps add the necessary seasonal reading of this difference. The identical EN 17037 sunlight exposure result does not describe the annual distribution of direct sunlight across the aperture.

4.1.3 SQ.2: How can SBI and SBI-Airmass influence early design decisions and urban planning?

SBI and SBI-airmass can support early-stage geometric design decisions at building, façade, and aperture level because their calculation is based on spatial configuration (Table 5; Figures 15-27). They allow direct sunlight access to be assessed during the definition of orientation, aperture size, setback, and external obstruction. Solar exposure can therefore inform the development of building form before later stages of design.

SBI supports the formulation of geometric design rules for early-stage decision-making. The relationship between spatial configuration and sunlight access can be used to define conditions for aperture placement, building spacing, and orientation in relation to solar exposure.

SBI can reduce the design solution space by filtering out geometries that do not meet minimum solar access conditions. Early identification of non-performing options supports a more efficient progression towards viable design solutions.

SBI therefore provides a geometric basis for assessing solar access across urban planning and architectural design, as shown by the single-aperture and room-based urban analyses (Figures 39 and 49; see also Appendix B, Table 1 and Appendix C, Table 1). Its application supports consistency between decisions made at the scale of the urban layout and those developed at the building level.

4.2 Proposal for SBI Thresholds

4.2.1 Provisional threshold transfer equation from EN 17037 sunlight exposure to SBI

As a recently proposed metric, SBI is not currently benchmarked, and no advisable targets are proposed. These would require quite extensive surveys. However, a proposal for thresholds could be based on anchoring SBI to the current EN 17037 sunlight exposure targets.

This subsection presents a conceptual method for transferring EN 17037 sunlight exposure thresholds to SBI. The method defines a transferable formulation rather than a fixed threshold. The objective is to establish the structure of the conversion across EN 17037 sunlight exposure levels, without deriving calibrated thresholds.

The EN 17037 sunlight exposure thresholds of 1.50 h, 3.00 h, and 4.00 h are used as reference conditions. These correspond to the fail/pass boundary, medium, good and high levels. The thresholds are defined within a seasonal evaluation period and do not represent annual sunlight availability.

A direct annualization of these values is obtained as H_EN × 365. This results in 547.50 h for 1.50 h, 1 095.00 h for 3.00 h, and 1 460.00 h for 4.00 h. This step assumes uniform daily transfer across the year. The assumption is not consistent with the seasonal basis of EN 17037 sunlight exposure and introduces an overestimation of annual equivalent exposure.

To address this, a seasonal transfer factor k_s is introduced. This factor reduces the annualised values to account for the difference between the EN 17037 sunlight exposure evaluation period and annual solar availability. The factor is location-dependent and relates to solar path and availability. A fixed value is not derived in the present study. The formulation therefore retains k_s as a variable.

The conversion is expressed using a reference aperture area A_ref. EN 17037 sunlight exposure is evaluated at point level and does not depend on aperture size, while SBI is directly proportional to aperture area. The introduction of A_ref provides a bridge between these definitions. The reference area represents a typical or average aperture size associated with the evaluated space. A fixed value is not imposed in the present study. The parameter is retained as a variable due to the variability of aperture sizes across buildings and contexts.

An angular transfer factor k_theta is introduced to account for incidence-angle effects in the conversion from time-based EN 17037 sunlight exposure thresholds to aperture-based SBI. This factor represents the reduction in effective exposure due to non-perpendicular solar incidence on the aperture. It captures the average projection of solar rays onto the aperture surface over the evaluation period. The factor is dependent on solar geometry, orientation, and location, and is therefore retained as a variable in the formulation.

The resulting transfer is expressed as:

$$SBI\_th = H\_EN \times 365 \times k\_s \times A\_ref \times k\_theta \quad (3)$$

For the EN 17037 sunlight exposure thresholds, the corresponding expressions are:

$$SBI\_1.5h = 1.5 \times 365 \times k\_s \times A\_ref \times k\_theta \quad (4)$$
$$SBI\_3.0h = 3.0 \times 365 \times k\_s \times A\_ref \times k\_theta \quad (5)$$
$$SBI\_4.0h = 4.0 \times 365 \times k\_s \times A\_ref \times k\_theta \quad (6)$$

The thresholds are therefore expressed as functions of k_s, A_ref, and k_theta, not as fixed values. The formulation defines a consistent transfer structure between EN 17037 sunlight exposure levels and SBI.

The resulting thresholds depend on the values of k_s, A_ref, and k_theta, all of which vary with location, solar geometry, and aperture configuration. The method is presented as a provisional approach, and its validity is limited by the differences between EN 17037 sunlight exposure and SBI identified in this study.

4.3 Limitations of the study

The analyses carried out were divided into two stages: the shoebox reference model and the analysis of real-case models. The introduction of the shoebox model allowed for the control of geometric variables but limited the generalisability of the results to more complex spatial configurations.

The analysis of real-case models was carried out based on available models, the surrounding area of which was in most cases limited to a radius of 100.0 m from the subject building. This limitation was due to data availability and may have affected the accuracy of the representation of shading conditions on a larger urban scale. The individual models differed in terms of their environmental configuration; consequently, the influence of context was not analysed in a standardised manner. In addition, neighbouring buildings were modelled as simplified geometric solids, without considering architectural details such as balconies, recesses or shading elements. This simplifies the analysis and facilitates the comparison of cases but may lead to an underestimation of local shading.

Analyses based on real-case models were carried out at two levels: the single aperture and the room. At the single-aperture level, each window was analysed individually, regardless of whether it was accompanied by additional architectural elements such as balconies, recesses or adjacent walls. This means that the results at this level of analysis maintain the local variability of exposure conditions, but do not always allow for a complete separation of the influence of individual geometric features.

In the case of certain contextual variables, their representation was simplified. Also, the urban density index was treated as a general contextual feature; not all local spatial differences could be represented in quantitative terms.

ASE results are contingent on the assumed interior model, including surface properties and computational grid configuration. As such, comparison with aperture-based metrics (SBI and SBI-airmass) is, by definition, methodological and not directly equivalent.

The analysis relies exclusively on numerical simulations and lacks validation under real-world conditions, representing a limitation in sunlight access modelling studies.

5 Conclusions

This thesis concerned the evaluation of SBI and SBI-airmass as aperture-based indicators of sunlight access, with emphasis on their response to aperture geometry, orientation, and external obstruction, their relationship to EN 17037 sunlight exposure, ASE, and ASH, and their possible use in early-stage design assessment where only geometric information is available.

The analysis establishes that SBI and SBI-airmass are governed directly by aperture geometry, orientation, and external obstruction. The results show that variations in aperture surface area, angular orientation, and surrounding shading conditions produce direct and proportional changes in the calculated values, which indicates that the metrics respond consistently to geometric input parameters.

SBI and SBI-airmass exhibit consistent responses to geometric variation across the analysed conditions. Across the parametric cases, aperture area acts as the main driver, orientation governs the temporal distribution of exposure, and obstruction reduces the effective sunlit portion of the aperture through shading, while SBI-airmass moderates this response by reducing the contribution of low-angle solar rays.

SBI and SBI-airmass differ structurally from EN 17037 sunlight exposure and ASH, which rely on point-based evaluation, through their area-based and continuous temporal formulation that integrates both the duration and spatial extent of direct sunlight exposure into a single annual value. This formulation produces a representation that combines exposure across both time and aperture extent within a single metric.

SBI and SBI-airmass require temporal distribution data to interpret annual behaviour, as the results alone do not indicate when sunlight occurs or how its magnitude varies over time. The annual values therefore require interpretation through temporal maps to reveal the seasonal and diurnal distribution of sunlight exposure and to identify periods of concentration or absence within the aggregated result.

SBI and SBI-airmass are applicable in early-stage design conditions based on geometric inputs and extend beyond apertures to evaluate sunlight access across exterior surfaces and openings. Their formulation allows evaluation under conditions where only geometric information is available and enables the assessment of sunlight access at the level of façades or other exterior elements within an urban context.

- SBI and SBI-airmass are directly affected by aperture geometry, orientation, and external obstruction.

- SBI and SBI-airmass outperformed EN 17037 sunlight exposure, ASH, and ASE as they provided both an overall yearly distribution of sunlight access and a better representation of sunlight access for rooms with more than one opening.

- SBI temporal maps support the interpretation of SBI by visualising the annual distribution of direct sunlight on an aperture. The comparisons suggest that EN 17037 sunlight exposure alone does not fully capture the annual and temporal characteristics of sunlight exposure.

  SBI and EN 17037 sunlight exposure showed similar general trends, but these trends did not always lead to the same EN 17037 sunlight exposure threshold category or SBI-based interpretation.

- SBI and SBI-airmass showed potential for early-stage design assessment where only geometric information is available.

5.1 Practical applicability and limitations

SBI and SBI-airmass can support design decisions at stages where detailed building information is not yet available. In this context, SBI and SBI-airmass can be used as comparative indicators to test how changes in geometric configuration affect direct sunlight access.

The method is feasible within a parametric modelling environment, as demonstrated through the Rhino–Grasshopper and Python implementation used in this thesis. This makes it suitable for design studies, option testing, and research-based evaluation. Routine use in architectural or urban design practice would require a simplified interface, clear input conventions, an optimised computational script, and interpretation ranges that allow designers to understand the results without detailed case-by-case analysis.

The urban-context analysis is based on available case models and simplified surrounding geometry. Vegetation was not represented in the obstruction geometry. This may affect the calculated exposure values in cases where trees or other landscape elements contribute to local shading.

The interpretation of SBI and SBI-airmass is limited by the current lack of established performance thresholds. Current research does not yet define how their values should be interpreted in terms of sufficient exposure, excessive exposure, comfort, health, or energy performance. Their annual values benefit from interpretation through temporal maps, because a single aggregated value does not show when sunlight occurs during the year or during the day.

Further development could proceed in three directions. Larger datasets would allow SBI and SBI-airmass to be tested across more climates, building types, and urban forms. Temporal interpretation could be developed further so that annual SBI values can be read together with seasonal and hourly exposure patterns. Threshold development would also be needed before SBI and SBI-airmass can move from comparative assessment towards practical evaluation criteria.

6 Future work

6.1 Possible directions for further research

The direction for further work does not extend the formulation of the Sunlight Beam Index (SBI) or its airmass variant, as both are already defined through a complete geometric and temporal aggregation of direct sunlight at the aperture level (Mardaljevic and Roy, 2016). SBI quantifies the cross-sectional area of beam sunlight passing through an opening and aggregates this quantity over time, producing an annual measure of geometric solar access. The future work is therefore located in how these quantities are interpreted, positioned in relation to existing methods, and translated into design use within design and planning contexts.

A first line of investigation concerns the interpretation of SBI as a performance-relevant indicator. SBI describes the geometrical capacity of an aperture to admit direct sunlight over time, expressed as an accumulated beam cross-section. This definition remains independent of interior conditions and therefore does not directly indicate whether a space receives sufficient or excessive sunlight. The relationship between this geometric measure and environmental performance is therefore unresolved. Previous work has shown that existing sunlight metrics fail to provide a consistent aggregate description of sunlight potential across geometries (Mardaljevic and Roy, 2016), yet the translation of SBI into performance domains remains open. Future work should examine how SBI and SBI-airmass relate to conditions associated with adequate sunlight exposure, overexposure, and secondary effects such as thermal gains or visual discomfort. Without this step, SBI remains a descriptive metric, with its implications for building performance left undefined.

A second direction addresses the positioning of SBI within existing sunlight evaluation methods. Current approaches differ in both spatial and temporal formulation. EN 17037 sunlight exposure evaluates sunlight access at a single point under fixed temporal conditions, while climate-based metrics and ASH-type approaches extend the analysis over longer periods and across spatial grids. SBI introduces an aperture-based, time-integrated formulation that does not conform to either structure. These differences are embedded in the definition of the metrics and cannot be reduced to direct equivalence. Further work should therefore clarify where SBI provides information not captured by point-based or grid-based methods, where partial overlap occurs, and how these approaches can be applied in parallel without conflict. This need for positioning reflects broader findings that different solar access indicators respond differently to geometry and density, while maintaining partial relationships (Czachura, 2023).

A third direction follows the development of aperture-based daylight modelling as a method. SBI represents one component within this line of research, where the aperture is treated as the primary unit of evaluation. Its use in isolation limits the scope of analysis, as sunlight access is only one aspect of façade performance. Previous research indicates that evaluation methods may require the combination of several indicators to support design and planning processes (Czachura, 2023). Future work should therefore extend the evaluation towards combined aperture-based indicators, where multiple façade-related quantities are considered simultaneously, forming an aperture-level method.

A fourth direction concerns the translation of SBI into design outputs. The metric is directly dependent on geometry, as it responds to aperture size, orientation, and external obstruction. This relationship is observable in the results but is not yet structured in a way that can inform design decisions. Early-stage design processes rely on geometric parameters such as orientation, spacing, and massing, while detailed interior definitions are not yet available (Dervishaj and Gudmundsson, 2025). Future work should investigate how SBI values can be mapped to façade configuration decisions, how variations in aperture geometry influence the metric in a predictable manner, and how this relationship can be embedded into early-stage workflows.

A fifth direction extends the application of aperture-based indicators to early-stage urban design. At this stage, available information is limited to building massing, spacing, and orientation, while interior configuration and material properties are not yet defined. Existing research indicates that evaluation methods used at this level must rely on simple, geometry-based indicators due to these limitations (Czachura, 2023). SBI shares this characteristic through its dependence on aperture geometry and external obstruction, which suggests potential applicability beyond the building scale. Further work should examine how façade-level SBI results can be related to urban form parameters such as building height, spacing, and orientation, and whether the metric can function within neighbourhood-scale assessments alongside established indicators such as VSC, SVF, and ASH-type measures. This direction is consistent with the need to introduce solar access considerations into planning processes through suitable performance indicators (Czachura, 2023).

The progression defined by these directions follows a sequence from geometric measurement to interpretation, from interpretation to design application, and from building-scale evaluation to urban-scale applicability. This sequence reflects the current state of SBI as a defined metric that has not yet been fully integrated into performance assessment or design decision-making processes.

6.2 Evidence-based derivation of SBI thresholds

This subsection outlines a pathway for deriving SBI thresholds through an evidence-based approach. The procedure differs from the previous section, where thresholds were transferred from EN 17037 sunlight exposure through a structured conversion. Here, the objective is to define how SBI thresholds could be established directly from observed performance and measurable outcomes. The approach assumes access to extended datasets and validation steps beyond the present study.

Threshold derivation requires a clearly defined unit of analysis. SBI can be evaluated at aperture, room, or dwelling level. Each choice produces a different threshold range. In this context, the room is taken as the primary unit. This reflects the scale at which sunlight conditions are experienced and evaluated. The definition of the unit directly influences how SBI values are interpreted.

The temporal basis of the metric must also be defined. SBI is calculated on an annual basis, while EN 17037 sunlight exposure relies on a limited seasonal condition. A single annual value may not capture periods of low sunlight availability. This introduces the need to consider whether thresholds should rely on annual SBI alone or include a seasonal component. A combined temporal structure may be required to represent both annual exposure and critical periods.

SBI is directly proportional to aperture area. Larger apertures increase SBI independently of sunlight duration. This creates a scaling effect that must be addressed during threshold derivation. The use of raw SBI values introduces dependence on opening size. Alternative formulations may include normalisation by aperture area or floor area. The choice of representation influences how thresholds are defined and compared.

Location introduces additional variation. Solar altitude, day length, and annual sun-path distribution change with latitude. The same geometry produces different SBI values under different solar conditions. Thresholds derived for one location cannot be applied directly to another without adjustment. This indicates that SBI thresholds are expected to vary across climate regions.

Access to direct sunlight is associated with physiological and perceptual effects. Reduced sunlight exposure is linked to lower circadian stimulus and seasonal variation in daily light availability. Minimum exposure conditions can therefore be interpreted not only as geometric thresholds but also as indicators of environmental adequacy. This introduces a human-centred basis for defining lower SBI limits.

Perceived adequacy of sunlight varies across spaces and occupants. A room may be considered acceptable at one level of exposure and insufficient at another. These categories can be structured into categories such as insufficient, acceptable, and good. SBI values can be mapped to these categories, providing a basis for defining threshold levels.

SBI thresholds can be examined alongside existing metrics. EN 17037 sunlight exposure and ASH provide reference points for current practice. The relationship between these metrics and SBI can be used to identify overlapping and diverging ranges. This comparison supports the positioning of SBI within established evaluation methods.

A single threshold is unlikely to capture the full range of conditions. Multiple criteria may be required to represent different aspects of sunlight exposure. This may include total SBI and a normalised form of SBI.

Thresholds may also be defined at multiple levels, corresponding to minimum and higher performance conditions. This leads to a graded structure rather than a single pass–fail limit.

The derivation of such thresholds requires extensive data. Large datasets covering variations in geometry, location, and obstruction are necessary. Both simulated and real building cases are required to capture the full range of conditions. This allows consistent patterns in SBI behaviour to be identified.

Calibration against observed outcomes is required to define threshold values. These outcomes include perceived adequacy, user response, and patterns of space use. Relationships between SBI and these indicators can be used to identify threshold ranges. This step provides a basis for linking geometric exposure to evaluation criteria.

Bibliography

Brembilla E and Mardaljevic J, 2019. Climate-Based Daylight Modelling for Compliance Verification: Benchmarking Multiple State-of-The-Art Methods. Building and Environment, vol. 158, pp. 151–164. https://doi.org/10.1016/j.buildenv.2019.04.051.

Bournas I, 2020. Daylight Compliance of Residential Spaces: Comparison of Different Performance Criteria and Association with Room Geometry and Urban Density. Division of Energy and Building Design, Department of Architecture and Built Environment. Building and Environment, vol. 185, 107276. https://doi.org/10.1016/j.buildenv.2020.107276.

Czachura A, 2023. Solar Access Indicators for Urban Planning. Lund University. Available at: portal.research.lu.se/en/publications/solar-access-indicators-for-urban-planning/ (accessed 19 Apr. 2026).

Czachura A, et al., 2022. "Identifying Potential Indicators of Neighbourhood Solar Access in Urban Planning." Buildings, vol. 12, no. 10, p. 1575. https://doi.org/10.3390/buildings12101575.

Dervishaj, A., Dervishaj, G., Gudmundsson, K. and Björk, F. (2023) 'EN 17037 a step forward: New computational methods with Sunlight, Daylight, and Quality Views for Regenerative Design', *REHVA Journal*, 4, pp. 20–28. Available at: https://www.rehva.eu/rehva-journal/chapter/en-17037-a-step-forward-new-computational-methods-with-sunlight-daylight-and-quality-views-for-regenerative-design (Accessed: 18 May 2026).

Dervishaj A and Gudmundsson K, 2025. "Sunlight Autonomy for Buildings: A New Methodology for Evaluating Sunlight Performance in Urban and Architectural Design." LEUKOS, pp. 1–31. https://doi.org/10.1080/15502724.2023.2297967.

Google Earth, 2026. *Satellite and site imagery*. Available at: Google Earth. Accessed May 2026.

Hraška J and Čurpek J, 2024. "The Practical Implications of the EN 17037 Minimum Target Daylight Factor for Building Design and Urban Daylight in Several European Countries." Heliyon, vol. 10, no. 1, e23297. https://doi.org/10.1016/j.heliyon.2023.e23297.

Ibarra DI and Reinhart CF, 2009. "Daylight Factor Simulations – How Close Do Simulation Beginners 'Really' Get?" Available at: www.researchgate.net/publication/241410294_Daylight_factor_simulations_-_how_close_do_simulation_beginners_ (accessed 19 Apr. 2026).

Illuminating Engineering Society, 2012. IES LM-83-12: Approved Method for Spatial Daylight Autonomy (sDA) and Annual Sunlight Exposure (ASE). New York: IES.

Jin Z, Chen X, Rogers P, Perez Morata A, Rasmussen HF and Gentile N, 2025. "Proposal for Revised Criteria for Daylight Provision in the European Daylight Standard Based on Calculations for Swedish Multifamily Residential Buildings." Lighting Research & Technology, vol. 57, no. 6–7, pp. 473–498. https://doi.org/10.1177/14771535241306970.

Ladybug Tools, 2021. Ladybug Tools | Home Page. Available at: https://www.ladybug.tools/

Lawrie LK and Crawley DB, 2026. Development of Global Typical Meteorological Years (TMYx): GBR_ENG_Blackwall.037820_TMYx – EnergyPlus Weather File (EPW), London (Blackwall), United Kingdom. Available at: https://climate.onebuilding.org (accessed 3 May 2026).

Lawrie LK and Crawley DB, 2026. Development of Global Typical Meteorological Years (TMYx): SWE_OR_Orebro-Eekeby.020740_TMYx – EnergyPlus Weather File (EPW), Örebro, Sweden. Available at: https://climate.onebuilding.org (accessed 3 May 2026).

Lawrie LK and Crawley DB, 2026. Development of Global Typical Meteorological Years (TMYx): SWE_ST_Skarpo-Stavnas.024870_TMYx – EnergyPlus Weather File (EPW), Stockholm (Skarpö-Stavnäs), Sweden. Available at: https://climate.onebuilding.org (accessed 3 May 2026).

Lawrie LK and Crawley DB, 2026. Development of Global Typical Meteorological Years (TMYx): SWE_VG_Gothenburg-Landvetter.AP.025260_TMYx – EnergyPlus Weather File (EPW), Gothenburg-Landvetter Airport, Sweden. Available at: https://climate.onebuilding.org (accessed 3 May 2026).

Liu Y, Brembilla E and Rafiee A, 2026. "Cloud-Based Application for Indoor Daylight Performance Analysis through BIM-GIS Integration." Building and Environment, vol. 293, p. 114376. https://doi.org/10.1016/j.buildenv.2026.114376.

Mardaljevic J, 2019. "Aperture-Based Daylight Modelling: Introducing the 'View Lumen'." Proceedings of Building Simulation 2019: 16th Conference of IBPSA, pp. 1129–1136. https://doi.org/10.26868/25222708.2019.210810.

Mardaljevic J and Brembilla E, 2021. "Aperture-Based Daylight Modelling: Evaluating the Airmass Refinement for the Sunlight Beam Index." Building Simulation Conference Proceedings, vol. 17. https://doi.org/10.26868/25222708.2021.30604.

Mardaljevic J and Roy N, 2016. "The Sunlight Beam Index." Lighting Research & Technology, vol. 48, no. 1, pp. 55–69. https://doi.org/10.1177/1477153515621486.

Python Software Foundation, 2024. Python Programming Language. Available at: https://www.python.org

Reinhart CF, Mardaljevic J and Rogers Z, 2013. "Dynamic Daylight Performance Metrics for Sustainable Building Design." LEUKOS, vol. 3, pp. 7–31. https://doi.org/10.1582/LEUKOS.2006.03.01.001.

Reinhart CF and Walkenhorst O, 2001. "Validation of Dynamic RADIANCE-Based Daylight Simulations for a Test Office with External Blinds." Energy and Buildings, vol. 33, pp. 683–697. https://doi.org/10.1016/S0378-7788(01)00058-5.

Robert McNeel & Associates, 2024. Grasshopper for Rhinoceros 3D.

Robert McNeel & Associates, 2024. Rhinoceros 3D, Version 7.

Rogers P, Dubois M-C, Tillberg M, Östbring M, Bournas I, Alenius M, et al., 2018. Moderniserad dagsljusstandard. Report No. 13209. Stockholm: SBUF.

Schober, P., Boer, C., and Schwarte, L. A. (2018). *Correlation coefficients: Appropriate use and interpretation*. Anesthesia & Analgesia, 126(5), 1763–1768,https://doi.org/10.1213/ANE.0000000000002864.

Solemma LLC, 2024. ClimateStudio – Environmental Performance Simulation Software.

SSI and CEN, 2021. SS-EN 17037:2018+A1:2021 Daylight in Buildings. European Committee for Standardization (CEN).

Tregenza P and Mardaljevic J, 2018. "Daylighting Buildings: Standards and the Needs of the Designer." Lighting Research & Technology, vol. 50, no. 1, pp. 63–79. https://doi.org/10.1177/1477153517740611.

Volf, C., Bueno, B., Edwards, P., Hobday, R., Mäder, S., Matusiak, B.S., Wulff, K., Osterhaus, W., Manoli, G., Della Giustina, C., Joshi, J., Kämpf, J.H., Vega, K. and Kueffer, C. (2024) 'Why daylight should be a priority for urban planning', Journal of Urban Management, 13(2), pp. 175–182. doi: 10.1016/j.jum.2024.02.002.

Appendix A

Custom Python Script Components

A.1 Point-based ray casting and sunlit aperture area computation component

The timestep-based sunlit aperture area was computed using point-sampled aperture geometry and ray-based obstruction testing (Figure 1). Each evaluation point was placed at the centre of its assigned aperture subdivision, and each area weight represents the portion of aperture area assigned to that point. The inputs included evaluation points on the aperture (P_out), corresponding area weights (w), sun direction vectors per timestep (sun_dir), cosine values per timestep (cos_list), surrounding geometry (context), and an optional maximum ray distance (max_dist). The outputs consisted of the sunlit aperture area per timestep (A_i), the sunlit area fraction (f_sunlit), and the number of sunlit points (sunlit_count).

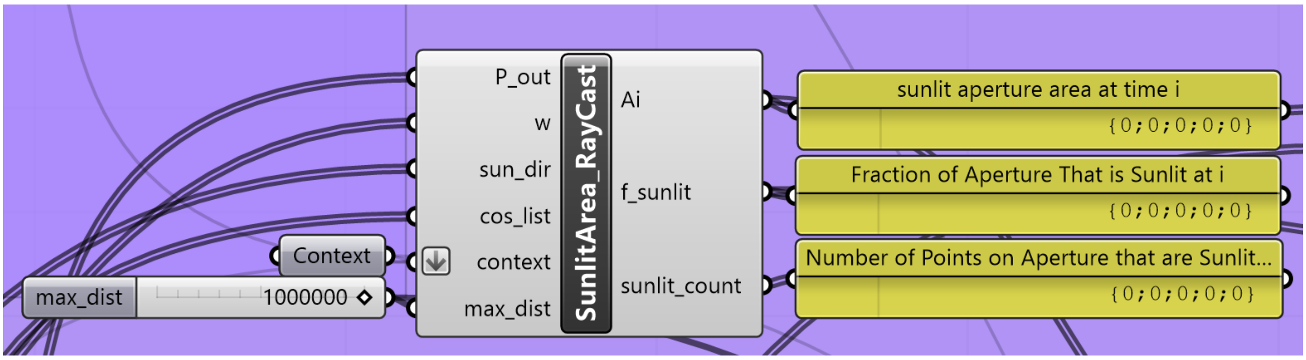

Figure 1 Point-based ray-casting and sunlit aperture area computation component used for sunlight aperture metric calculations.

All inputs were converted to list form. The context geometry was coerced into a Brep representation from Breps, Extrusions, or Rhino object GUIDs. This established a consistent geometry type for intersection testing.

Input consistency was checked before execution. The number of aperture points was required to match the number of weights, and the number of sun direction vectors was required to match the number of cosine values. The total aperture area was computed as the sum of the weights.

The evaluation was performed per timestep. For each timestep, if no context geometry was provided, and the cosine value was positive, the entire aperture was classified as sunlit. If the cosine value was non-positive, the timestep contribution was set to zero.

When context geometry was present, the cosine value was evaluated first. Non-positive values resulted in zero contribution. For positive values, the sun direction vector was unitised, and rays were cast from each aperture point towards the sun. Each ray was tested against the context geometry using 'Intersection.RayShoot'. This RhinoCommon method returns intersections between a ray and the supplied Brep geometry.

A point was classified as sunlit when no intersection occurred within the specified ray distance. The weights of sunlit points were summed to obtain the sunlit aperture area for the timestep, and the number of sunlit points was recorded.

After all timesteps were processed, the sunlit area fraction was computed as the ratio of sunlit area to total aperture area.

A.2 Midpoint-based ray casting and annual sunlight evaluation component

Timestep-based Boolean sunlight exposure at a single evaluation point was computed (Figure 2). The inputs included a point (P_mid, Point3d), sun direction vectors (sun_dir, list of Vector3d), cosine values (cos_list, list of floats), surrounding geometry (context, list of Brep), a maximum ray distance (max_dist, float or None), and an offset value (eps, float). The outputs consisted of a Boolean list (sunlit_mid) and an integer (count_mid).

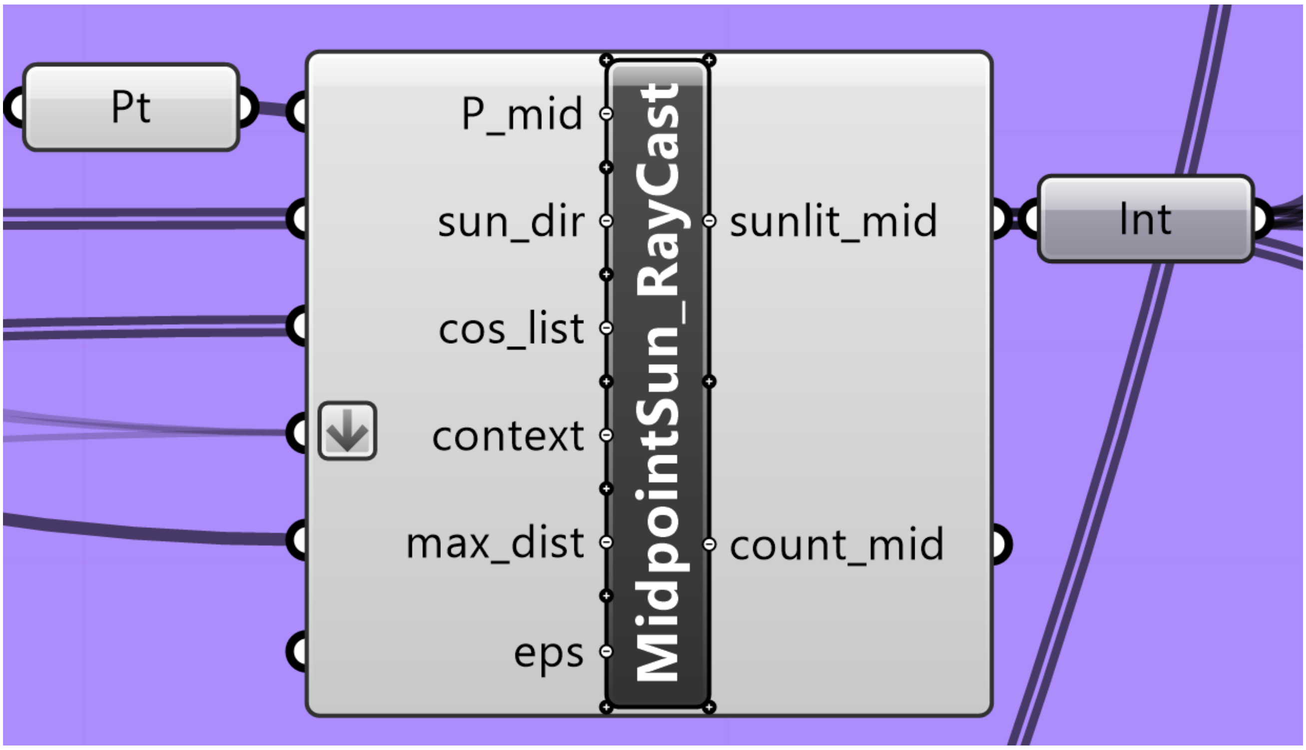

Figure 2 Midpoint-based ray-casting and annual sunlight evaluation component used for point-based sunlight exposure calculations.

Inputs were converted to list form where required. The sun direction and cosine lists were checked for equal length. The evaluation point was cast to Point3d. The surrounding geometry was used directly as a list of Breps for intersection testing.

The computation was performed per timestep. If no context geometry was provided, the Boolean result was determined directly from the cosine values, where cos_list[t] > 0 yielded 'True', and otherwise 'False'.

When context geometry was present, the cosine values were evaluated first. For timesteps with cos_list[i] ≤ 0, the result was set to 'False'. For positive cosine values, the corresponding sun direction vector was validated and unitised.

The ray origin was defined at P_mid. If eps was non-zero, the origin was translated along the sun direction by eps to avoid self-intersection. A ray was then constructed and tested against the Brep geometry using 'Intersection.RayShoot'.

The Boolean result for each timestep was defined as:
sunlit_mid[t] = not is_blocked(origin, direction, context, max_dist).

The final output count_mid was computed as the sum of True values in the Boolean list.

A.3 Airmass weighting, SBI and SBI-airmass computation component

Timestep-based SBI and SBI-airmass values were computed from numerical timestep series (Figure 3). The inputs consisted of lists of floats, including the sunlit aperture area per timestep (A_i), cosine values (cos_list), and solar altitude in degrees (alt_deg). Additional scalar inputs included the timestep duration (dt, in hours) and a numerical tolerance (eps). The outputs comprised float lists for timestep SBI (SBI_t), airmass (AM_t), SBI-airmass (SBI_AM_t), and scalar totals (SBI_total, SBI_AM_total).

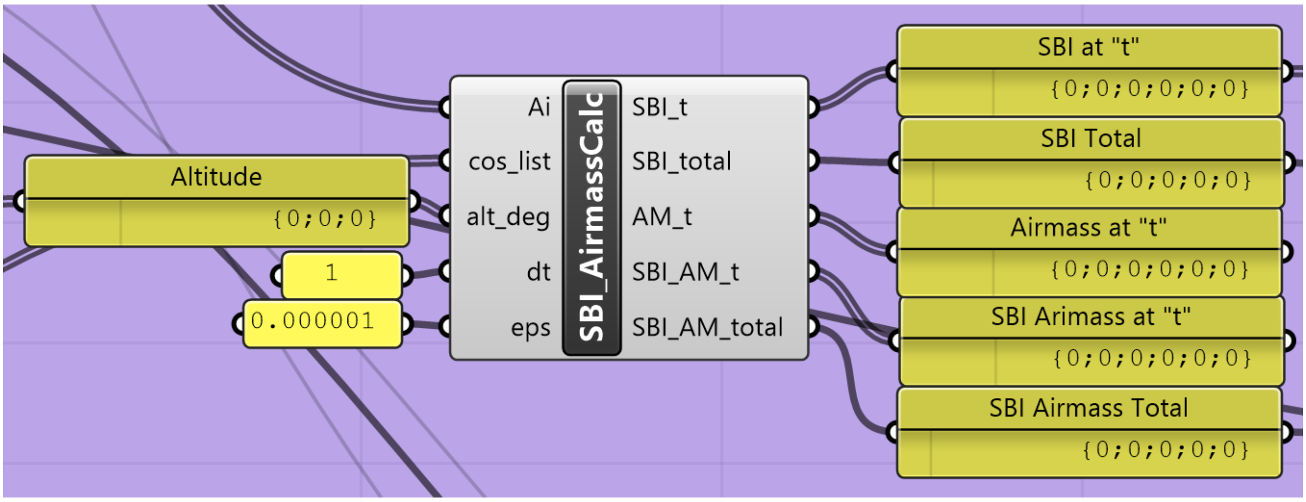

Figure 3 Airmass-weighting component used for the computation of SBI and SBI-airmass metrics across annual simulation timesteps.

All inputs were cast to list form and reduced to a common length so that each index corresponded to a single timestep. The computation was performed over this timestep index. The timestep duration was applied as a scalar multiplier during accumulation. A small tolerance value was used to avoid division by zero.

At each timestep 'i', SBI was computed as:

$$SBI\_t_{[i]} = A\_i_{[i]} \times cos\_list_{[i]} \quad (1)$$

Airmass was computed using the Kasten–Young formulation based on solar altitude:

$$AM\_t_{[i]} = \frac{1}{\sin h - 0{,}505\,72(h + 6{,}079\,95)^{-1{,}636\,4}} \quad (2)$$

where h was the solar altitude in degrees. Altitude values below zero were set to zero prior to evaluation. SBI-airmass was computed per timestep as:

$$SBI\_AM\_t_{[i]} = \frac{\mathrm{SBI}\_t_{[i]}}{\max(\mathrm{AM}\_t_{[i]}, \mathrm{eps})} \quad (3)$$

The total values were obtained by summing the timestep series and scaling by the timestep duration:

$$SBI_{total} = \sum SBI\_t_{[i]} \times dt \quad (4)$$

$$SBI\_\mathrm{AM}_{total} = \sum SBI\_\mathrm{AM}\_t_{[i]} \times dt \quad (5)$$

A.4 Date-range filtering and daily aggregation for EN 17037 sunlight exposure evaluation component

Timestep-indexed Boolean sunlight data were processed into daily aggregates within a specified calendar range (Figure 4). The inputs included hour-of-year values (hoys_ash, list of floats), Boolean sunlight values (sunlit_mid, list of bool), timestep resolution (timestep_per_hour, integer), and start and end dates (start_m, start_d, end_m, end_d). The outputs consisted of integer lists (day_keys, day_counts, day_steps) and a float list (day_hours).

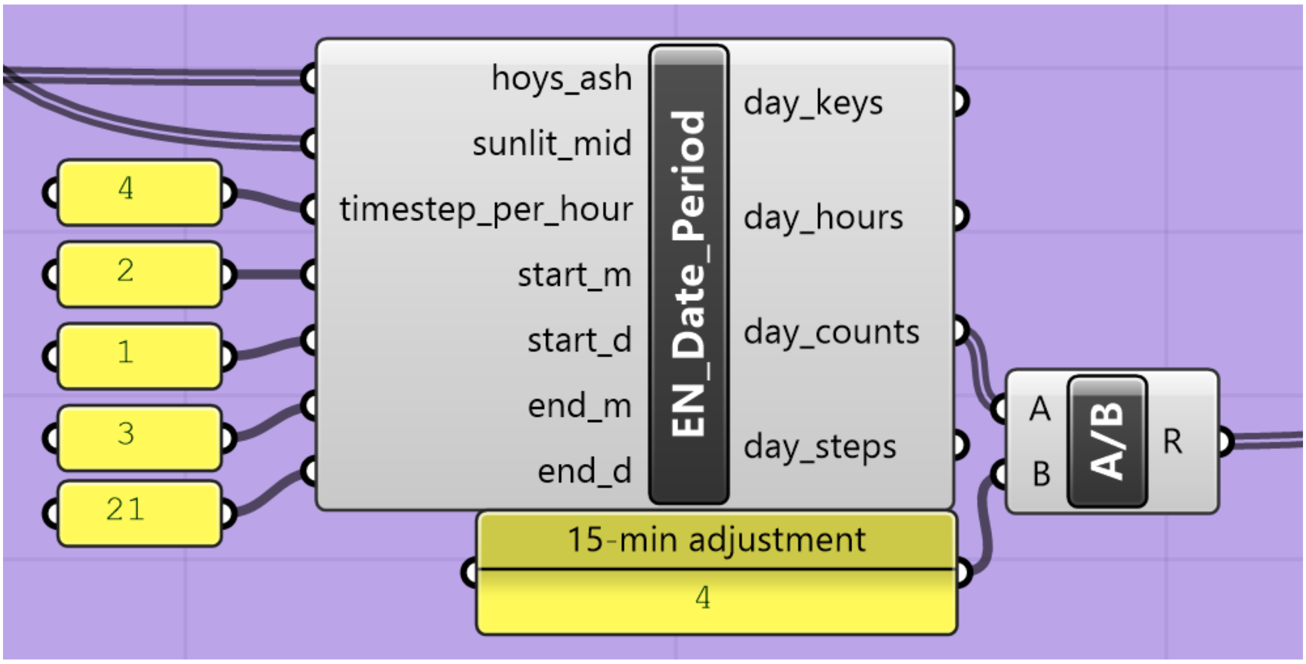

Figure 4 Date-range filtering and daily aggregation component used for EN 17037 sunlight exposure evaluation.

Input sequences were cast to list form and checked for equal non-zero length. The timestep resolution (tph) was defined as an integer representing the number of timesteps per hour.

Each HOY value was converted to a datetime representation by mapping it to minutes from the start of a reference year. This provided discrete month (m) and day (d) values for each timestep. A date filter was applied using the condition:

$$(\mathrm{start\_m}, \mathrm{start\_d}) \leq (\mathrm{m}, \mathrm{d}) \leq (\mathrm{end\_m}, \mathrm{end\_d}) \quad (6)$$

Timesteps outside this interval were excluded.

The remaining timesteps were grouped by day using an integer key defined as:

$$key = m \times 100 + d \quad (7)$$

For each key, two accumulators were maintained:

- day_steps: total number of timesteps for the day
- day_counts: number of timesteps where sunlit_mid[t] = True

Daily sunlight duration was computed as:

$$day\_hours = \frac{day\_counts}{tph} \quad (8)$$

The outputs represented day-wise sunlight exposure as timestep counts and as hours.

A.5 Temporal reconstruction and annual data tree generation component

Timestep-indexed SBI and SBI-airmass series were reconstructed into an annual sequence and organised into day-based structures (Figure 5). The inputs included hour-of-year values (hoys_ash, list of floats), timestep values for SBI (vals_1), timestep values for SBI-airmass (vals_2), timestep resolution (timestep_per_hour, integer), and a leap-year flag (is_leap). The outputs consisted of Grasshopper DataTrees (grid1_tree, grid2_tree), full-year float arrays (flat_1, flat_2), maximum values (max_1, max_2), and the total number of days (day_count).

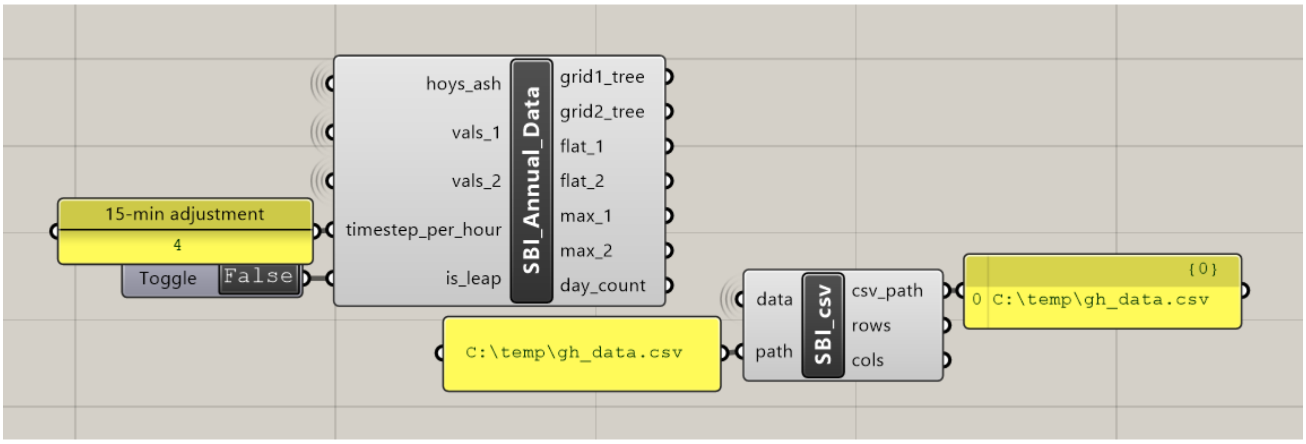

Figure 5 Temporal reconstruction and annual data-tree generation component used for SBI annual dataset processing and export.

Input sequences were converted to list form and checked for equal length. The timestep resolution (tph) defined the number of samples per hour. The number of timesteps per day was computed as 24 × tph. The annual length was defined as:

$$total\_steps = days \times 24 \times tph \tag{9}$$

Two full-year arrays (flat_1, flat_2) were initialised as lists of floats with length total_steps, filled with 0.0. These arrays represented the annual domain, including timesteps not present in the input series.

Each HOY value was mapped to an integer timestep index using:

$$idx = int\big(round\ (hoy \times tph)\big) \tag{10}$$

This mapping converted fractional HOY values into discrete timestep positions. Values falling outside the valid range [0, total_steps) were ignored. For valid indices, the corresponding SBI and SBI-airmass values were assigned:

$$\text{flat\_1}[idx] = float\ (\text{vals\_1}_{[i]}) \tag{11}$$
$$\text{flat\_2}[idx] = float\ (\text{vals\_2}_{[i]}) \tag{12}$$

This produced a dense annual representation in which missing timesteps remained 0.0.

The flat arrays were then reorganised into Grasshopper DataTrees. For each day d, a branch was created using GH_Path(d). Each branch contained steps_per_day consecutive values extracted from the flat arrays:

$$start = d \times steps\_per\_day \tag{13}$$
$$end = start \times steps\_per\_day \tag{14}$$

Values were appended sequentially to each branch, preserving timestep order within the day.

Maximum values were computed using standard list operations:

$$\text{max\_1} = \text{max(flat\_1)} \tag{15}$$
$$\text{max\_2} = \text{max(flat\_2)} \tag{16}$$

The number of days was returned as day_count. This component converted sparse timestep series into a continuous annual structure and organised the data into per-day sequences suitable for temporal mapping and comparison.

Appendix B

The aperture naming follows the format Orientation_Floor_Number_Area. The orientation field uses compass abbreviations such as S, E, W, N, SW, SSW, or similar directional codes. In cases where a building has more than one façade with the same orientation, an additional number is added to distinguish them. For example, W1 and W2 indicate different west-facing façades, with W1 assigned to the west-facing façade located furthest west in the building geometry. The following number indicates the floor level, the next number indicates the aperture number, and the final number indicates the aperture area in cm². Aperture numbers are assigned from left to right within each façade. For example, W1_2_4_178 refers to the W1 façade, second floor, aperture number 4, with an aperture area of 178 cm².

Table 6 Complete dataset of single-aperture-level sunlight access metrics calculated for urban context models computations.

Name	Orientation	Floor	Number	Aperture area (cm²)	SBI (m²·hrs)	SBI_airmass (m²·hrs)	EN 17037 sunlight exposure (hrs)	ASH (hrs)	Urban density (m³/m²)
S_3_1_148	S	3	1	148.00	1 645.15	611.72	8.00	1 446.00	3.02
S_1_1_266	S	1	1	266.00	985.82	423.99	5.75	867.25	3.02
S_1_3_266	S	1	3	266.00	994.07	431.21	5.25	930.25	3.02
S_3_3_148	S	3	3	148.00	1 656.83	613.72	8.00	1 443.00	3.02
S_3_5_148	S	3	5	148.00	1 672.43	616.18	8.00	1 440.25	3.02
S_2_2_148	S	2	2	148.00	1 413.05	568.91	7.75	1 246.25	3.02
S_2_4_148	S	2	4	148.00	1 427.45	570.13	7.75	1 243.25	3.02
E_1_1_362	E	1	1	362.00	1 218.57	477.43	2.75	639.00	3.02
E_2_3_148	E	2	3	148.00	1 039.85	381.88	3.25	889.25	3.02
E_3_2_269	E	3	2	269.00	1 966.47	683.55	5.50	1 412.00	3.02
E_2_5_148	E	2	5	148.00	1 013.99	378.79	2.75	877.00	3.02
E_3_4_148	E	3	4	148.00	1 200.02	405.42	3.25	1 034.25	3.02
E_2_1_148	E	2	1	148.00	1 057.53	382.57	3.75	898.75	3.02
E_2_2_269	E	2	2	269.00	1 743.63	661.73	6.25	1 404.50	3.02
W_2_1_148	W	2	1	148.00	832.46	333.08	1.25	667.00	3.02
W_3_1_148	W	3	1	148.00	1 023.05	377.16	3.75	840.50	3.02
W_1_1_266	W	1	1	266.00	317.49	93.88	0.00	67.75	3.02
W_2_2_148	W	2	2	148.00	612.10	226.89	0.00	453.25	3.02

W_3_2_148	W	3	2	148.00	945.95	350.36	0.75	754.75	3.02
N_1_1_266	N	1	1	266.00	0.32	0.07	0.00	0.00	3.02
N_3_1_148	N	3	1	148.00	18.21	3.04	0.00	0.00	3.02
N_1_3_266	N	1	3	266.00	0.32	0.07	0.00	0.00	3.02
N_3_3_148	N	3	3	148.00	18.21	3.04	0.00	0.00	3.02
ENE_1_1_190	ENE	1	1	190.00	762.76	217.48	2.50	693.25	0.76
ENE_2_1_190	ENE	2	1	190.00	820.66	229.27	3.00	707.75	0.76
ENE_3_1_190	ENE	3	1	190.00	982.10	241.21	3.00	684.50	0.76
ENE_1_3_190	ENE	1	3	190.00	555.10	186.39	3.00	704.50	0.76
ENE_2_3_190	ENE	2	3	190.00	727.63	222.24	3.00	724.75	0.76
ENE_3_3_190	ENE	3	3	190.00	977.51	241.20	3.00	708.75	0.76
ENE_1_5_363	ENE	1	5	363.00	998.88	370.03	1.75	691.75	0.76
ENE_2_5_363	ENE	2	5	363.00	1 339.25	424.79	1.75	855.75	0.76
ENE_3_5_363	ENE	3	5	363.00	1 913.88	464.78	2.75	1 055.25	0.76
ENE_1_6_302	ENE	1	6	302.00	937.93	343.75	1.75	581.50	0.76
ENE_2_6_302	ENE	2	6	302.00	1 308.32	416.78	2.25	644.25	0.76
ENE_3_6_302	ENE	3	6	302.00	1 842.60	474.29	3.50	800.50	0.76
ENE_1_7_462	ENE	1	7	462.00	1 233.49	470.88	1.75	639.25	0.76
ENE_2_7_462	ENE	2	7	462.00	1 745.62	572.58	2.25	817.50	0.76
ENE_3_7_462	ENE	3	7	462.00	2 551.27	676.27	3.00	1 119.75	0.76
SSE_1_1_230	SSE	1	1	230.00	1 711.05	759.80	4.50	1 242.75	0.76
SSE_2_1_230	SSE	2	1	230.00	1 982.46	837.42	5.00	1 376.00	0.76
SSE_3_1_230	SSE	3	1	230.00	2 321.42	903.43	6.00	1 530.75	0.76
SSE_1_2_434	SSE	1	2	434.00	3 420.69	1 477.53	7.00	1 715.25	0.76
SSE_2_2_434	SSE	2	2	434.00	3 883.95	1 615.77	8.25	1 890.50	0.76
SSE_3_2_434	SSE	3	2	434.00	4 943.20	2 114.63	8.50	2 377.25	0.76
WSW_1_1_140	WSW	1	1	140.00	558.31	275.37	2.75	877.75	0.76
WSW_2_1_140	WSW	2	1	140.00	726.98	344.11	3.75	1 077.75	0.76
WSW_3_1_140	WSW	3	1	140.00	897.91	386.01	4.50	1 194.50	0.76
WSW_1_2_133	WSW	1	2	133.00	402.18	222.79	1.50	738.50	0.76
WSW_2_2_133	WSW	2	2	133.00	583.48	299.11	2.25	957.25	0.76

WSW_3_2_133	WSW	3	2	133.00	774.44	350.46	3.00	1 124.00	0.76
WSW_1_4_268	WSW	1	4	268.00	882.88	471.66	2.25	676.50	0.76
WSW_2_4_268	WSW	2	4	268.00	1 291.43	640.60	3.00	833.00	0.76
WSW_3_4_268	WSW	3	4	268.00	1 705.61	741.73	3.25	848.00	0.76
WSW_1_6_133	WSW	1	6	133.00	598.41	267.70	3.00	971.75	0.76
WSW_2_6_133	WSW	2	6	133.00	762.85	336.45	3.00	1 164.25	0.76
WSW_3_6_133	WSW	3	6	133.00	931.36	378.82	3.25	1 274.50	0.76
NNW_1_1_172	NNW	1	1	172.00	59.84	20.22	0.00	91.75	0.76
NNW_2_1_172	NNW	2	1	172.00	85.98	27.92	0.00	131.25	0.76
NNW_3_1_172	NNW	3	1	172.00	112.06	33.45	0.00	163.75	0.76
NNW_1_2_268	NNW	1	2	268.00	62.41	24.60	0.25	111.75	0.76
NNW_2_2_268	NNW	2	2	268.00	139.95	48.50	0.25	199.25	0.76
NNW_3_2_268	NNW	3	2	268.00	228.67	68.80	0.25	282.50	0.76
S_1_1_218	S	1	1	218.00	557.13	197.00	1.75	203.50	3.96
W_1_9_218	W	1	9	218.00	751.80	298.06	0.75	437.00	3.96
S_2_1_338	S	2	1	338.00	1 147.50	556.10	2.25	370.25	3.96
W_2_8_218	W	2	8	218.00	851.15	334.81	0.75	484.25	3.96
S_3_1_338	S	3	1	338.00	1 344.03	651.59	2.50	480.50	3.96
W_3_8_218	W	3	8	218.00	951.71	366.61	1.00	533.25	3.96
S_4_1_338	S	4	1	338.00	1 603.41	759.00	2.75	601.75	3.96
W_4_8_218	W	4	8	218.00	1 043.90	391.17	2.25	578.50	3.96
S_5_1_338	S	5	1	338.00	1 931.60	870.46	4.75	744.25	3.96
W_5_8_218	W	5	8	218.00	1 167.22	417.68	4.75	640.00	3.96
S_6_1_338	S	6	1	338.00	2 841.53	1 258.71	4.75	1 181.00	3.96
W_6_8_218	W	6	8	218.00	1 263.48	390.71	4.75	564.25	3.96
S_1_2_218	S	1	2	218.00	730.27	317.28	1.50	208.75	3.96
S_2_2_218	S	2	2	218.00	1 079.33	539.80	2.75	709.25	3.96
S_3_2_218	S	3	2	218.00	1 218.82	605.09	2.75	825.25	3.96
S_4_2_218	S	4	2	218.00	1 399.28	675.51	3.25	951.00	3.96
S_5_2_218	S	5	2	218.00	1 627.73	746.99	5.00	1 096.00	3.96
S_6_2_218	S	6	2	218.00	2 016.00	818.99	5.50	1 304.75	3.96

S_1_4_218	S	1	4	218.00	599.51	217.02	1.75	168.25	3.96
E_1_1_218	E	1	1	218.00	72.02	36.98	1.00	127.50	3.96
S_2_4_338	S	2	4	338.00	1 358.22	655.27	3.00	448.75	3.96
E_2_1_218	E	2	1	218.00	111.72	58.72	1.00	177.75	3.96
S_3_4_338	S	3	4	338.00	1 552.13	739.45	3.25	553.50	3.96
E_3_1_218	E	3	1	218.00	216.11	118.61	1.00	285.25	3.96
S_4_4_338	S	4	4	338.00	1 807.55	832.12	3.75	671.75	3.96
E_4_1_218	E	4	1	218.00	406.43	209.37	0.00	374.50	3.96
S_5_4_338	S	5	4	338.00	2 110.80	918.99	4.25	819.00	3.96
E_5_1_218	E	5	1	218.00	626.43	287.56	0.00	479.50	3.96
S_6_4_338	S	6	4	338.00	2 958.15	1 277.66	4.25	1 240.00	3.96
E_6_1_218	E	6	1	218.00	888.58	351.35	0.00	607.50	3.96
E_1_2_218	E	1	2	218.00	85.38	40.72	0.00	133.25	3.96
E_2_2_218	E	2	2	218.00	165.00	84.71	0.75	227.25	3.96
E_3_2_218	E	3	2	218.00	268.17	139.17	0.50	319.50	3.96
E_4_2_218	E	4	2	218.00	434.66	210.40	0.75	417.25	3.96
E_5_2_218	E	5	2	218.00	610.14	259.00	2.25	537.75	3.96
E_6_2_218	E	6	2	218.00	1 049.17	386.62	3.00	669.25	3.96
E_1_3_320	E	1	3	320.00	197.96	79.30	0.00	67.50	3.96
E_2_3_320	E	2	3	320.00	492.86	242.76	0.50	290.25	3.96
E_3_3_320	E	3	3	320.00	757.21	373.81	0.50	413.00	3.96
E_4_3_320	E	4	3	320.00	958.50	438.39	0.25	496.00	3.96
E_5_3_320	E	5	3	320.00	1 511.13	631.38	2.25	726.50	3.96
E_6_3_320	E	6	3	320.00	2 473.15	943.71	3.00	1 063.50	3.96
E_1_5_320	E	1	5	320.00	436.78	168.54	0.00	112.25	3.96
E_2_5_384	E	2	5	384.00	543.10	208.40	0.25	222.25	3.96
E_3_5_384	E	3	5	384.00	717.54	284.76	0.50	322.25	3.96
E_4_5_384	E	4	5	384.00	1 120.67	461.51	0.50	530.25	3.96
E_5_5_384	E	5	5	384.00	1 597.26	611.56	1.25	729.25	3.96
E_6_5_384	E	6	5	384.00	2 219.07	787.60	3.00	996.75	3.96
E_1_7_218	E	1	7	218.00	395.15	152.54	0.00	150.00	3.96

E_2_7_218	E	2	7	218.00	493.90	202.61	0.00	228.00	3.96
E_3_7_218	E	3	7	218.00	613.24	253.32	0.00	293.25	3.96
E_4_7_218	E	4	7	218.00	812.73	320.02	0.75	382.75	3.96
E_5_7_218	E	5	7	218.00	1 050.34	381.81	1.50	493.25	3.96
E_6_7_218	E	6	7	218.00	1 281.10	420.94	2.25	597.25	3.96
N_1_1_218	N	1	1	218.00	29.22	2.72	0.00	39.00	3.96
N_2_1_338	N	2	1	338.00	34.35	3.40	0.00	41.25	3.96
N_3_1_338	N	3	1	338.00	40.36	4.25	0.00	50.00	3.96
N_4_1_338	N	4	1	338.00	43.64	4.62	0.00	54.25	3.96
N_5_1_338	N	5	1	338.00	56.19	5.97	0.00	68.00	3.96
N_6_1_338	N	6	1	338.00	73.93	7.45	0.00	82.50	3.96
N_1_2_218	N	1	2	218.00	7.59	0.73	0.00	12.00	3.96
N_2_2_218	N	2	2	218.00	8.12	0.88	0.00	15.75	3.96
N_3_2_218	N	3	2	218.00	11.86	1.40	0.00	20.25	3.96
N_4_2_218	N	4	2	218.00	17.45	2.03	0.00	26.50	3.96
N_5_2_218	N	5	2	218.00	26.63	2.99	0.00	39.25	3.96
N_6_2_218	N	6	2	218.00	51.25	5.30	0.00	67.50	3.96
N_1_4_218	N	1	4	218.00	0.00	0.00	0.00	0.00	3.96
W_1_1_218	W	1	1	218.00	281.69	131.33	1.25	407.50	3.96
N_2_4_338	N	2	4	338.00	0.00	0.00	0.00	0.00	3.96
W_2_1_218	W	2	1	218.00	336.10	156.28	1.75	463.00	3.96
N_3_4_338	N	3	4	338.00	0.00	0.00	0.00	0.00	3.96
W_3_1_218	W	3	1	218.00	423.21	196.03	2.25	522.25	3.96
N_4_4_338	N	4	4	338.00	3.79	0.45	0.00	2.25	3.96
W_4_1_218	W	4	1	218.00	609.08	274.09	2.25	569.75	3.96
N_5_4_338	N	5	4	338.00	8.70	0.93	0.00	6.00	3.96
W_5_1_218	W	5	1	218.00	829.10	317.47	2.50	502.25	3.96
N_6_4_338	N	6	4	338.00	35.91	3.87	0.00	29.75	3.96
W_6_1_218	W	6	1	218.00	938.85	269.68	3.00	417.25	3.96
W_1_3_218	W	1	3	218.00	467.28	198.75	1.25	379.75	3.96
W_2_3_320	W	2	3	320.00	1 366.77	619.03	2.00	700.50	3.96

W_3_3_320	W	3	3	320.00	1 446.23	631.15	2.50	728.00	3.96
W_4_3_320	W	4	3	320.00	1 712.85	730.50	3.25	830.25	3.96
W_5_3_320	W	5	3	320.00	2 223.38	891.80	3.50	1 009.25	3.96
W_6_3_320	W	6	3	320.00	2 765.79	1 001.77	3.75	1 204.25	3.96
W_1_5_437	W	1	5	437.00	1 040.44	385.56	1.00	239.25	3.96
W_2_5_384	W	2	5	384.00	1 006.86	395.00	1.75	363.13	3.96
W_3_5_384	W	3	5	384.00	1 123.67	426.53	2.00	402.38	3.96
W_4_5_384	W	4	5	384.00	1 260.35	460.64	2.00	443.75	3.96
W_5_5_384	W	5	5	384.00	1 501.95	507.04	2.00	505.00	3.96
W_6_5_384	W	6	5	384.00	1 972.68	645.81	2.25	659.13	3.96
W_1_7_218	W	1	7	218.00	738.99	307.70	1.00	451.50	3.96
W_2_7_218	W	2	7	218.00	825.97	337.76	1.00	493.00	3.96
W_3_7_218	W	3	7	218.00	913.42	363.14	2.00	538.25	3.96
W_4_7_218	W	4	7	218.00	1 008.76	386.21	2.50	580.50	3.96
W_5_7_218	W	5	7	218.00	1 114.07	401.87	3.00	617.75	3.96
W_6_7_218	W	6	7	218.00	1 037.74	274.19	2.75	413.25	3.96
S_1_1_37	S	1	1	37.00	60.49	20.54	1.50	325.00	3.57
W1_1_4_167	W	1	4	167.00	1 288.98	369.28	2.00	942.50	3.57
S_2_1_86	S	2	1	86.00	223.56	83.23	1.50	557.75	3.57
S_2_2_86	S	2	2	86.00	195.83	68.32	1.50	470.75	3.57
S_3_1_167	S	3	1	167.00	539.74	202.16	3.00	892.75	3.57
S_4_1_167	S	4	1	167.00	573.86	220.45	3.25	912.00	3.57
S_5_1_167	S	5	1	167.00	672.24	278.32	3.50	929.00	3.57
S_6_1_86	S	6	1	86.00	437.35	196.40	3.50	1 150.25	3.57
S_6_2_86	S	6	2	86.00	371.08	163.90	3.25	995.50	3.57
S_1_2_37	S	1	2	37.00	18.10	4.61	0.50	73.25	3.57
W2_1_1_93	W	1	1	93.00	741.92	232.29	1.75	1 078.25	3.57
W2_1_2_204	W	1	2	204.00	1 514.51	446.50	1.75	941.00	3.57
W2_1_3_93	W	1	3	93.00	619.13	166.11	1.50	777.50	3.57
W2_1_4_167	W	1	4	167.00	1 028.13	254.21	1.50	712.25	3.57
S_2_2_37	S	2	2	37.00	5.33	1.38	0.00	0.00	3.57

W2_2_3_204	W	2	3	204.00	1 489.83	464.18	1.50	947.75	3.57
W2_2_4_235	W	2	4	235.00	1 548.64	441.51	1.25	775.75	3.57
S_2_3_167	S	2	3	167.00	378.08	47.05	0.75	631.75	3.57
S_2_4_167	S	2	4	167.00	523.80	67.87	0.00	915.75	3.57
S_2_5_204	S	2	5	204.00	563.28	394.14	0.00	750.00	3.57
S_2_6_86	S	2	6	86.00	271.74	35.64	0.00	936.00	3.57
S_2_7_86	S	2	7	86.00	271.72	35.64	0.00	939.00	3.57
S_2_8_204	S	2	8	204.00	644.88	84.50	0.00	940.75	3.57
S_2_9_167	S	2	9	167.00	523.89	67.90	0.00	917.50	3.57
S_2_10_37	S	2	10	37.00	61.49	6.30	0.00	395.50	3.57
W4_2_3_204	W	2	3	204.00	1 221.00	438.41	1.75	770.50	3.57
W4_2_4_235	W	2	4	235.00	1 296.42	422.06	1.00	624.50	3.57
S_2_11_167	S	2	11	167.00	278.40	27.57	0.00	403.00	3.57
S_3_2_99	S	3	2	99.00	157.03	20.59	0.00	475.25	3.57
W2_3_3_204	W	3	3	204.00	1 614.97	553.98	1.50	1 107.50	3.57
W2_3_4_235	W	3	4	235.00	1 743.42	583.09	1.25	1 007.00	3.57
S_3_3_167	S	3	3	167.00	507.73	62.60	0.00	848.50	3.57
S_3_4_167	S	3	4	167.00	512.24	63.73	0.00	852.50	3.57
S_3_5_167	S	3	5	167.00	512.35	63.76	0.00	851.00	3.57
S_3_6_167	S	3	6	167.00	507.88	62.64	0.00	848.00	3.57
S_3_7_99	S	3	7	99.00	49.18	33.08	0.50	156.00	3.57
W4_3_4_204	W	3	4	204.00	1 307.50	505.78	1.75	907.50	3.57
W4_3_5_235	W	3	5	235.00	1 466.59	539.94	1.25	841.25	3.57
S_4_2_99	S	4	2	99.00	156.60	20.41	0.00	475.25	3.57
W2_4_2_204	W	4	2	204.00	1 682.46	603.01	1.25	1 233.25	3.57
W2_4_3_235	W	4	3	235.00	1 924.77	700.47	1.25	1 192.00	3.57
S_4_3_167	S	4	3	167.00	621.39	380.72	3.75	792.75	3.57
S_4_4_167	S	4	4	167.00	665.61	406.57	4.25	911.25	3.57
S_4_5_167	S	4	5	167.00	656.81	401.44	4.75	909.75	3.57
S_4_6_167	S	4	6	167.00	591.07	364.24	3.50	786.00	3.57
S_4_7_99	S	4	7	99.00	143.17	102.79	0.25	472.00	3.57

W4_4_4_204	W	4	4	204.00	1 354.94	530.48	1.50	1 015.50	3.57
W4_4_5_235	W	4	5	235.00	1 628.03	634.67	1.00	1 008.00	3.57
S_5_2_99	S	5	2	99.00	134.57	16.18	0.00	381.00	3.57
W2_5_2_204	W	5	2	204.00	1 356.07	418.89	6.00	1 069.00	3.57
W2_5_3_235	W	5	3	235.00	1 858.90	680.37	5.25	1 274.00	3.57
S_5_3_167	S	5	3	167.00	381.45	32.29	4.25	505.50	3.57
S_5_4_167	S	5	4	167.00	376.02	31.22	4.50	495.00	3.57
S_5_5_167	S	5	5	167.00	374.82	31.02	4.75	495.25	3.57
S_5_6_167	S	5	6	167.00	373.09	30.90	4.25	496.50	3.57
S_5_7_99	S	5	7	99.00	131.64	21.62	0.00	522.00	3.57
W4_5_2_204	W	5	2	204.00	1 027.56	344.26	4.00	821.75	3.57
W4_5_3_235	W	5	3	235.00	1 538.88	595.83	2.75	1 066.00	3.57
S_6_2_99	S	6	2	99.00	104.25	8.40	0.00	232.75	3.57
W4_6_3_204	W	6	3	204.00	516.36	90.15	5.00	425.25	3.57
W4_6_4_235	W	6	4	235.00	870.95	250.35	6.00	649.75	3.57
S_6_3_77	S	6	3	77.00	480.19	214.82	5.50	1 447.00	3.57
S_6_4_77	S	6	4	77.00	484.47	216.45	5.50	1 456.75	3.57
S_6_5_77	S	6	5	77.00	481.71	216.00	5.75	1 445.00	3.57
S_6_6_77	S	6	6	77.00	464.69	212.79	5.75	1 408.75	3.57
S_6_7_77	S	6	7	77.00	459.60	211.63	5.75	1 402.25	3.57
S_6_8_77	S	6	8	77.00	443.23	207.54	5.75	1 368.50	3.57
S_6_9_77	S	6	9	77.00	430.71	204.27	5.50	1 342.50	3.57
S_6_10_77	S	6	10	77.00	460.91	252.61	5.50	1 085.75	3.57
S_6_11_77	S	6	11	77.00	486.93	267.78	5.25	1 088.00	3.57
W4_6_3_204	W	6	3	204.00	330.71	58.64	3.50	241.00	3.57
W4_6_4_235	W	6	4	235.00	610.25	187.25	4.50	435.50	3.57
S_3_11_167	S	3	11	167.00	329.18	29.38	0.00	410.25	3.57
S_4_11_167	S	4	11	167.00	438.01	241.07	0.25	402.25	3.57
S_5_11_167	S	5	11	167.00	284.82	21.36	0.00	313.25	3.57
S_6_12_77	S	6	12	77.00	285.74	144.37		932.25	3.57
S_6_13_77	S	6	13	77.00	320.14	162.39	3.25	1 048.75	3.57

W1_1_1_167	W	1	1	167.00	1 256.31	302.17	2.25	937.75	3.57
W1_1_2_235	W	1	2	235.00	1 666.16	315.06	3.00	893.75	3.57
W1_1_3_204	W	1	3	204.00	1 620.69	458.38	2.25	984.00	3.57
W1_3_1_235	W	3	1	235.00	1 648.15	313.07	3.00	887.50	3.57
W1_3_2_204	W	3	2	204.00	1 285.64	282.94	4.50	786.75	3.57
W1_3_3_167	W	3	3	167.00	1 375.69	473.20	1.75	1 214.50	3.57
W1_5_1_235	W	5	1	235.00	1 646.85	313.52	3.00	882.00	3.57
W1_5_2_204	W	5	2	204.00	769.96	100.72	2.50	491.25	3.57
W2_5_1_93	W	5	1	93.00	123.58	9.91	1.00	189.50	3.57
W2_5_2_93	W	5	2	93.00	132.81	12.34	2.50	224.75	3.57
W3_3_1_37	W	3	1	37.00	128.26	24.73	4.75	713.25	3.57
N_3_17_167	N	3	17	167.00	101.15	8.77	0.00	184.25	3.57
W3_5_1_37	W	5	1	37.00	83.52	11.44	3.25	417.50	3.57
N_5_17_167	N	5	17	167.00	101.79	8.97	0.00	184.25	3.57
W3_6_1_147	W	6	1	147.00	120.94	10.28	0.75	122.50	3.57
N_6_17_37	N	6	17	37.00	25.43	1.67	0.00	85.75	3.57
W4_2_1_93	W	2	1	93.00	505.88	210.46	1.75	811.75	3.57
W4_2_2_93	W	2	2	93.00	525.83	211.43	1.75	830.50	3.57
W4_3_1_167	W	3	1	167.00	962.63	395.37	1.75	886.50	3.57
W4_4_1_167	W	4	1	167.00	811.11	284.95	3.25	698.75	3.57
W4_5_1_167	W	5	1	167.00	479.08	116.33	4.25	393.50	3.57
W4_6_1_93	W	6	1	93.00	71.50	6.71	1.00	92.25	3.57
W4_6_2_93	W	6	2	93.00	81.75	8.43	1.25	114.50	3.57
E1_2_1_93	E	2	1	93.00	696.02	232.09	1.25	1 045.75	3.57
E1_2_1_37	E	2	1	37.00	289.57	98.38	1.25	1 126.75	3.57
E1_3_1_198	E	3	1	198.00	175.54	73.33	0.50	280.00	3.57
E1_3_2_198	E	3	2	198.00	221.18	87.44	0.75	329.50	3.57
E1_3_3_204	E	3	3	204.00	1 785.52	374.65	5.75	1 402.75	3.57
E1_3_4_235	E	3	4	235.00	1 933.70	377.83	5.75	1 300.00	3.57
E1_4_1_198	E	4	1	198.00	258.04	125.70	0.50	380.75	3.57
E1_4_2_198	E	4	2	198.00	300.67	137.33	0.75	426.00	3.57

E1_4_3_204	E	4	3	204.00	1 493.94	258.23	5.75	1 193.00	3.57
E1_4_4_235	E	4	4	235.00	1 639.60	266.12	4.50	1 150.50	3.57
E1_5_1_198	E	5	1	198.00	394.43	199.80	0.75	474.75	3.57
E1_5_2_198	E	5	2	198.00	438.62	211.54	0.75	515.25	3.57
E1_5_3_204	E	5	3	204.00	1 111.86	140.48	4.75	870.00	3.57
E1_5_4_235	E	5	4	235.00	1 215.97	144.63	4.50	796.50	3.57
E1_6_1_93	E	6	1	93.00	183.67	37.29	6.00	387.00	3.57
E1_6_2_93	E	6	2	93.00	133.22	18.32	2.50	256.00	3.57
E1_6_3_93	E	6	3	93.00	102.77	7.81	1.00	172.50	3.57
E1_6_4_93	E	6	4	93.00	101.03	7.08	1.00	155.50	3.57
E1_6_5_204	E	6	5	204.00	529.22	38.73	1.75	420.25	3.57
E1_6_6_235	E	6	6	235.00	512.03	34.89	0.75	300.00	3.57
E2_2_1_93	E	2	1	93.00	428.90	128.65	1.25	741.00	3.57
E2_2_2_93	E	2	2	93.00	459.77	132.19	1.00	790.75	3.57
E2_3_1_167	E	3	1	167.00	716.99	271.49	1.75	709.75	3.57
E2_3_2_235	E	3	2	235.00	1 151.16	346.13	1.25	829.75	3.57
E2_4_1_167	E	4	1	167.00	796.27	319.57	1.75	846.00	3.57
E2_4_2_235	E	4	2	235.00	1 042.35	258.01	3.75	694.50	3.57
E2_4_3_204	E	4	3	204.00	267.51	68.53	0.00	181.50	3.57
E2_4_4_93	E	4	4	93.00	455.16	73.53	4.75	818.00	3.57
N_4_15_167	N	4	15	167.00	101.15	8.77	0.00	184.25	3.57
N_4_16_37	N	4	16	37.00	7.82	0.55	0.00	14.00	3.57
E2_5_1_167	E	5	1	167.00	769.07	286.97	5.00	920.75	3.57
E2_5_2_235	E	5	2	235.00	879.85	160.57	4.00	570.50	3.57
E2_6_1_93	E	6	1	93.00	227.56	50.59	5.25	495.00	3.57
E2_6_2_93	E	6	2	93.00	164.55	25.71	4.75	344.75	3.57
E2_6_3_93	E	6	3	93.00	128.67	11.23	2.75	217.75	3.57
E2_6_4_93	E	6	4	93.00	122.28	9.06	1.00	188.25	3.57
E2_6_5_93	E	6	5	93.00	123.56	8.25	0.75	172.25	3.57
E2_6_6_204	E	6	6	204.00	359.14	98.16	0.00	250.50	3.57
E2_6_7_93	E	6	7	93.00	231.92	54.04	0.00	37.25	3.57

N_6_15_37	N	6	15	37.00	7.82	0.55	0.00	14.00	3.57
N_6_16_93	N	6	16	93.00	35.11	2.66	0.00	39.75	3.57
N_2_1_93	N	2	1	93.00	34.20	2.50	0.00	39.75	3.57
N_2_2_93	N	2	2	93.00	33.85	2.44	0.00	39.75	3.57
N_2_3_167	N	2	3	167.00	91.86	6.95	0.00	175.75	3.57
N_2_4_167	N	2	4	167.00	90.78	6.87	0.00	175.75	3.57
N_2_5_167	N	2	5	167.00	90.84	6.94	0.00	161.25	3.57
N_2_6_167	N	2	6	167.00	82.48	5.85	0.00	133.75	3.57
N_2_7_93	N	2	7	93.00	24.13	1.32	0.00	39.75	3.57
N_2_8_93	N	2	8	93.00	19.46	0.95	0.00	39.75	3.57
N_2_9_93	N	2	9	93.00	35.13	2.66	0.00	39.75	3.57
N_2_10_93	N	2	10	93.00	35.30	2.72	0.00	39.75	3.57
N_2_11_93	N	2	11	93.00	35.14	2.67	0.00	39.75	3.57
N_2_12_93	N	2	12	93.00	36.00	2.90	0.00	39.75	3.57
N_3_1_167	N	3	1	167.00	13.16	1.76	0.00	41.75	3.57
N_3_3_93	N	3	3	93.00	15.13	1.69	0.00	0.00	3.57
N_3_4_93	N	3	4	93.00	17.03	1.82	0.00	0.00	3.57
N_3_5_265	N	3	5	265.00	116.09	13.40	0.00	88.50	3.57
N_3_6_37	N	3	6	37.00	6.26	0.50	0.00	4.50	3.57
N_3_7_167	N	3	7	167.00	93.16	7.58	0.00	174.50	3.57
N_3_14_167	N	3	14	167.00	51.67	2.92	0.00	64.50	3.57
N_3_15_167	N	3	15	167.00	0.24	0.06	0.00	0.00	3.57
N_3_16_167	N	3	16	167.00	101.15	8.77	0.00	184.25	3.57
N_4_2_167	N	4	2	167.00	20.28	2.45	0.00	61.75	3.57
N_4_8_167	N	4	8	167.00	90.16	6.79	0.00	176.00	3.57
N_4_9_204	N	4	9	204.00	95.36	8.52	0.00	127.25	3.57
N_4_10_235	N	4	10	235.00	71.30	4.60	0.00	65.00	3.57
N_4_13_167	N	4	13	167.00	51.65	2.92	0.00	64.50	3.57
N_4_15_167	N	4	15	167.00	101.15	8.77	0.00	184.25	3.57
N_4_16_167	N	4	16	167.00	142.35	13.60	0.00	201.25	3.57
N_5_1_167	N	5	1	167.00	9.08	1.34	0.00	14.25	3.57

N_5_3_93	N	5	3	93.00	9.95	0.85	0.00	0.00	3.57
N_5_4_93	N	5	4	93.00	12.31	1.05	0.00	0.00	3.57
N_5_5_265	N	5	5	265.00	97.90	10.29	0.00	50.00	3.57
N_5_6_37	N	5	6	37.00	5.90	0.44	0.00	4.50	3.57
N_5_7_167	N	5	7	167.00	88.31	6.86	0.00	149.75	3.57
N_5_8_167	N	5	8	167.00	91.14	7.17	0.00	166.50	3.57
N_5_11_235	N	5	11	235.00	60.07	3.08	0.00	36.25	3.57
N_5_12_204	N	5	12	204.00	63.49	4.91	0.00	111.00	3.57
N_5_14_167	N	5	14	167.00	171.03	29.52	0.00	139.15	3.57
N_5_16_167	N	5	16	167.00	142.35	13.60	0.00	201.25	3.57
N_6_1_93	N	6	1	93.00	1.21	0.20	0.00	0.00	3.57
N_6_2_93	N	6	2	93.00	1.71	0.25	0.00	0.00	3.57
N_6_3_167	N	6	3	167.00	15.97	2.45	0.00	42.00	3.57
N_6_6_93	N	6	6	93.00	14.00	0.97	0.00	18.00	3.57
N_6_7_167	N	6	7	167.00	62.43	5.55	0.00	109.25	3.57
N_6_8_93	N	6	8	93.00	23.41	1.40	0.00	36.00	3.57
N_6_11_204	N	6	11	204.00	75.16	6.20	0.00	96.50	3.57
N_6_12_235	N	6	12	235.00	508.65	43.42	0.00	266.50	3.57
N_6_21_93	N	6	21	93.00	35.13	2.66	0.00	39.75	3.57
N_6_22_93	N	6	22	93.00	35.91	2.86	0.00	39.75	3.57
SSE1_2_1_249	SSE	2	1	249.00	2 319.21	996.29	7.25	1 963.25	2.57
SSE1_2_2_221	SSE	2	2	221.00	1 919.69	825.57	5.75	1 694.50	2.57
SSE1_2_4_250	SSE	2	4	250.00	2 609.20	1 036.25	7.75	2 103.25	2.57
SSE1_2_5_250	SSE	2	5	250.00	2 315.13	920.64	5.75	1 614.00	2.57
SSE1_2_9_251	SSE	2	9	251.00	2 730.82	1 095.38	7.25	2 084.75	2.57
SSE1_3_3_210	SSE	3	3	210.00	2 100.79	820.93	6.50	1 804.50	2.57
SSE1_3_6_214	SSE	3	6	214.00	2 092.44	836.76	4.25	1 684.50	2.57
SSE1_3_7_256	SSE	3	7	256.00	2 962.21	1 144.40	7.50	2 224.00	2.57
SSE1_3_8_211	SSE	3	8	211.00	2 128.63	839.23	5.75	1 718.75	2.57
SSE1_4_1_249	SSE	4	1	249.00	2 954.02	1 122.06	8.25	2 370.50	2.57
SSE1_4_3_210	SSE	4	3	210.00	2 306.08	859.26	6.50	1 944.75	2.57

SSE1_4_5_250	SSE	4	5	250.00	2 669.63	993.11	6.25	1 819.50	2.57
SSE1_4_7_256	SSE	4	7	256.00	3 227.31	1 184.95	8.00	2 395.50	2.57
SSE1_4_9_251	SSE	4	9	251.00	3 185.51	1 164.42	8.00	2 400.75	2.57
SSE2_3_1_232	SSE	3	1	232.00	1 948.68	809.95	4.25	1 295.75	2.57
SSE3_1_1_360	SSE	1	1	360.00	3 306.37	1 282.78	7.00	2 067.00	2.57
SSE3_1_2_105	SSE	1	2	105.00	946.60	351.91	7.00	1 556.00	2.57
SSE3_1_3_257	SSE	1	3	257.00	1 192.89	262.62	0.75	889.25	2.57
SW1_1_1_209	SW	1	1	209.00	1 102.60	257.20	2.75	916.00	2.57
SSE3_2_4_257	SSE	2	4	257.00	1 192.46	220.18	1.75	806.75	2.57
SSE3_2_5_105	SSE	2	5	105.00	188.74	28.24	1.00	662.75	2.57
SSE3_2_6_360	SSE	2	6	360.00	1 303.25	211.56	1.50	638.75	2.57
SSE3_3_7_360	SSE	3	7	360.00	3 545.40	1327.46	7.00	2300.50	2.57
SSE3_3_8_105	SSE	3	8	105.00	527.52	166.90	4.00	1320.50	2.57
SSE3_3_9_257	SSE	3	9	257.00	940.71	123.11	1.75	564.75	2.57
SSE3_4_1_360	SSE	4	1	360.00	3 349.26	1168.62	6.50	2024.75	2.57
SSE3_4_2_105	SSE	4	2	105.00	609.96	195.65	4.00	1422.75	2.57
SSE3_4_3_257	SSE	4	3	257.00	780.41	112.05	2.25	492.75	2.57
SW1_4_1_209	SW	4	1	209.00	202.26	15.70	1.50	204.75	2.57
SSE3_2_1_257	SSE	2	1	257.00	1 933.18	619.18	5.00	1589.00	2.57
SSW_2_2_360	SSW	2	2	360.00	807.83	111.31	0.75	903.25	2.57
SSW_3_1_360	SSW	3	1	360.00	1 674.85	517.71	7.00	1051.25	2.57
SW2_3_2_257	SW	3	2	257.00	1 604.33	606.22	5.00	1337.50	2.57
SSW_4_1_257	SSW	4	1	257.00	1 695.53	468.13	5.25	1188.75	2.57
SW2_4_2_360	SW	4	2	360.00	399.22	25.54	0.75	330.50	2.57
NW1_1_7_209	NW	1	7	209.00	551.49	114.09	1.00	588.00	2.57
NW1_1_8_244	NW	1	8	244.00	697.24	140.96	0.50	474.50	2.57
NW1_2_3_209	NW	2	3	209.00	580.95	117.08	1.00	607.25	2.57
NW1_2_4_244	NW	2	4	244.00	741.02	145.29	0.50	495.50	2.57
NW1_2_6_209	NW	2	6	209.00	601.97	118.28	1.00	614.25	2.57
NW1_3_1_244	NW	3	1	244.00	711.35	142.71	0.50	401.00	2.57
NW1_3_2_209	NW	3	2	209.00	579.51	116.33	1.00	605.50	2.57

NW1_3_7_209	NW	3	7	209.00	649.79	119.30	1.00	631.00	2.57
NW1_4_3_209	NW	4	3	209.00	632.59	112.31	1.00	577.25	2.57
NW1_4_4_244	NW	4	4	244.00	798.96	137.97	0.50	495.50	2.57
NW1_4_5_244	NW	4	5	244.00	826.57	140.12	0.50	506.50	2.57
NW1_4_6_209	NW	4	6	209.00	673.57	116.52	1.00	601.75	2.57
NW2_2_1_206	NW	2	1	206.00	52.42	5.79	0.00	19.05	2.57
NW2_3_1_206	NW	3	1	206.00	80.60	6.90	0.00	33.00	2.57
NW3_3_4_257	NW	3	4	257.00	356.00	70.20	0.75	331.75	2.57
NW3_3_5_105	NW	3	5	105.00	114.98	16.87	0.50	418.50	2.57
NW3_4_2_105	NW	4	2	105.00	389.04	92.56	0.50	621.50	2.57
NW3_4_3_257	NW	4	3	257.00	460.88	88.95	0.00	413.50	2.57
SW3_2_1_209	SW	2	1	209.00	1 457.30	632.11	3.75	1 243.25	2.57
NW4_3_2_105	NW	3	2	105.00	463.14	112.35	3.00	899.00	2.57
NW4_3_3_257	NW	3	3	257.00	455.35	88.94	0.00	388.00	2.57
NW4_4_5_105	NW	4	5	105.00	92.47	13.13	0.00	248.25	2.57
NW4_4_6_257	NW	4	6	257.00	1 719.22	311.63	4.75	903.75	2.57
SW3_4_1_209	SW	4	1	209.00	1 933.16	678.86	4.00	1 422.00	2.57
SW3_3_1_209	SW	3	1	209.00	1 745.13	706.42	4.00	1 470.25	2.57
NE1_2_1_217	NE	2	1	217.00	0.00	0.00	0.00	0.00	2.57
NE1_3_1_217	NE	3	1	217.00	0.00	0.00	0.00	0.00	2.57
NE1_4_1_217	NE	4	1	217.00	0.00	0.00	0.00	0.00	2.57
NE2_2_1_248	NE	2	1	248.00	1 028.38	315.77	2.00	726.25	2.57
SSE2_2_1_232	SSE	2	1	232.00	0.00	0.00	0.00	0.00	2.57
NE2_2_5_218	NE	2	5	218.00	990.26	271.15	2.00	738.25	2.57
NE2_2_6_215	NE	2	6	215.00	732.92	166.86	1.25	586.75	2.57
NE2_3_3_215	NE	3	3	215.00	754.95	169.72	1.25	601.00	2.57
NE2_3_4_212	NE	3	4	212.00	1 024.78	265.74	2.25	774.75	2.57
NE2_3_7_215	NE	3	7	215.00	816.63	173.88	1.25	625.75	2.57
SSE2_4_1_232	SSE	4	1	232.00	0.00	0.00	0.00	0.00	2.57
NE2_4_1_248	NE	4	1	248.00	1 256.98	303.84	2.00	646.25	2.57
NE2_4_2_215	NE	4	2	215.00	819.42	174.49	1.75	643.50	2.57

NE2_4_5_218	NE	4	5	218.00	1 135.48	275.83	2.50	752.75	2.57
NE2_4_6_215	NE	4	6	215.00	848.35	176.12	1.50	650.75	2.57
NE3_2_2_212	NE	2	2	212.00	871.67	205.14	0.75	522.75	2.57
NE3_2_3_215	NE	2	3	215.00	1 209.93	407.70	4.25	722.75	2.57
NE3_2_6_212	NE	2	6	212.00	969.73	241.79	1.75	791.25	2.57
NE3_3_1_214	NE	3	1	214.00	518.36	82.07	0.00	140.75	2.57
NE3_3_4_215	NE	3	4	215.00	157.28	108.02	0.50	140.75	2.57
NE3_3_5_212	NE	3	5	212.00	1 019.52	242.32	2.00	765.00	2.57
NE3_3_8_215	NE	3	8	215.00	298.75	123.86	0.50	288.75	2.57
NE3_3_9_259	NE	3	9	259.00	915.16	295.00	0.75	597.00	2.57
NE3_4_2_212	NE	4	2	212.00	907.27	200.16	0.50	519.00	2.57
NE3_4_3_215	NE	4	3	215.00	864.39	418.79	1.75	535.50	2.57
NE3_4_6_212	NE	4	6	212.00	1 091.88	243.49	2.25	799.50	2.57
NE3_4_7_215	NE	4	7	215.00	888.07	419.54	1.75	615.75	2.57
SW2_2_1_213	SW	2	1	213.00	1 105.15	512.64	3.75	996.75	2.57
SW2_2_3_257	SW	2	3	257.00	1 597.60	302.41	2.25	820.50	2.57
SW2_2_4_105	SW	2	4	105.00	385.71	172.45	3.50	1 043.75	2.57
SW2_2_5_360	SW	2	5	360.00	1 828.82	332.36	2.00	768.75	2.57
SW2_2_9_210	SW	2	9	210.00	1 444.85	621.58	4.50	1 333.75	2.57
SW2_2_11_257	SW	2	11	257.00	1 391.15	252.83	1.75	829.50	2.57
SW2_2_12_105	SW	2	12	105.00	856.45	173.85	3.75	821.50	2.57
SW2_2_13_360	SW	2	13	360.00	1 443.44	236.24	2.50	758.25	2.57
SW2_3_2_210	SW	3	2	210.00	1 567.56	646.25	4.50	1 368.25	2.57
SW2_3_6_360	SW	3	6	360.00	1 480.20	213.23	1.50	574.50	2.57
SW2_3_7_105	SW	3	7	105.00	349.02	48.55	1.00	529.75	2.57
SW2_3_8_257	SW	3	8	257.00	1 288.56	193.88	1.75	636.75	2.57
SW2_3_10_210	SW	3	10	210.00	1 603.08	642.85	4.75	1 479.50	2.57
SW2_4_1_213	SW	4	1	213.00	1 574.22	557.83	4.00	1 121.75	2.57
SW2_4_3_257	SW	4	3	257.00	712.76	63.85	1.00	332.50	2.57
SW2_4_4_105	SW	4	4	105.00	600.23	217.46	4.50	1 354.50	2.57
SW2_4_5_360	SW	4	5	360.00	719.36	55.70	0.75	275.75	2.57

SW2_4_9_210	SW	4	9	210.00	1 706.55	578.99	4.25	1 320.25	2.57
SW2_4_11_257	SW	4	11	257.00	612.96	56.70	2.00	357.75	2.57
SW2_4_12_105	SW	4	12	105.00	397.79	60.23	3.00	473.75	2.57
SW2_4_13_360	SW	4	13	360.00	768.36	131.03	2.25	452.50	2.57
WSW_2_1_360	WSW	2	1	360.00	2 195.36	1022.89	5.50	1 492.25	2.57
WSW_2_2_361	WSW	2	2	105.00	657.94	289.83	5.25	1 333.50	2.57
WSW_2_3_257	WSW	2	9	257.00	1 138.52	457.37	4.75	1 404.75	2.57
WSW_2_5_209	WSW	2	5	209.00	1 653.40	719.92	3.25	1 123.75	2.57
WSW_2_9_360	WSW	2	9	360.00	1 967.60	952.30	2.75	1 374.00	2.57
WSW_2_10_105	WSW	2	10	105.00	477.01	223.19	3.25	1 201.25	2.57
WSW_2_11_257	WSW	2	11	257.00	935.66	389.15	2.50	1 162.00	2.57
WSW_2_9_257	WSW	2	9	257.00	1 797.74	815.91	3.25	1 736.07	2.57
WSW_3_4_213	WSW	3	4	213.00	1 910.59	786.24	3.50	1 255.75	2.57
WSW_3_6_257	WSW	3	6	257.00	1 282.75	470.07	4.75	1 385.25	2.57
WSW_3_7_105	WSW	3	7	105.00	920.02	143.44	3.50	863.25	2.57
WSW_3_8_360	WSW	3	8	360.00	2 409.67	1046.88	5.50	1 607.50	2.57
WSW_3_12_214	WSW	3	12	214.00	1 501.22	654.16	0.50	870.25	2.57
WSW_4_1_360	WSW	4	1	360.00	1 926.19	742.71	6.00	1 289.25	2.57
WSW_4_2_105	WSW	4	2	105.00	220.83	17.51	1.00	273.75	2.57
WSW_4_3_257	WSW	4	3	257.00	1 220.45	402.02	5.50	1 224.50	2.57
WSW_4_5_209	WSW	4	5	209.00	1 728.07	615.69	3.75	932.25	2.57
WSW_4_9_360	WSW	4	9	360.00	2 603.23	1108.11	6.25	1 711.75	2.57
WSW_4_10_105	WSW	4	10	105.00	595.14	253.58	5.00	1 255.25	2.57
WSW_4_11_257	WSW	4	11	257.00	1 285.43	457.86	5.75	1 331.25	2.57
E_1_1_271	E	1	1	271.00	2 047.68	849.10	3.00	1 404.00	1.25
E_1_2_160	E	1	2	160.00	1 316.10	534.53	3.00	1 494.00	1.25
E_2_5_160	E	2	5	160.00	1 784.62	634.12	5.50	1 888.25	1.25
E_2_6_271	E	2	6	271.00	3 044.42	1078.86	5.50	1 890.75	1.25
E_3_9_160	E	3	9	160.00	2 095.40	659.92	6.00	2 150.25	1.25
E_3_10_271	E	3	10	271.00	3 558.64	1118.91	6.00	2 153.50	1.25
E_4_7_271	E	4	7	271.00	3 665.73	1122.62	6.00	2 202.50	1.25

E_4_8_160	E	4	8	160.00	2 162.66	662.31	6.00	2 202.50	1.25
E_5_3_271	E	5	3	271.00	3 665.73	1122.62	6.00	2 202.50	1.25
E_5_4_160	E	5	4	160.00	2 162.66	662.31	6.00	2 202.50	1.25
E_6_1_271	E	6	1	271.00	3 665.73	1122.62	6.00	2 202.50	1.25
E_6_2_160	E	6	2	160.00	2 162.66	662.31	6.00	2 202.50	1.25
E_7_5_160	E	7	5	160.00	2 162.66	662.31	6.00	2 202.50	1.25
E_7_6_271	E	7	6	271.00	3 665.73	1122.62	6.00	2 202.50	1.25
E_8_9_160	E	8	9	160.00	2 162.66	662.31	6.00	2 202.50	1.25
E_8_10_271	E	8	10	271.00	3 665.73	1122.62	6.00	2 202.50	1.25
E_9_7_271	E	9	7	271.00	3 665.73	1122.62	6.00	2 202.50	1.25
E_9_8_160	E	9	8	160.00	2 162.66	662.31	6.00	2 202.50	1.25
W_1_1_271	W	1	1	271.00	2 711.71	1038.90	5.00	1 652.75	1.25
W_1_2_160	W	1	2	160.00	1 588.90	609.75	5.00	1 635.25	1.25
W_2_5_271	W	2	5	271.00	2 896.71	1060.22	5.50	1 733.25	1.25
W_2_6_160	W	2	6	160.00	1 672.36	619.55	5.50	1 689.25	1.25
W_4_7_160	W	4	7	160.00	2 162.66	662.31	6.00	2 202.50	1.25
W_4_8_271	W	4	8	271.00	3 665.73	1122.62	6.00	2 202.50	1.25
W_5_3_160	W	5	3	160.00	2 162.66	662.31	6.00	2 202.50	1.25
W_5_4_271	W	5	4	271.00	3 665.73	1122.62	6.00	2 202.50	1.25
W_6_1_271	W	6	1	271.00	3 665.73	1122.62	6.00	2 202.50	1.25
W_6_2_160	W	6	2	160.00	2 162.66	662.31	6.00	2 202.50	1.25
W_7_5_271	W	7	5	271.00	3 665.73	1122.62	6.00	2 202.50	1.25
W_7_6_160	W	7	6	160.00	2 162.66	662.31	6.00	2 202.50	1.25
W_9_7_160	W	9	7	160.00	2 162.66	662.31	6.00	2 202.50	1.25
W_9_8_271	W	9	8	271.00	3 665.73	1122.62	6.00	2 202.50	1.25

Appendix C

The room naming follows the format R_BuildingID_RoomNumber_Floor. The letter R indicates a room. The following number indicates the building model ID, the next number indicates the room number within that building model, and the final number indicates the floor level. For example, R_52_21_6 refers to room 21 in building model 52, located on the sixth floor.

Table 7 Complete dataset of room-level sunlight access metrics calculated for urban context models computations.

Room ID	Model	Floor	Orientation	Aperture count	Aperture area (total) (cm^2)	SBI ($m^2 \cdot hrs$)	SBI_airmas ($m^2 \cdot hrs$)	EN 17037 sunlight exposure (hrs)	ASH (hrs)	Urban density (m^3/m^2)
S_3_1_1	ID_5	3	S	1	148.00	1 645.15	611.72	8.00	1 446.00	3.02
S_1_1_266	ID_5	1	S	1	266.00	985.82	423.99	5.75	867.25	3.02
S_1_3_266	ID_5	1	S	1	266.00	994.07	431.21	5.25	930.25	3.02
S_3_3_148	ID_5	3	S	1	148.00	1 656.83	613.72	8.00	1 443.00	3.02
S_3_5_148	ID_5	3	S	1	148.00	1 672.43	616.18	8.00	1 440.25	3.02
S_2_2_148	ID_5	2	S	1	148.00	1 413.05	568.91	7.75	1 246.25	3.02
S_2_4_148	ID_5	2	S	1	148.00	1 427.45	570.13	7.75	1 243.25	3.02
E_1_1_362	ID_5	1	E	1	362.00	1 218.57	477.43	2.75	639.00	3.02
E_2_3_148	ID_5	2	E	1	148.00	1 039.85	381.88	3.25	889.25	3.02
E_3_2_269	ID_5	3	E	1	269.00	1 966.47	683.55	5.50	1 412.00	3.02
E_2_5_148	ID_5	2	E	1	148.00	1 013.99	378.79	2.75	877.00	3.02
E_3_4_148	ID_5	3	E	1	148.00	1 200.02	405.42	3.25	1 034.25	3.02
E_2_1_148	ID_5	2	E	1	148.00	1 057.53	382.57	3.75	898.75	3.02
E_2_2_269	ID_5	2	E	1	269.00	1 743.63	661.73	6.25	1 404.50	3.02
W_2_1_148	ID_5	2	W	1	148.00	832.46	333.08	1.25	667.00	3.02
W_3_1_148	ID_5	3	W	1	148.00	1 023.05	377.16	3.75	840.50	3.02
W_1_1_266	ID_5	1	W	1	266.00	317.49	93.88	0.00	67.75	3.02
W_2_2_148	ID_5	2	W	1	148.00	612.10	226.89	0.00	453.25	3.02
W_3_2_148	ID_5	3	W	1	148.00	945.95	350.36	0.75	754.75	3.02
N_1_1_266	ID_5	1	N	1	266.00	0.32	0.07	0.00	0.00	3.02
N_3_1_148	ID_5	3	N	1	148.00	18.21	3.04	0.00	0.00	3.02

N_1_3_266	ID_5	1	N	1	266.00	0.32	0.07	0.00	0.00	3.02
N_3_3_148	ID_5	3	N	1	148.00	18.21	3.04	0.00	0.00	3.02
ENE_1_3_190	ID_18	1	ENE	1	190.00	555.10	186.39	3.00	704.50	0.76
ENE_2_3_190	ID_18	2	ENE	1	190.00	727.63	222.24	3.00	724.75	0.76
ENE_3_3_190	ID_18	3	ENE	1	190.00	977.51	241.20	3.00	708.75	0.76
ENE_1_5_363	ID_18	1	ENE	1	363.00	998.88	370.03	1.75	691.75	0.76
ENE_2_5_363	ID_18	2	ENE	1	363.00	1 339.25	424.79	1.75	855.75	0.76
ENE_3_5_363	ID_18	3	ENE	1	363.00	1 913.88	464.78	2.75	1 055.25	0.76
ENE_1_6_302	ID_18	1	ENE	1	302.00	937.93	343.75	1.75	581.50	0.76
ENE_2_6_302	ID_18	2	ENE	1	302.00	1 308.32	416.78	2.25	644.25	0.76
ENE_3_6_302	ID_18	3	ENE	1	302.00	1 842.60	474.29	3.50	800.50	0.76
SSE_1_2_434	ID_18	1	SSE	1	434.00	3 420.69	1 477.53	7.00	1 715.25	0.76
SSE_2_2_434	ID_18	2	SSE	1	434.00	3 883.95	1 615.77	8.25	1 890.50	0.76
SSE_3_2_434	ID_18	3	SSE	1	434.00	4 943.20	2 114.63	8.50	2 377.25	0.76
WSW_1_1_14	ID_18	1	WSW	1	140.00	558.31	275.37	2.75	877.75	0.76
WSW_2_1_14	ID_18	2	WSW	1	140.00	726.98	344.11	3.75	1 077.75	0.76
WSW_3_1_14	ID_18	3	WSW	1	140.00	897.91	386.01	4.50	1 194.50	0.76
WSW_1_2_13	ID_18	1	WSW	1	133.00	402.18	222.79	1.50	738.50	0.76
WSW_2_2_13	ID_18	2	WSW	1	133.00	583.48	299.11	2.25	957.25	0.76
WSW_3_2_13	ID_18	3	WSW	1	133.00	774.44	350.46	3.00	1 124.00	0.76
WSW_1_4_26	ID_18	1	WSW	1	268.00	882.88	471.66	2.25	676.50	0.76
WSW_2_4_26	ID_18	2	WSW	1	268.00	1 291.43	640.60	3.00	833.00	0.76
WSW_3_4_26	ID_18	3	WSW	1	268.00	1 705.61	741.73	3.25	848.00	0.76
WSW_1_6_13	ID_18	1	WSW	1	133.00	598.41	267.70	3.00	971.75	0.76
WSW_2_6_13	ID_18	2	WSW	1	133.00	762.85	336.45	3.00	1 164.25	0.76
WSW_3_6_13	ID_18	3	WSW	1	133.00	931.36	378.82	3.25	1 274.50	0.76
NNW_1_2_26	ID_18	1	NNW	1	268.00	62.41	24.60	0.25	111.75	0.76
NNW_2_2_26	ID_18	2	NNW	1	268.00	139.95	48.50	0.25	199.25	0.76
NNW_3_2_26	ID_18	3	NNW	1	268.00	228.67	68.80	0.25	282.50	0.76
R_18_1_1	ID_18	1	R	2	420.00	2 473.80	977.28	4.50	1 242.75	0.76
R_18_1_2	ID_18	2	R	2	420.00	2 803.12	1 066.68	5.00	1 376.00	0.76

R_18_1_3	ID_18	3	R	2	420.00	3 303.52	1 144.64	6.00	1 530.75	0.76
R_18_2_1	ID_18	1	R	2	634.00	1 293.32	491.09	1.75	639.25	0.76
R_18_2_2	ID_18	2	R	2	634.00	1 831.60	600.50	2.25	817.50	0.76
R_18_2_3	ID_18	3	R	2	634.00	2 663.33	709.73	3.00	1 119.75	0.76
R_29_1_1	ID_29	1	S+W	2	436.00	1 308.93	495.06	1.75	437.00	3.96
R_29_1_2	ID_29	2	S+W	2	556.00	1 998.64	890.91	2.25	484.25	3.96
R_29_1_3	ID_29	3	S+W	2	556.00	2 295.74	1 018.20	2.50	533.25	3.96
R_29_1_4	ID_29	4	S+W	2	556.00	2 647.30	1 150.17	2.75	601.75	3.96
R_29_1_5	ID_29	5	S+W	2	556.00	3 098.82	1 288.15	4.75	744.25	3.96
R_29_1_6	ID_29	6	S+W	2	556.00	4 105.01	1 649.42	4.75	1 181.00	3.96
S_1_2_218	ID_29	1	S	1	218.00	730.27	317.28	1.50	208.75	3.96
S_2_2_218	ID_29	2	S	1	218.00	1 079.33	539.80	2.75	709.25	3.96
S_3_2_218	ID_29	3	S	1	218.00	1 218.82	605.09	2.75	825.25	3.96
S_4_2_218	ID_29	4	S	1	218.00	1 399.28	675.51	3.25	951.00	3.96
S_5_2_218	ID_29	5	S	1	218.00	1 627.73	746.99	5.00	1 096.00	3.96
S_6_2_218	ID_29	6	S	1	218.00	2 016.00	818.99	5.50	1 304.75	3.96
R_29_2_1	ID_29	1	S+E	2	436.00	671.53	254.01	1.75	168.25	3.96
R_29_2_2	ID_29	2	S+E	2	556.00	1 469.94	713.99	3.00	448.75	3.96
R_29_2_3	ID_29	3	S+E	2	556.00	1 768.24	858.06	3.25	553.50	3.96
R_29_2_4	ID_29	4	S+E	2	556.00	2 213.98	1 041.49	3.75	671.75	3.96
R_29_2_5	ID_29	5	S+E	2	556.00	2 737.23	1 206.54	4.25	819.00	3.96
R_29_2_6	ID_29	6	S+E	2	556.00	3 846.73	1 629.01	4.25	1 240.00	3.96
E_1_2_218	ID_29	1	E	1	218.00	85.38	40.72	0.00	133.25	3.96
E_2_2_218	ID_29	2	E	1	218.00	165.00	84.71	0.75	227.25	3.96
E_3_2_218	ID_29	3	E	1	218.00	268.17	139.17	0.50	319.50	3.96
E_4_2_218	ID_29	4	E	1	218.00	434.66	210.40	0.75	417.25	3.96
E_5_2_218	ID_29	5	E	1	218.00	610.14	259.00	2.25	537.75	3.96
E_6_2_218	ID_29	6	E	1	218.00	1 049.17	386.62	3.00	669.25	3.96
E_1_3_320	ID_29	1	E	1	320.00	197.96	79.30	0.00	67.50	3.96
E_2_3_320	ID_29	2	E	1	320.00	492.86	242.76	0.50	290.25	3.96
E_3_3_320	ID_29	3	E	1	320.00	757.21	373.81	0.50	413.00	3.96

E_4_3_320	ID_29	4	E	1	320.00	958.50	438.39	0.25	496.00	3.96
E_5_3_320	ID_29	5	E	1	320.00	1 511.13	631.38	2.25	726.50	3.96
E_6_3_320	ID_29	6	E	1	320.00	2 473.15	943.71	3.00	1 063.50	3.96
E_1_5_320	ID_29	1	E	1	320.00	436.78	168.54	0.00	112.25	3.96
E_2_5_384	ID_29	2	E	1	384.00	543.10	208.40	0.25	222.25	3.96
E_3_5_384	ID_29	3	E	1	384.00	717.54	284.76	0.50	322.25	3.96
E_4_5_384	ID_29	4	E	1	384.00	1 120.67	461.51	0.50	530.25	3.96
E_5_5_384	ID_29	5	E	1	384.00	1 597.26	611.56	1.25	729.25	3.96
E_6_5_384	ID_29	6	E	1	384.00	2 219.07	787.60	3.00	996.75	3.96
E_1_7_218	ID_29	1	E	1	218.00	395.15	152.54	0.00	150.00	3.96
E_2_7_218	ID_29	2	E	1	218.00	493.90	202.61	0.00	228.00	3.96
E_3_7_218	ID_29	3	E	1	218.00	613.24	253.32	0.00	293.25	3.96
E_4_7_218	ID_29	4	E	1	218.00	812.73	320.02	0.75	382.75	3.96
E_5_7_218	ID_29	5	E	1	218.00	1 050.34	381.81	1.50	493.25	3.96
E_6_7_218	ID_29	6	E	1	218.00	1 281.10	420.94	2.25	597.25	3.96
N_1_1_218	ID_29	1	N	1	218.00	29.22	2.72	0.00	39.00	3.96
N_2_1_338	ID_29	2	N	1	338.00	34.35	3.40	0.00	41.25	3.96
N_3_1_338	ID_29	3	N	1	338.00	40.36	4.25	0.00	50.00	3.96
N_4_1_338	ID_29	4	N	1	338.00	43.64	4.62	0.00	54.25	3.96
N_5_1_338	ID_29	5	N	1	338.00	56.19	5.97	0.00	68.00	3.96
N_6_1_338	ID_29	6	N	1	338.00	73.93	7.45	0.00	82.50	3.96
N_1_2_218	ID_29	1	N	1	218.00	7.59	0.73	0.00	12.00	3.96
N_2_2_218	ID_29	2	N	1	218.00	8.12	0.88	0.00	15.75	3.96
N_3_2_218	ID_29	3	N	1	218.00	11.86	1.40	0.00	20.25	3.96
N_4_2_218	ID_29	4	N	1	218.00	17.45	2.03	0.00	26.50	3.96
N_5_2_218	ID_29	5	N	1	218.00	26.63	2.99	0.00	39.25	3.96
N_6_2_218	ID_29	6	N	1	218.00	51.25	5.30	0.00	67.50	3.96
R_29_3_1	ID_29	1	N+W	2	436.00	281.69	131.33	1.25	407.50	3.96
R_29_3_2	ID_29	2	N+W	2	556.00	336.10	156.28	1.75	463.00	3.96
R_29_3_3	ID_29	3	N+W	2	556.00	423.21	196.03	2.25	522.25	3.96
R_29_3_4	ID_29	4	N+W	2	556.00	612.86	274.54	2.25	569.75	3.96

R_29_3_5	ID_29	5	N+W	2	556.00	837.81	318.40	2.50	502.25	3.96
R_29_3_6	ID_29	6	N+W	2	556.00	974.77	273.55	3.00	417.25	3.96
W_1_3_218	ID_29	1	W	1	218.00	467.28	198.75	1.25	379.75	3.96
W_2_3_320	ID_29	2	W	1	320.00	1 366.77	619.03	2.00	700.50	3.96
W_3_3_320	ID_29	3	W	1	320.00	1 446.23	631.15	2.50	728.00	3.96
W_4_3_320	ID_29	4	W	1	320.00	1 712.85	730.50	3.25	830.25	3.96
W_5_3_320	ID_29	5	W	1	320.00	2 223.38	891.80	3.50	1 009.25	3.96
W_6_3_320	ID_29	6	W	1	320.00	2 765.79	1 001.77	3.75	1 204.25	3.96
W_1_5_437	ID_29	1	W	1	437.00	1 040.44	385.56	1.00	239.25	3.96
W_2_5_384	ID_29	2	W	1	384.00	1 006.86	395.00	1.75	363.13	3.96
W_3_5_384	ID_29	3	W	1	384.00	1 123.67	426.53	2.00	402.38	3.96
W_4_5_384	ID_29	4	W	1	384.00	1 260.35	460.64	2.00	443.75	3.96
W_5_5_384	ID_29	5	W	1	384.00	1 501.95	507.04	2.00	505.00	3.96
W_6_5_384	ID_29	6	W	1	384.00	1 972.68	645.81	2.25	659.13	3.96
W_1_7_218	ID_29	1	W	1	218.00	738.99	307.70	1.00	451.50	3.96
W_2_7_218	ID_29	2	W	1	218.00	825.97	337.76	1.00	493.00	3.96
W_3_7_218	ID_29	3	W	1	218.00	913.42	363.14	2.00	538.25	3.96
W_4_7_218	ID_29	4	W	1	218.00	1 008.76	386.21	2.50	580.50	3.96
W_5_7_218	ID_29	5	W	1	218.00	1 114.07	401.87	3.00	617.75	3.96
W_6_7_218	ID_29	6	W	1	218.00	1 037.74	274.19	2.75	413.25	3.96
R_52_1_1	ID_52	1	S+W	2	204.00	1 349.47	389.82	2.00	942.50	3.57
R_52_1_2	ID_52	2	S	2	172.00	419.39	151.55	1.50	557.75	3.57
S_3_1_167	ID_52	3	S	1	167.00	539.74	202.16	3.00	892.75	3.57
S_4_1_167	ID_52	4	S	1	167.00	573.86	220.45	3.25	912.00	3.57
S_5_1_167	ID_52	5	S	1	167.00	672.24	278.32	3.50	929.00	3.57
R_52_1_6	ID_52	6	S	2	172.00	808.43	360.30	3.50	1 150.25	3.57
R_52_2_1	ID_52	1	S+W	5	594.00	3 921.79	1 103.72	1.75	1 078.25	3.57
R_52_3_2	ID_52	2	S+W	3	476.00	3 043.80	907.06	1.50	947.75	3.57
S_2_3_167	ID_52	2	S	1	167.00	378.08	47.05	0.75	631.75	3.57
S_2_4_167	ID_52	2	S	1	167.00	523.80	67.87	0.00	915.75	3.57
R_52_4_2	ID_52	2	S	2	290.00	835.02	429.78	0.00	936.00	3.57

R_52_4_2	ID_52	2	S	2	290.00	916.60	120.14	0.00	0.00	3.57
S_2_9_167	ID_52	2	S	1	167.00	523.89	67.90	0.00	917.50	3.57
R_52_5_2	ID_52	2	S+W	3	476.00	2 578.92	866.76	1.75	770.50	3.57
S_2_11_167	ID_52	2	S	1	167.00	278.40	27.57	0.00	403.00	3.57
R_52_3_3	ID_52	3	S+W	3	538.00	3 515.42	1 157.66	1.50	1 107.50	3.57
S_3_3_167	ID_52	3	S	1	167.00	507.73	62.60	0.00	848.5	3.57
S_3_4_167	ID_52	3	S	1	167.00	512.24	63.73	0.00	852.50	3.57
S_3_5_167	ID_52	3	S	1	167.00	512.35	63.76	0.00	851.00	3.57
S_3_6_167	ID_52	3	S	1	167.00	507.88	62.64	0.00	848.00	3.57
R_52_3_3	ID_52	3	S+W	3	538.00	2 823.27	1 078.80	1.75	907.50	3.57
R_52_3_4	ID_52	4	S+W	3	538.00	3 763.82	1 323.89	1.25	1 233.25	3.57
S_3_3_167	ID_52	3	S	1	167.00	621.39	380.72	3.75	792.75	3.57
S_3_4_167	ID_52	3	S	1	167.00	665.61	406.57	4.25	911.25	3.57
S_3_5_167	ID_52	3	S	1	167.00	656.81	401.44	4.75	909.75	3.57
S_3_6_167	ID_52	3	S	1	167.00	591.07	364.24	3.50	786.00	3.57
R_52_3_4	ID_52	4	S+W	3	538.00	3 126.13	1 267.94	1.50	1 015.50	3.57
R_52_3_5	ID_52	5	S+W	3	538.00	3 349.54	1 115.44	6.00	1 274.00	3.57
S_5_3_167	ID_52	5	S	1	167.00	381.45	32.29	4.25	505.50	3.57
S_5_4_167	ID_52	5	S	1	167.00	376.02	31.22	4.50	495.00	3.57
S_5_5_167	ID_52	5	S	1	167.00	374.82	31.02	4.75	495.25	3.57
S_5_6_167	ID_52	5	S	1	167.00	373.09	30.90	4.25	496.50	3.57
R_52_3_4	ID_52	5	S+W	3	538.00	2 698.08	961.72	4.00	1 066.00	3.57
R_52_3_4	ID_52	6	S+W	3	538.00	1 491.57	348.90	6.00	649.75	3.57
R_52_6_6	ID_52	6	S	2	154.00	964.66	431.27	5.50	1 456.75	3.57
R_52_4_6	ID_52	6	S	2	154.00	946.40	428.79	5.75	1 445.00	3.57
R_52_4_6	ID_52	6	S	2	154.00	902.83	419.17	5.75	1 402.25	3.57
R_52_6_6	ID_52	6	S	2	154.00	891.62	456.88	5.50	1 342.50	3.57
R_52_3_4	ID_52	6	S+W	3	538.00	1 427.89	513.67	5.25	1 088.00	3.57
S_3_11_167	ID_52	3	S	1	167.00	329.18	29.38	0.00	410.25	3.57
S_4_11_167	ID_52	4	S	1	167.00	438.01	241.07	3.25	1 048.75	3.57
S_5_11_167	ID_52	5	S	1	167.00	284.82	21.36	0.00	313.25	3.57

R_52_7_6	ID_52	6	S	2	154.00	605.88	306.76	1048.75	3.25	3.57
W1_1_1_167	ID_52	1	W	1	167.00	1 256.31	302.17	2.25	937.75	3.57
R_52_8_1	ID_52	1	W	2	439.00	3 286.85	773.44	3.00	984.00	3.57
R_52_9_3	ID_52	3	W	2	439.00	2 933.79	596.01	4.50	887.50	3.57
W1_3_3_167	ID_52	3	W	1	167.00	1 375.69	473.20	1.75	1 214.50	3.57
R_52_9_5	ID_52	5	W	2	439.00	2 416.81	414.24	3.00	882.00	3.57
R_52_10_5	ID_52	5	W	2	186.00	256.39	22.26	2.50	224.75	3.57
R_52_11_3	ID_52	3	W+N	2	204.00	229.41	33.50	5.75	713.25	3.57
R_52_11_3	ID_52	5	W+N	2	204.00	185.31	20.41	3.50	713.25	3.57
R_52_11_6	ID_52	6	W+N	2	184.00	146.37	11.95	0.75	417.50	3.57
R_52_12_2	ID_52	3	W	2	186.00	1 031.72	421.89	1.75	830.50	3.57
W4_3_1_167	ID_52	3	W	1	167.00	962.63	395.37	1.75	886.50	3.57
W4_4_1_167	ID_52	4	W	1	167.00	811.11	284.95	3.25	698.75	3.57
W4_5_1_167	ID_52	5	W	1	167.00	479.08	116.33	4.25	393.50	3.57
R_52_12_6	ID_52	6	W	2	186.00	153.25	15.14	1.25	114.50	3.57
R_52_13_2	ID_52	2	E	2	130.00	985.59	330.47	1.25	1 126.75	3.57
E1_3_1_198	ID_52	3	E	1	198.00	175.54	73.33	0.50	280.00	3.57
E1_3_2_198	ID_52	3	E	1	198.00	221.18	87.44	0.75	329.50	3.57
R_52_14_2	ID_52	3	E	2	439.00	3 719.22	752.48	5.75	1 402.75	3.57
E1_4_1_198	ID_52	4	E	1	198.00	258.04	125.70	0.50	380.75	3.57
E1_4_2_198	ID_52	4	E	1	198.00	300.67	137.33	0.75	426.00	3.57
R_52_14_4	ID_52	4	E	2	439.00	3 133.54	524.35	5.75	1 193.00	3.57
E1_5_1_198	ID_52	5	E	1	198.00	394.43	199.80	0.75	474.75	3.57
E1_5_2_198	ID_52	5	E	1	198.00	438.62	211.54	0.75	515.25	3.57
R_52_14_5	ID_52	5	E	2	439.00	2 327.82	285.11	4.75	870.00	3.57
R_52_15_6	ID_52	6	E	2	186.00	316.89	55.61	6.00	387.00	3.57
R_52_16_6	ID_52	6	E	2	186.00	203.80	14.89	1.00	172.50	3.57
R_52_14_6	ID_52	6	E	2	439.00	1 041.25	73.62	1.75	420.25	3.57
R_52_17_2	ID_52	2	E	2	186.00	888.67	260.84	1.25	790.75	3.57
E2_3_1_167	ID_52	3	E	1	167.00	716.99	271.49	1.75	709.75	3.57
E2_3_2_235	ID_52	3	E	1	235.00	1 151.16	346.13	1.25	829.75	3.57

E2_4_1_167	ID_52	4	E	1	167.00	796.27	319.57	1.75	846.00	3.57
E2_4_2_235	ID_52	4	E	1	235.00	1 042.35	258.01	3.75	694.50	3.57
R_52_18_2	ID_52	4	E+N	4	501.00	831.64	151.38	4.75	818.00	3.57
E2_5_1_167	ID_52	5	E	1	167.00	769.07	286.97	5.00	920.75	3.57
E2_5_2_235	ID_52	5	E	1	235.00	879.85	160.57	4.00	570.50	3.57
R_52_19_2	ID_52	6	E	2	186.00	392.12	76.30	5.25	495.00	3.57
R_52_17_6	ID_52	6	E	3	279.00	374.51	28.55	2.75	217.75	3.57
R_52_18_6	ID_52	6	E+N	4	427.00	633.99	155.41	0.00	250.50	3.57
R_52_20_6	ID_52	2	N	2	186.00	68.05	4.94	0.00	39.75	3.57
R_52_21_2	ID_52	2	N	2	334.00	182.64	13.82	0.00	175.75	3.57
R_52_21_2	ID_52	2	N	2	334.00	173.32	12.79	0.00	161.25	3.57
R_52_20_2	ID_52	2	N	2	186.00	43.59	2.27	0.00	39.75	3.57
R_52_21_2	ID_52	2	N	2	186.00	70.43	5.38	0.00	39.75	3.57
R_52_22_2	ID_52	2	N	2	186.00	71.14	5.57	0.00	39.75	3.57
N_3_1_167	ID_52	3	N	1	167.00	13.16	1.76	0.00	41.75	3.57
R_52_23_3	ID_52	3	N	2	186.00	32.16	3.51	0.00	0.00	3.57
R_52_24_3	ID_52	3	N	3	469.00	215.51	21.48	0.00	174.50	3.57
N_3_14_167	ID_52	3	N	1	167.00	51.67	2.92	0.00	64.50	3.57
N_3_15_167	ID_52	3	N	1	167.00	0.24	0.06	0.00	0.00	3.57
N_3_16_167	ID_52	3	N	1	167.00	101.15	8.77	0.00	184.25	3.57
N_4_2_167	ID_52	4	N	1	167.00	20.28	2.45	0.00	61.75	3.57
N_4_8_167	ID_52	4	N	1	167.00	0.54	0.04	0.00	176.00	3.57
R_52_21_2	ID_52	4	N	2	439.00	166.66	13.12	0.00	127.25	3.57
N_4_13_167	ID_52	4	N	1	167.00	51.65	2.92	0.00	64.50	3.57
N_4_15_167	ID_52	4	N	1	167.00	101.15	8.77	0.00	184.25	3.57
N_4_16_167	ID_52	4	N	1	167.00	142.35	13.60	0.00	201.25	3.57
N_5_1_167	ID_52	5	N	1	167.00	9.08	1.34	0.00	14.25	3.57
R_52_23_3	ID_52	5	N	2	186.00	22.26	1.90	0.00	0.00	3.57
R_52_24_3	ID_52	5	N	3	469.00	192.11	17.59	0.00	149.75	3.57
N_5_8_167	ID_52	5	N	1	167.00	91.14	7.17	0.00	166.50	3.57
R_52_21_6	ID_52	5	N	2	439.00	123.56	7.99	0.00	111.00	3.57

N_5_14_167	ID_52	5	N	1	167.00	171.03	29.52	0.00	139.15	3.57
N_5_16_167	ID_52	5	N	1	167.00	142.35	13.60	0.00	201.25	3.57
R_52_24_3	ID_52	6	N	2	186.00	2.92	0.45	0.00	0.00	3.57
N_6_3_167	ID_52	6	N	1	167.00	15.97	2.45	0.00	42.00	3.57
R_52_24_3	ID_52	6	N	3	353.00	99.84	7.92	0.00	109.25	3.57
R_52_21_6	ID_52	6	N	2	439.00	583.81	49.62	0.00	266.50	3.57
R_52_20_6	ID_52	6	N	2	186.00	71.04	5.52	0.00	39.75	3.57
SSE1_2_1_249	ID_60	2	SSE	1	249.00	2 319.21	996.29	7.25	1 963.25	2.57
SSE1_2_2_221	ID_60	2	SSE	1	221.00	1 919.69	825.57	5.75	1 694.50	2.57
SSE1_2_4_250	ID_60	2	SSE	1	250.00	2 609.20	1 036.25	7.75	2 103.25	2.57
SSE1_2_5_250	ID_60	2	SSE	1	250.00	2 315.13	920.64	5.75	1 614.00	2.57
SSE1_2_9_251	ID_60	2	SSE	1	251.00	2 730.82	1 095.38	7.25	2 084.75	2.57
SSE1_3_3_210	ID_60	3	SSE	1	210.00	2 100.79	820.93	6.50	1 804.50	2.57
SSE1_3_6_214	ID_60	3	SSE	1	214.00	2 092.44	836.76	4.25	1 684.50	2.57
SSE1_3_7_256	ID_60	3	SSE	1	256.00	2 962.21	1 144.40	7.50	2 224.00	2.57
SSE1_3_8_211	ID_60	3	SSE	1	211.00	2 128.63	839.23	5.75	1 718.75	2.57
SSE1_4_1_249	ID_60	4	SSE	1	249.00	2 954.02	1 122.06	8.25	2 370.50	2.57
SSE1_4_3_210	ID_60	4	SSE	1	210.00	2 306.08	859.26	6.50	1 944.75	2.57
SSE1_4_5_250	ID_60	4	SSE	1	250.00	2 669.63	993.11	6.25	1 819.50	2.57
SSE1_4_7_256	ID_60	4	SSE	1	256.00	3 227.31	1 184.95	8.00	2 395.50	2.57
SSE1_4_9_251	ID_60	4	SSE	1	251.00	3 185.51	1 164.42	8.00	2 400.75	2.57
SSE2_3_1_232	ID_60	3	SSE	1	232.00	1 948.68	809.95	4.25	1 295.75	2.57
R_60_1_1	ID_60	1	SSE+SW	4	931.00	6 548.47	2 154.52	7.00	2 067.00	2.57
R_60_1_2	ID_60	2	SSE	3	722.00	2 684.46	459.97	1.75	2 108.25	2.57
R_60_1_3	ID_60	3	SSE	3	722.00	5 013.62	1 617.47	7.00	2 300.50	2.57
R_60_1_4	ID_60	4	SSE+SW	4	931.00	4 941.88	1 492.02	6.50	2 024.75	2.57
R_60_2_2	ID_60	2	SSE+SSW	2	617.00	2 741.01	730.49	5.00	1 589.00	2.57
R_60_2_3	ID_60	3	SSW+SW	2	617.00	3 279.18	1 123.93	7.00	1 337.50	2.57
R_60_2_4	ID_60	4	SSW+SW	2	617.00	2 094.75	493.67	5.25	1 188.75	2.57
NW1_1_1_244	ID_60	1	NW	1	244.00	628.39	135.84	0.50	445.50	2.57
NW1_1_2_209	ID_60	1	NW	1	209.00	519.81	111.24	1.00	570.25	2.57

NW1_1_7_209	ID_60	1	NW	1	209.00	551.49	114.09	1.00	588.00	2.57
NW1_1_8_244	ID_60	1	NW	1	244.00	697.24	140.96	0.50	474.50	2.57
NW1_2_3_209	ID_60	2	NW	1	209.00	580.95	117.08	1.00	607.25	2.57
NW1_2_4_244	ID_60	2	NW	1	244.00	741.02	145.29	0.50	495.50	2.57
NW1_2_5_244	ID_60	2	NW	1	244.00	750.39	145.85	0.50	499.75	2.57
NW1_2_6_209	ID_60	2	NW	1	209.00	601.97	118.28	1.00	614.25	2.57
NW1_3_1_244	ID_60	3	NW	1	244.00	711.35	142.71	0.50	401.00	2.57
NW1_3_2_209	ID_60	3	NW	1	209.00	579.51	116.33	1.00	605.50	2.57
NW1_3_7_209	ID_60	3	NW	1	209.00	649.79	119.30	1.00	631.00	2.57
NW1_3_8_244	ID_60	3	NW	1	244.00	826.07	149.89	0.50	531.75	2.57
NW1_4_3_209	ID_60	4	NW	1	209.00	632.59	112.31	1.00	577.25	2.57
NW1_4_4_244	ID_60	4	NW	1	244.00	798.96	137.97	0.50	495.50	2.57
NW1_4_5_244	ID_60	4	NW	1	244.00	826.57	140.12	0.50	506.50	2.57
NW1_4_6_209	ID_60	4	NW	1	209.00	673.57	116.52	1.00	601.75	2.57
NW2_1_1_206	ID_60	1	NW	1	206.00	25.62	2.82	0.00	32.00	2.57
NW2_2_1_206	ID_60	2	NW	1	206.00	52.42	5.79	0.00	19.05	2.57
NW2_3_1_206	ID_60	3	NW	1	206.00	80.60	6.90	0.00	33.00	2.57
R_60_3_2	ID_60	2	NW	3	722.00	3 219.75	951.34	6.00	1 216.25	2.57
R_60_4_3	ID_60	3	NW	3	722.00	3 094.12	548.30	6.50	1 149.25	2.57
R_60_3_4	ID_60	4	NW	3	722.00	1 382.03	243.20	0.75	621.50	2.57
R_60_4_2	ID_60	2	NW+SW	4	931.00	6 191.33	1 955.44	9.25	2 215.75	2.57
R_60_4_3	ID_60	3	NW	3	722.00	3 443.41	606.12	6.75	1 127.75	2.57
R_60_4_4	ID_60	4	NW+SW	4	931.00	4 186.52	1 067.79	4.75	1 422.00	2.57
SW3_3_1_209	ID_60	3	SW	1	209.00	1 745.13	706.42	4.00	1 470.25	2.57
NE1_2_1_217	ID_60	2	NE	1	217.00	0.00	0.00	0.00	0.00	2.57
NE1_3_1_217	ID_60	3	NE	1	217.00	0.00	0.00	0.00	0.00	2.57
NE1_4_1_217	ID_60	4	NE	1	217.00	0.00	0.00	0.00	0.00	2.57
R_60_5_2	ID_60	2	NE+SSE	2	480.00	1 028.38	315.77	2.00	726.25	2.57
NE2_2_5_218	ID_60	2	NE	1	218.00	990.26	271.15	2.00	738.25	2.57
NE2_2_6_215	ID_60	2	NE	1	215.00	732.92	166.86	1.25	586.75	2.57
NE2_3_3_215	ID_60	3	NE	1	215.00	754.95	169.72	1.25	601.00	2.57

NE2_3_4_212	ID_60	3	NE	1	212.00	1024.78	265.74	2.25	774.75	2.57
NE2_3_7_215	ID_60	3	NE	1	215.00	816.63	173.88	1.25	625.75	2.57
R_60_5_2	ID_60	4	NE+SSE	2	480.00	1 256.98	303.84	2.00	646.25	2.57
NE2_4_2_215	ID_60	4	NE	1	215.00	819.42	174.49	1.75	643.50	2.57
NE2_4_5_218	ID_60	4	NE	1	218.00	1 135.48	275.83	2.50	752.75	2.57
NE2_4_6_215	ID_60	4	NE	1	215.00	848.35	176.12	1.50	650.75	2.57
NE3_2_2_212	ID_60	2	NE	1	212.00	871.67	205.14	0.75	522.75	2.57
NE3_2_3_215	ID_60	2	NE	1	215.00	1 209.93	407.70	4.25	722.75	2.57
NE3_2_6_212	ID_60	2	NE	1	212.00	969.73	241.79	1.75	791.25	2.57
NE3_2_7_215	ID_60	2	NE	1	215.00	3 088.20	1 226.96	7.25	2 134.75	2.57
NE3_3_1_214	ID_60	3	NE	1	214.00	518.36	82.07	0.00	140.75	2.57
NE3_3_4_215	ID_60	3	NE	1	215.00	157.28	108.02	0.50	140.75	2.57
NE3_3_5_212	ID_60	3	NE	1	212.00	1 019.52	242.32	2.00	765.00	2.57
NE3_3_8_215	ID_60	3	NE	1	215.00	298.75	123.86	0.50	288.75	2.57
NE3_3_9_259	ID_60	3	NE	1	259.00	915.16	295.00	0.75	597.00	2.57
NE3_4_2_212	ID_60	4	NE	1	212.00	907.27	200.16	0.50	519.00	2.57
NE3_4_3_215	ID_60	4	NE	1	215.00	864.39	418.79	1.75	535.50	2.57
NE3_4_6_212	ID_60	4	NE	1	212.00	1 091.88	243.49	2.25	799.50	2.57
NE3_4_7_215	ID_60	4	NE	1	215.00	888.07	419.54	1.75	615.75	2.57
SW2_2_1_213	ID_60	2	SW	1	213.00	1 105.15	512.64	3.75	996.75	2.57
R_60_4_2	ID_60	2	SW	3	722.00	4917.28	1 319.86	3.75	1 043.75	2.57
SW2_2_9_210	ID_60	2	SW	1	210.00	1 444.85	621.58	4.50	1 333.75	2.57
R_60_4_2	ID_60	2	SW	3	722.00	5135.88	1 284.51	4.50	1 333.75	2.57
SW2_3_2_210	ID_60	3	SW	1	210.00	1 567.56	646.25	4.50	1 368.25	2.57
R_60_6_3	ID_60	3	SW	3	722.00	4 685.35	1 101.91	4.50	1 368.25	2.57
SW2_3_10_210	ID_60	3	SW	1	210.00	1 603.08	642.85	4.75	1 479.50	2.57
SW2_4_1_213	ID_60	4	SW	1	213.00	1 574.22	557.83	4.00	1 121.75	2.57
R_60_4_4	ID_60	4	SW	3	722.00	3 606.85	894.84	4.50	1 354.50	2.57
SW2_4_9_210	ID_60	4	SW	1	210.00	1 706.55	578.99	4.25	1 320.25	2.57
R_60_4_4	ID_60	4	SW	3	722.00	3 485.65	826.95	4.25	1 320.25	2.57
R_60_6_2	ID_60	2	WSW	3	722.00	3 991.82	1 770.09	5.50	1 492.25	2.57

WSW_2_5_20	ID_60	2	WSW	1	209.00	1 653.40	719.92	3.25	1 123.75	2.57
R_60_6_2	ID_60	2	WSW	3	722.00	5 033.67	2 284.56	3.25	1 374.00	2.57
WSW_3_4_21	ID_60	3	WSW	1	213.00	1 910.59	786.24	3.50	1 255.75	2.57
R_60_4_3	ID_60	3	WSW	3	422.00	6 523.02	2 446.63	5.50	1 384.25	2.57
WSW_3_12_214	ID_60	3	WSW	1	214.00	1 501.22	654.16	0.50	870.25	2.57
R_60_6_4	ID_60	4	WSW	3	722.00	3 367.47	1 162.24	6.00	1 289.00	2.57
WSW_4_5_20	ID_60	4	WSW	1	209.00	1 728.07	615.69	3.75	932.25	2.57
R_60_6_4	ID_60	4	WSW	3	931.00	6 211.87	2 435.24	6.25	1 711.75	2.57
E_1_1_271	ID_75	1	E	1	271.00	2 047.68	849.10	3.00	1 404.00	1.25
E_1_2_160	ID_75	1	E	1	160.00	1 316.10	534.53	3.00	1 494.00	1.25
E_2_5_160	ID_75	2	E	1	160.00	1 784.62	634.12	5.50	1 888.25	1.25
E_2_6_271	ID_75	2	E	1	271.00	3 044.42	1 078.86	5.50	1 890.75	1.25
E_3_9_160	ID_75	3	E	1	160.00	2 095.40	659.92	6.00	2 150.25	1.25
E_3_10_271	ID_75	3	E	1	271.00	3 558.64	1 118.91	6.00	2 153.50	1.25
R_75_1_4	ID_75	4	E	2	431.00	5 828.39	1 784.93	6.00	2 202.50	1.25
R_75_1_5	ID_75	4	E	2	431.00	5 828.39	1 784.93	6.00	2 202.50	1.25
E_6_1_271	ID_75	6	E	1	271.00	3 665.73	1 122.62	6.00	2 202.50	1.25
E_6_2_160	ID_75	6	E	1	160.00	2 162.66	662.31	6.00	2 202.50	1.25
E_7_5_160	ID_75	7	E	1	160.00	2 162.66	662.31	6.00	2 202.50	1.25
E_7_6_271	ID_75	7	E	1	271.00	3 665.73	1 122.62	6.00	2 202.50	1.25
E_8_9_160	ID_75	8	E	1	160.00	2 162.66	662.31	6.00	2 202.50	1.25
E_8_10_271	ID_75	8	E	1	271.00	3 665.73	1 122.62	6.00	2 202.50	1.25
R_75_1_9	ID_75	9	E	2	431.00	5 828.39	1 784.93	6.00	2 202.50	1.25
W_1_1_271	ID_75	1	W	1	271.00	2 711.71	1 038.90	5.00	1 652.75	1.25
W_1_2_160	ID_75	1	W	1	160.00	1 588.90	609.75	5.00	1 635.25	1.25
W_2_5_271	ID_75	2	W	1	271.00	2 896.71	1 060.22	5.50	1 733.25	1.25
W_2_6_160	ID_75	2	W	1	160.00	1 672.36	619.55	5.50	1 689.25	1.25
R_75_2_4	ID_75	4	W	2	431.00	5 828.39	1 784.93	6.00	2 202.50	1.25
R_75_2_5	ID_75	5	W	2	431.00	5 828.39	1 784.93	6.00	2 202.50	1.25
W_6_1_271	ID_75	6	W	1	271.00	3 665.73	1 122.62	6.00	2 202.50	1.25
W_6_2_160	ID_75	6	W	1	160.00	2 162.66	662.31	6.00	2 202.50	1.25

W_7_5_271	ID_75	7	W	1	271.00	3 665.73	1 122.62	6.00	2 202.50	1.25
W_7_6_160	ID_75	7	W	1	160.00	2 162.66	662.31	6.00	2 202.50	1.25
R_75_2_9	ID_75	9	W	2	431.00	5 828.39	1 784.93	6.00	2 202.50	1.25

LUND UNIVERSITY

Divisions of Energy and Building Design, Building Physics and Building Services
Department of Building and Environmental Technology